Self-Assembling Modular Systems: Enhancing Efficiency and Accuracy in Robotic Lattice Assembly

by

John Romanishin

B.S. Mechanical Engineering, MIT, 2012
M.S. Mechanical Engineering, MIT, 2018

Submitted to the Department of Mechanical Engineering
in partial fulfillment of the requirements for the degree of

DOCTOR OF PHILOSOPHY IN MECHANICAL ENGINEERING

at the

MASSACHUSETTS INSTITUTE OF TECHNOLOGY

May 2024

Authored by:	John Romanishin Department of Mechanical Engineering May 20, 2024
Certified by:	Daniela Rus Professor of Electrical Engineering and Computer Science, Thesis Supervisor
Accepted by:	Amos Winter Professor of Mechanical Engineering

Self-Assembling Modular Systems: Enhancing Efficiency and Accuracy in Robotic Lattice Assembly

by

John Romanishin

B.S. Mechanical Engineering, MIT, 2012
M.S. Mechanical Engineering, MIT, 2018

Submitted to the Department of Mechanical Engineering
in partial fulfillment of the requirements for the degree of

DOCTOR OF PHILOSOPHY IN MECHANICAL ENGINEERING

ABSTRACT

This thesis introduces a robotic system designed to progress the concept of modular 'industrial Legos,' aiming to harness the advantages of modularity in new environments, such as CNC machines and factory automation. This vision intersects with the domain of modular self-reconfigurable robotics and robotically-assembled structures. The work presented here extends from existing research and is particularly focused on three key areas: (1) the development of improved modular connectors between system elements, (2) the advancement of modular linear actuator designs that not only facilitate component rearrangement but also contribute to task performance, and (3) improved performance and efficiency of lattice-assembler robots. All topics are examined in depth, and their relevance to prior work is carefully outlined.

Central to any modular system is the design of connectors, which enable the modules to assemble into various configurations. Although extensive research has been conducted in this area, existing connector solutions often fall short in terms of repeatability, affordability, and mechanical strength. This thesis addresses these shortcomings by introducing a new connector that utilizes a kinematic coupling for high-repeatability and incorporates a simple, screw-based latching mechanism for strong mechanical connections. Detailed design specifications for these connectors are provided; these designs are both relatively simple to implement and robust enough to withstand the harsh conditions encountered in industrial settings.

In CNC and industrial automation, linear actuators often pair with structural elements to form *gantry* systems, allowing for precise 3D-positioning of tools and end effectors. While there are self-contained linear actuators that offer some level of modularity—often termed 'superficial modularity'—traditional designs generally lack the capacity for what might be called 'deep modularity.' This refers to the unique ability to seamlessly join two actuators of length L to create a single actuator of length 2L. To address this, the thesis presents a high-strength, extensible modular linear actuator built on magnetic lead screws, capable of general linear motion and of cooperating with other modular elements to rearrange modules.

Lastly, this thesis introduces an assembly robot named Belty, equipped with proprioceptive actuators that feature large-diameter, high-torque-density brushless motors and minimal

gearing. These actuators offer several advantages, such as efficient motion, back-drivability, force sensing, and impact resilience. These features are especially valuable for assembly tasks within constrained spaces, as they enable simplified assembly algorithms through contact-rich motion primitives (e.g., dragging parts, bumping into objects). Following the hardware discussion, assembly algorithms are detailed to demonstrate the system's ability to construct a diverse array of structures quickly and energy-efficiently.

Thesis supervisor: Daniela Rus
Title: Professor of Electrical Engineering and Computer Science

Acknowledgments

Firstly, I would like to thank Daniela Rus for the support and mentorship over the last too-many years to count. From building a block-stacking robot in 6.141, to our class trip to a castle in Italy to play with robot arms, to your frantic hand-writing corrections for my undergraduate thesis; I knew that I wanted to continue as a graduate student in your lab after graduating. After finally getting in, it has been truly wonderful getting to know you and learning about robotics with the DRL family. All the way through the intense few years working with the M-Block robots, to having the freedom and resources to build my dream project described in the rest of this thesis, I have been truly lucky to have had this incredible opportunity. Thank you!

I would like to thank the rest of my thesis committee for their support and guidance throughout this process. Amos Winter for helping drag me kicking-and-screaming through the mechanical engineering qualification exam process, as well as for the constant support since then. I have many great memories from the long nights in the Stata basement happily attempting to electrify a small car for Professor Winter's Global Engineering class. Sangbae Kim, thank you for your support going all way back to being a great section leader for my 2.007 class all the way back in 2009 and for showing us inspiring high-performance robots year after year. Much of what I have learned about robotics is from your truly excellent biological-inspired robotics class. Finally, I would like to thank Beth Marcus for her support throughout the last part of my PhD. It has been a joy working with you and your group over the last several internships at Amazon Robotics and being reminded that there is a world outside of academia.

Thank you to all of the professional shop people and my fellow machinist friends on campus that helped me manufacture many of the elements for these robots in various campus shops, including the Hobby Shop, the LMP (Building 35) Shop, Mark Belinger at the Edgerton shop, and the MIT Central Machine Shop. I thoroughly enjoyed almost every minute of my time inside each of the different machine shops on campus. I would like thank Ron Wiken for his immense knowledge about making different parts and for keeping order in the CSAIL machine shop and making it a welcoming place to work. MakerWorkShop, a student-run community, has been such a great addition to my MIT tenure. MakerWorks is full of so many of the cool folks on campus who have a shared obsession in making things, often from scratch, and often just for the fun. I have learned greatly from chatting in the shop with people about random mostly educational topics, like discussing Magnetic Lead Screws with Marcel Thomas, or (attempting) to learn about the intricacies of motor control and magnetic circuits from Austin Brown. Thanks!

This PhD would have been much less exciting and educational without all of the wonder-

ful colleagues and friends in the Distributed Robotics Laboratory. I can't count how many shared papers, fun group retreats, and multi-hour conversations, from robots to politics, (usually late at night) with folks from the lab including: (in no particular order) Zach Patterson, Steven Ceron, Teddy Ort, Leo Zamora, Alyssa Pierson, Andy Marchese, Shuguang Li, Sebastian Claici, Robert Katzschmann, Joseph DelPreto, Brandon Araki, Robert MacCurdy, Cathy Wu, Bianca Homberg, Cenk Baykal, Ara Knaian, Mikhail Volkov, Stuart Baker, Ross Knepper, Cagdas Onal, Ankur Mehta, Lucas Liebenwein, Noam Buckman, Andy Spielberg, Lillian Chin, Annan Zhang, Mehmet Dogar, Cindy Sung, Thomas Bertossi, Stephanie Gil, Hunter Hansen, Stephane Bonardi, Ryan Truby, Josie Hughes, Veevee Cai, and probably more that my old brain has somehow forgot. In my defense, I have been here for a *long* time. Having such a fun crew around also meant that traveling to conferences was always an exciting adventure. A special shout-out to Jim Bern for helping me focus when important paper-deadlines are due, and for keeping the Omax CAD dream alive. Also to John Mamish for always being willing to draw random circuit diagrams on napkins in many different bars and restaurants around Cambridge. And a special thank you to Mieke Moran for always making the office a happier place to be, for the immense work involved with managing receipts, and for always telling us about the best free food opportunities.

Special gratitude to Kyle Gilpin for mentoring me at the beginning of my long DRL journey and showing me a great example of how to properly build exciting modular robots. I am grateful for the time you spent mailing circuit boards back and forth to Alaska to try enable the M-Blocks to keep working. And for all of the excellent advice throughout the years on topics ranging from electrical circuits to hiking in the Sierras. Hopefully I will soon have the time to actually come visit you in Bishop, CA!

Thanks to my friend and postdoc colleague Jeff Lipton. It has always been fun sharing the newest random things we built and talking late into the night about crazy robot ideas designed across the white boards in your office. Perhaps I would have graduated years earlier without these distractions but it would have been far less fun.

There are many other wonderful people I have met at MIT who have helped me achieve this goal in various ways. Professor Daniel Frey for running the incredible 2.007 robot competition class where I finally knew for sure that I had picked the right major. Professor Slocum for enthusiastically introducing everyone to the magic of kinematic couplings which are used extensively in this work, and for always keeping your lectures entertaining. Other people at MIT who have contributed towards this effort include my friends Bhargav Gajjar and Arya Azma who both encouraged me to learn about magnet power transmissions in different ways. Also, there always seem to be folks around like Matt Carney and Mike Nawrot who I can talk about random mechanical things like the intricacies of different types of bearings for hours. I owe a great debt to Kenny Cheung who (in addition to now leading the team working on the SOLL-E structure assembly robot mentioned throughout this thesis) was briefly my UROP advisor many many years ago, and *also* showed me the best places to mountain bike in the Fells. He passed down a slightly peculiar way of designing in 2D-CAD using OMAX layout software that I still use to this day. Someday there might be enough people that use this technique to fill a car, or maybe even a small bus?

A big shout out to the MIT mountain biking team and the MIT Outing Club, and all of the wonderful people that I have met on fun outdoor adventures throughout my time at MIT. It has been inspiring to have been able to go on so many trips with people like Matt

and Eric Gilbertson, who showed me how one can efficiently integrate hiking adventures into international conference trips. I have spent more time out in the mountains during my PhD than might be considered reasonable, but this provided a solid counter-balance to the academic rigors and somehow always managed to put the stresses of campus into the proper context. (There were even a few times where I actually read the papers that I printed out and brought with me, while chilling in a hammock on top of a mountain!)

I would like to acknowledge all of the funding support that has allowed me to experience many different projects as well as have the freedom to work through many of my own ideas. My very first project grant, the summer Eloranta Fellowship from the MIT UROP office may not have been the largest, but it was well-timed and truly had a large impact by giving me the confidence to attempt to develop my own projects. Additionally, I am thankful for the rest of the funding that I have received over the years, including the funding provided by Boeing, the office of Naval Research through the NDSEG fellowship, Amazon Robotics, and from various NSF grants.

To my friend Peter Lu, I can't thank you enough for generously volunteering your time to act as an impromptu project manager to help keep me on track during the final months before my defense. It is easy as a graduate student to get a little bit too comfortable and distracted by always trying to always expand the scope of your project... Who knew that having someone hold you accountable for the deadlines you set for yourself and talking through the details can actually accelerate your progress?

I would also like to thank my high school physics teacher David Askey. Besides being an amazing physics teacher, Mr Askey also ran the Botball robotics team for my high school where I first realized that I have a passion for building robots. I spent countless hours after school building robots out of Lego and (mostly) staying out of trouble. I did not realize at the time how special the team and your class environment were, but it's very clear now how your influence helped me get to where I am now.

Finally I would like to thank my family. My parents, Janet and Bill, put the very first Lego blocks into my toddler hands many years ago and supported me unceasingly all the way since (including actually reading through a draft of this and helping with valuable proofreading - thanks Mom!). And my brother Robert who is always down for road trip and hiking adventures, and who demonstrates how one can teach themselves almost anything related to making things; I am constantly in awe of what you create in your garage shop. Last but certainly not least, I would like to thank my wonderful girlfriend Cathy Melnikow who has managed to put up with a lot during my PhD journey, and whose patience and support I am truly grateful for. You have put up with many things from long nights away in lab, to the metal chips on the floor of the apartment, to the endless frustrating shifting paper deadlines...and somehow you seem to be able to sleep through all of the strange whirring and clunking sounds the robots make while hopping around late at night. Whirrrr, plop, buzz... clunk clunk... (oopsies!)....thunk.

Contents

List of Figures

List of Tables

Chapter 1

Introduction: The world of Modular Structure Assembling Robots

Researchers have long envisioned large-scale self-assembling and reconfigureable robotic and industrial systems that can solve real-world challenges in a flexible and adaptable manner. Imagine an industrial set of Lego blocks controlled through a Minecraft-like software interface that can be configured to autonomously retool a factory overnight in response to supply disruptions. Each component of the factory would be a simple physical Lego-like block that contains specific mechanical functionalities which are periodically re-arranged by a group of small assembler robots to tailor the factory for each new task. In addition to enabling flexible factories, these systems might someday build structures in space or set up infrastructure in inaccessible locations on earth. Existing development towards this vision have been constrained to the laboratory due to various challenges left mostly unsolved by related work. These challenges include prohibitively high costs, a general lack of robustness, and limitations in performance metrics like stiffness, accuracy, strength, and speed when compared to task-optimized systems that do not incur the costs involved with implementing a modular framework.

Building large-scale modular systems is difficult for many reasons including both theoretical and practical concerns. Modular systems need a well-designed conceptual framework and set of specifications that allow the system to manage both low-level hardware challenges as well as challenges only encountered once the system scales to many modules. The same framework must be able to simultaneously solve challenges ranging from how the connector accurately aligns and hold parts to how thousands of nodes are able to effectively communicate and coordinate to accomplish tasks as a collective. Building these systems is also challenging for practical reasons including the high cost of prototyping due to the difficulties involved with obtaining custom specified industrial machinery in low unit quantities. However, the benefits these systems could bring through increased adaptability and flexibility make their pursuit interesting. Recent advancements in actuator, sensor, and fabrication technologies have started to make achieving this dream seem more realistic.

This thesis aims to contribute meaningful progress toward the grand vision of modular reconfigurable general purpose machines. The ultimate objective is to create a conceptual framework and a set of standardized specifications for crafting these modular industrial systems. The system developed in this work could directly apply to some general industrial

automation systems as well as light-duty machines like 3D printers and pick-and-place machines. However, extending the system to machining tasks like milling and turning will require new designs for the bearings, connectors, and actuators that are more optimized for high stiffness. Existing systems shown in related work have progressed different facets of this comprehensive vision. However, one of the most fundamental difficulties lies in reconciling a multitude of conflicting design requirements within the limited space dictated by the lattice unit cell boundaries. To bring clarity and direction to this work, the following set of concrete functional requirements serve as the goals guiding this work:

- The system should be capable of relocating modular components to any position within the work space, including the ability to create cantilevered structures in the presence of gravity.
- The system should be designed to create stable structures using high-strength reversible connectors that ensure predictable levels of stiffness at each connection point, as well as along the entire structural loop between the system's tooling and work-pieces.
- The connectors should be engineered to withstand occasional impacts, as well as unpredictable forces such as those due to dragging and sliding, and should self-align with a high area of acceptance while mainaining high levels of repeatability and accuracy.
- The system should have the ability to continuously and accurately assess the state of its own configuration (i.e., what modules are attached to each other), for example by reading identification markers on each modular connector.
- Some of the actuators that power movements in the system should be *deeply* modular, and be able to be combined in order to extend the range of motion and force capability.
- The system should be able to identify and apply the suitable primitive motion algorithms in the context of the locally available parts to create the newly specified system configurations.

1.1 Challenges of Modularity

While films such as Big Hero 6 may give the impression that creating a modular system matching these proposed functional requirements is a straightforward task, the reality is quite different. Crafting such systems presents numerous formidable challenges. While the advantages that modularity brings — like flexibility, repairability, adaptability, and robustness — are substantial, they are hard to clearly describe, let alone quantify. Conversely, the downsides are quite tangible, encapsulated by the term the *Curse of Modularity*. This concept relates to the tendency for specific systems built around modular architectures to perform poorly on metrics like speed, stiffness, and overall performance while also costing more than an equivalent single purpose built machine. The primary reason for this curse is that all of the connectors and other modular hardware that are not involved in the functional operation of the machine are effectively expensive dead weight.

Take, for instance, a hypothetical car constructed from 1,000 modular components, each connected by modular robot style connectors. Such a vehicle would likely be heavier, costlier, less reliable, and slower than its traditionally fabricated counterpart, which would make for a tough sell to the average car buyer. A few of the benefits that this hypothetical modular car might bring - like the ability to temporarily expand a small trunk after a trip to the grocery store, or to easily upgrade its parts and quickly repair damage are interesting. However, neither these miscellaneous benefits nor the fact that the pieces of the car could transform into a small factory will be enough to convince the average car buyer to pay a (likely large) premium to purchase it. However, for a small factory owner, the ability to quickly re-arrange and upgrade their machines, to reuse older parts and quickly repair damaged components might be worth an extra initial cost - plus the parts might be able to turn into a car when business is slow! While this thesis will not attempt to quantify the merits of modular machines, the prevalence of modularity in various complex systems—from biological organisms to software frameworks and advanced microchips—suggests its potential value.

The connector serves as the linchpin of any modular system and epitomizes many of the associated challenges. Each connector must not only provide a secure, accurate, high-strength structural bond, but also facilitate electrical connections, possibly sense and interact with the external environment, and read and display information about itself to adjacent connectors. Moreover, it must accomplish these tasks within confined spatial limitations. For example, up to six connectors may need to fit within a single standard cubic lattice cell, while also allowing room for other crucial system components like actuators, sensors, and mechanical structure. This becomes particularly complex from a physical standpoint, as unlike a software API, which can virtually 'expand' as needed, these connectors are restricted by actual, finite physical dimensions.

As this thesis will further explore, simply enlarging the lattice cell to better accommodate more features is enticing, but brings its own set of problems. Larger lattice cells require an increase in the size of other elements including the actuators, and therefore also increase the cost and weight and complexity. The design requirements for modular systems encourages high density of functionality, and the metrics that should attempt to be met include stiffness, connector strength and power divided by the lattice cell size. An additional complication, as demonstrated by the struggles with backwards compatibility in physical connector standards like USB, is that once a system interface is defined and widely used, it is difficult to make changes to the parameters of the system without defining an entirely new system. The nature of this problem suggests that for a system to become widely used, the system has to be designed 'correctly' from the start, which ends as circular logic conundrum that discourages further system development.

Even if a mythical 'perfect connector' could be created that meets all of the necessary design requirements while having zero mass and volume, modular robotically assembled lattice systems still would face significant challenges related to the actual act of assembly. Assembly of anything, in all but the most perfectly controlled environment, is inherently a difficult task. Assembly requires repeated unpredictable contact between objects of varying sizes, shapes and material compositions. Additionally, there needs to be enough robots in the right places at the right times to actually perform the assembly tasks. Suitable algorithms to reliably implement the necessary reconfiguration sequences are also necessary and face

their own challenges. Detecting errors and misalignment further increases the difficulty for larger autonomous system that reconfigure themselves, as having a human in the loop can solve many unexpected edge-case problems that could cause disaster in fully autonomous systems.

Until recently, most of the robotics community has focused on avoiding contact wherever possible by implementing carefully calculated collision-free trajectories paired with stiff high-gain position-controlled actuators. While this approach works well in engineered environments like automobile factories, it is not realistic or safe for many other applications, especially those involving assembly tasks or environments where humans are present. Many of the same contact and impact challenges inherent in assembling objects also affect the task of legged robot locomotion. Recent work developing more effective actuator designs for legged robot locomotion mostly focused on low-gear-ratio proprioceptive actuators perhaps hint at the direction that the modular robot community should take.

However, simply adapting the quasi-direct-drive proprioceptive actuators from these systems to modular assembly robots is difficult because of the constrained physical dimensions of lattice based systems. Decisions need to be made about what size and kinematic structure assembly robots should have that best optimizes for factors such as assembly time, total energy expenditure, and reliability and robustness. Most modular lattice systems use some form of magnetic connection to align modules into place, and this presents a unique set of requirements on the actuators. High short-duration forces are required during the connection and disconnection from the lattice, interspersed with more gentle force-sensitive motions while moving the modules through open air. There are likely new mechanisms and designs for actuators that are yet to be developed that are even better optimized to match these unique requirements than electric motor based proprioceptive actuators, but they are a good starting point.

1.2 Modular System Metrics: Benchmarking Progress

As modular assembly systems transition from laboratory-scale prototypes to configurations encompassing hundreds or thousands of modules, they are likely to encounter novel sets of challenges not faced by prototype systems. While existing work has included many clever designs and impressive demonstrations, little attention has been dedicated to these future challenges. Looking into the future we believe that the following challenges will increasingly dominate the design requirements for useful large-scale self-assembling systems:

- Energy *efficiency* of the reconfiguration motions.
- *Repeatability* and accuracy of the structures built from modular components.
- *Affordability* and ease of manufacturing of the hardware.

In many of the impressive simulations and hardware systems shown in related work that involve robots assembling structures, the expenditure of energy is not often an important consideration. Since it is difficult to compare the energy use for existing systems due to the lack of published data, this thesis will present and discuss in Section 7.2 a new metric

called the *Lattice Assembly Efficiency Factor* that is similar to the existing cost of transport metric. This new metric aims to create a single number that is roughly representative of the amount of energy require to move a modular element along a 3D path through a lattice normalized to the payload weight and lattice cell dimension. While energy use is not that important when the number of reconfiguration steps in a system is small, or when the robots are powered externally (as is the case with many of the systems found in related work), its importance will grow as systems scale. Assembling structures with even hundreds of components will involve *thousands* of individual movements, resulting in significant exponentially increasing energy expenditures. Additionally, one of the fundamental factors limiting the *rate* of movement for traditional robotic systems are limitations on the allowable *power* of heat related losses generated during motion. This implies that energy efficient systems are also likely to ultimately be faster than inefficient systems. This thesis will make an argument in Chapter 6 that using quasi-direct-drive actuators to power the assembly robots is the clearest path towards fast and efficient lattice assembly robots.

One of the primary disadvantages that modular machines have compared to monolithic systems is the inaccuracies in the positioning of the final configuration due to the cumulative nature of the positional errors introduced through the connectors in the system. For machines such as CNC machines built with a monolithic frame (i.e., single welded structure or machined metal frame), relative accuracy only depends on the physical loads and thermal distortions encountered during operation, for which many existing compensation strategies exist. However, even in a relatively simple modular structure, the errors introduced from the connectors are often so significant that accurate operation can only be accomplished with extensive error mapping and calibration every time the configuration changes. A requirement for constant calibration would make real-world use of modular systems for tasks requiring high levels of precision intractable. This thesis investigates in Chapter 4 how kinematic couplings have the ability to create highly repeatable modular robot connectors while retaining a large connector *area of acceptance* and therefore ease of forming new connections. While kinematic couplings are already in use in various industrial settings, this work focuses on the design of one suitable to the specific requirements of lattice modular robots. In order to evaluate this claim we present a metric called the *Lattice Repeatability Factor* (LRF) in Section 4.4, which aims to provide a single number encapsulating the likely final positional errors for a 3D structure connected by modular connectors.

The final challenge is that of affordability or that of cost per unit of performance. Due to the nature of small-scale prototyping and the constraints and peculiarities of academia, cost considerations have been neglected in much of the related work. As an example, the 3D M-Blocks which were the basis of much of this thesis and are summarized in [1] and discussed in Section 2.5, cost somewhere on the order of $1000 dollars per 50 mm lattice sized module for a small set of prototypes. This results in a theoretical cost of eight *million* dollars for the 8,000 robots needed to fill a cubic meter volume, which clearly dramatically limits their practicality. While in practice this cost would come down substantially if they were able to be mass produced in quantities of millions of units, having millions of independent modules each with its own batteries, actuators, and control electronics will still likely be orders of magnitude more expensive than structures built out of simpler passive modules.

In many modular self-reconfigurable robots (MSRR) each module includes a full system including control circuitry, actuator(s), and batteries. Realizing the poor scalability of such

systems, many researchers are moving towards heterogeneous systems which split up the assembly operations from the modules forming the structure. These systems, which are alternatively called *digital materials* or robotically assembled structures involve a small set of assembler robots rearranging simple mostly-passive components to form structures and machines. This approach is analogous to a child (the assembly robots) assembling structures out of Lego (the digital materials) as opposed to the MSRR approach where the Lego blocks are able to magically assemble themselves on their own. This thesis doesn't included a detailed cost estimate due to the same problems discussed in related work, as well as the fact that most of the hardware was artisanally hand-assembled and machined in the CSAIL machine shop. However, many of the designs presented throughout the thesis focus on simplicity and cost-effective manufacturing strategies both due to necessity, as well as a desire to simplify the path to potentially moving towards large scale production in the future.

1.3 Modularity and Abstraction as a Solution to Complexity

The interrelated concepts of modularity and abstraction provide the foundation for entire fields of engineering, and are integral to the existence of many of our complex modern engineered systems. Abstraction of specific implementation details through a modular interface allow for quicker iteration of combinations of the lower level system building blocks, as well as embedding and preserving expertise and best practices. A particularly literal form of this concept seen in modular robotic systems is the concept of *metamodules*, which refers to a group of modules that coordinate to perform useful functions like creating a robotic arm to help move other modules around a structure. Similarly the ability for modern software engineering to create programs with millions of lines of code that generally work would be impossible if there were not extensive levels of abstraction built into the code and its libraries. Additional levels of abstraction can be found in software systems down through the languages and compilers, all the way to the layers of abstracted transistors on which the software runs. It is perhaps understandable due to the practical realities of developing hardware that physical machines have fewer, and less well codified and developed levels of abstraction and modular interfaces than are found in software systems. It is much less costly to modify a piece of software by adding a new API on top of existing functions than it would be to perform an analogous action on a physical systems, such as to attach a new axis to a CNC machine.

In light of the many fundamental limitations related to modular hardware there is certainly no clear answer to the challenge of how to balance any specific system between the flexibility allowed by modularity and the performance optimization possible through fixed-use designs. Many of the drawbacks inherent in over-optimized fixed-use systems are only apparent during rare events like supply chain disruptions or over long time horizons like maintenance and repairability. The short time horizon lens that industry commonly views the world might not properly value the benefits that are possible through modular systems. Whatever the reasons, deeply modular human-engineered *physical* systems are rare, and are

perhaps most commonly encountered as toys. Once a successful design for a product or device has been created, it is often subsequently improved upon, and refined along a somewhat linear path, with all parts not integral to its primary function optimized away in pursuit of cost savings. As future derivative designs are created, complexity accumulates as industries and supply chains develop around the particularities of each product and different aspects are refined, upgraded and extended. In some cases the accumulated costs of this complexity becomes so great that it forces industries to work to create a modular interface abstraction layer that allows for new types of potential design combinations. This often results in moving the focus for the new development up a level in abstraction, thereby enabling new more powerful capabilities. I believe that such a transition is due to happen for industrial machines at some point, although exactly when, how or why is up to researchers and engineers, but considering a few examples from other fields provides inspiration.

It can be argued that many industries have followed this general trajectory of being forced to develop modular interfaces as a response to increasing complexity. The computer industry, and now increasingly the high performance semi-conductor industry have undergone such transitions. Once the design of analog electronic circuits was standardized and embedded into chips, less effort was put into their continued development, and the industry with the exception of the cutting-edge in terms of performance or cost-efficiency moved on to solving more complex problems. A similar illuminating example of this transition is happening right now with high-performance semi-conductors.

Chiplets [2], which are an interface for creating high-end semiconductors out of modular tiles instead of the previous monolithic approach, and are a case study in the trade-offs involved with modular architectures. The semiconductor industry used to have a large number of manufacturers each making roughly equivalent chips, all using what is termed a *monolithic* approach where the circuitry is etched into a single piece of silicon. However, as the complexity of the manufacturing and design tools increased, at some point after 2010 it reached the point that only a small number of companies remained that could make any claim to be at the leading-edge of either design or manufacturing.

New leading semiconductor fabrication facilities cost on the order of *tens* of *billions* of dollars and the cost of simply *verifying* new designs, excluding the cost of the actual design itself, at leading edge nodes has been estimated to approach 1.5 billion dollars [2]. Not only has this made it difficult for niche companies to design or make new chips, but it has caused the leading companies to struggle for both cost and timeline related reasons. For monolithic designs, *all* of the components, (e.g., for a CPU this includes high bandwidth memory, logic, iGPU, etc.) are on the same physical piece of silicon which has to be manufactured and verified using the newest process node for all of these components at once. This adds unnecessary design and verification complexity, and wastes resources, since some of the components, for example some types of memory, do not gain much from the switch to a newer node, but are forced to come along for the ride anyway.

The solution to this problem that the industry is now currently in the midst of realizing is to (you might have guessed it!) create a new modular interface layer and an abstract interface to allow for what is either termed chiplets, or 'disaggregated' designs for semiconductors. By developing chiplets, manufacturers and designers are able to capture some of the many benefits brought by a modular architecture. This transition will help to increase the rate of new design iteration and verification through the ability to more effectively reuse

and repurpose design blocks and through manufacturing efficiencies brought by the ability to combine silicon manufactured on different processes into a single device. Chiplets are basically little cut-up parts of silicon that are connected to each other through what is effectively an ultra-high-performance circuit board called a silicon interposer. A disaggregated CPU is able to use chiplets from different manufacturers and process nodes all combined into a single package. This allows for only the parts (i.e., logic cores) that really *need* the new cutting-edge process nodes to be manufactured in the high-end fabs, while the other parts can be fabricated by older nodes. This solution has involved immense engineering costs, and has introduced significant trade-offs in terms of performance and overall system complexity. However, almost all of the leading semiconductor companies have embraced chiplets, and now many of the newest highest performance chips are created this way. This transition has helped to invigorate the industry, and will allow small hyper-specialized companies and groups of people to focus on one part that can then be packaged with and interface directly to the other chips.

The progression up the complexity-hierarchy as designs mature is a concept resonating with many in the modular robotics community. This idea is notably discussed in a conversation between Neil Gershenfeld, who advises the researchers creating the Bill-E family of robots discussed further in Section 2.3, and Lex Fridman [3]. In this podcast, Gershenfeld illustrates how biology embodies the essence of modularity and abstraction. Every protein is constructed from diverse configurations of approximately 20 fundamental building blocks. As cells evolved, their development wasn't just about increasing in size. Instead, they integrated as modular units with other evolved counterparts, forming higher-level organizational structures. These structures, harnessing the intricate complexity of their individual components, can achieve significantly more than isolated cells. This modular progression is evident up the entire chain from amino acids, proteins, DNA, organelles, cells, tissues, organs, etc. Creating intricate designs like humans, would be challenging without the distinct boundaries between these layers, and the flexibility to rearrange these foundational units to conceive new designs. Throughout this thesis, I aim to transpose these principles to industrial machinery, believing that machines can reap benefits analogous to those seen in biology, software, or chiplets through an intentional embrace of modularity and abstraction.

1.4 Economics of Reconfigurable Machines

Once the initial costs of setting up a modular system are covered, these systems offer compelling economic advantages. They allow for parts to be reused and interchanged, enabling a limited capital investment in modular units to achieve a diverse range of functionalities. However, it's worth noting that they can't perform all functions simultaneously, which is a crucial trade-off. A common example of this is general-purpose computers. We don't use separate computers for emailing, viewing cat pictures, etc. Instead, we rely on one device that can switch its functionality almost instantly to adapt to each new task. Below are some of the potential economic benefits that modular industrial machines could introduce to industry:

- **Reuse**: Salvaging functional parts from outdated or retired machines can reduce the need to spend on new equipment.

- **Repair and Upgrade**: Enhancing the ability to quickly and seamlessly repair or upgrade specific components in machines can boost operational times and decrease maintenance expenses, especially over the longer term as specialized spare parts become more difficult to source.
- **Adaptability**: Boosting the flexibility of industrial tools to adapt to shifting demands can yield higher profits, especially during market shortfalls and disturbances, like the 2020 global pandemic.
- **Quality over Quantity**: By being able to swap expensive rarely-used parts between multiple machines, it becomes more feasible to invest in higher-quality, more efficient, and dependable components, since their high cost can be amortized over more uses.
- **Standardization**: Greater standardization facilitates faster expansion and scaling of promising new manufacturing designs, given the readily available pool of compatible components.

When manufacturing industrial equipment, costly components with specialized and optimized designs are often utilized. Consider a high-stiffness linear stage, such as one found in a waterjet machine, equipped with precision components like linear bearings and ball screws. If there is a subsequent need for a gantry machine to test medical devices instead of waterjets, these precision components can't be effectively repurposed. This is in some ways a fundamental problem, as the more each machine is optimized for cost and function, the more specific and tightly integrated these components are likely to be. Although industries do reuse and re-purpose equipment to some extent, the construction methodology of machines, particularly high-end ones, tends to render component re-purposing impractical. The extensive availability of industrial components available on platforms like Ebay, seemingly extracted from old machines and sold at a fraction of their original price, underscores this issue.

The heightened retooling speed and adaptability in reconfigurable factories can offer advantages while concurrently mitigating the impact of market fluctuations. For instance, had the factories producing office furniture been swiftly reconfigured to manufacture medical testing equipment and ventilators, the upheaval during the 2020 COVID pandemic might have been less severe. It's crucial not to overemphasize this argument to the point of imagining that *everything* should interlock like Lego bricks, which isn't realistic. Yet, it seems our society has chosen to ignore the potential risks of relying solely on the ongoing trend of globalization, specialization, and economies of scale. I believe that a renewed focus on resiliency and adaptability of our manufacturing equipment, even with an increase in cost, will eventually be forced upon us whether we have prepared or not.

1.5 Thesis Contributions

While many of the aspects of this system are directly inspired and borrowed from existing research, this section provides a concise listing of the specific novel contributions presented in this thesis, organized by the categories of Devices, Algorithms and Systems and Applications.

1.5.1 Mechanism and Devices Contributions

The core focus of this work has been on developing new mechanical designs that help to solve existing gaps in the related work literature that concern modular robotically assembled structures. This thesis contributes the following four mechanical designs:

1. The mechanical design of a deeply **modular linear actuator** based on a modified magnetic lead screw power transmission is detailed in Chapter 5. Most traditional power transmission elements like belts and lead and ball screws are not able to be combined end-to-end in a modular way. However, magnetic power transmissions are amenable to this task as their 'gear teeth' are able to gracefully attach, detach and transition between different parts. This contribution includes two parts that together are called the MagnaCarta system; *carts* are active robotic modules that move along passive *tracks*.

2. The design for a new **modular connector** based on kinematic couplings which provide a high area of acceptance as well as high accuracy, two design requirements which usually conflict. This is presented in Chapter 4.

3. The mechanical design for a novel **automatic self-bolting connector** is introduced and characterized. This mechanism is potentially the first MSRR self-bolting connector that is non-gendered while also able being able support the weight of hundreds of modules.

4. The design of Belty, a new relative lattice traversing **assembler robot**. This robot uses similar proprioceptive actuators as the MIT Mini Cheetah, and has by far the highest power for any single-axis of any lattice-assembler robot presented to date in the modular robotics community that we are aware of with the exception of NASA's SOLL-E [4]. This high power-to-weight ratio allows for high-speed lattice movements and assembly operations, and also allows for dynamic motions like hopping while carrying modular elements.

1.5.2 Algorithm Contributions

There has been extensive existing work relating to high level control for modular robotic assembly systems, and the algorithmic contributions presented in this work are more focused on lower-level hardware-specific algorithms. These specific algorithmic contributions include:

5. Algorithms that allow robots like Belty to traverse a lattice, to rearrange blocks, and to pass parts between different robots.

6. The development of a practical algorithm to allow for an assembler robot to carry a module and move through hopping.

7. Algorithms for rearranging modular linear actuators using the trackbot meta-module are presented in Chapter 7 based on work with Jim Bern [5].

8. An algorithm for assembling linear cantilevered beams out of structural blocks using both a single and dual-assembler teams of robots is presented and discussed.

1.5.3 System and Application Contributions

All of the algorithms and designs presented here are components that work together in a larger modular machine system. In the context of this larger system the following system contributions are presented:

8. A new comparison metric, termed the 'Lattice Assembly Efficiency Factor', in Section 7.2 aims to benchmark the efficiency of reconfiguration normalized against the size and weight of the lattice cells.

9. A second comparison metric called the 'Lattice Repeatability Factor' is introduced in Section 4.4 which is intended to compare assembly systems in regards to the accuracy and repeatability of the structures that they create.

10. System experiments using a mostly fully-functioning proof of concept system which is able to implement the algorithmic contributions while being evaluated on the two new metrics are presented in Chapter 8. These experiments involve coordinate between multiple robots which communicate through a distributed CAN bus network.

1.6 Thesis Outline

The remainder of this thesis is organized as follows. Chapter 2 provides a discussion of selected related works. Topics from related work include a discussion of modular self-reconfigurable robots, connector mechanisms and modular linear actuators and digital materials. Chapter 3 provides an overview of the experimental hardware system built as part of this thesis, as well as describing some of the important concepts like metamodules. Details regarding the overall system including the systems for communication between modules and broad categories of modules are presented.

Chapter 4 introduces the design and characterization details for a new modular robotic connector. A new 100 mm connector designed around a preloaded kinematic coupling and a non-gendered automatic bolting mechanism are discussed. Designs and experiments relating to various connector systems including the electrical power and ID detection systems, as well as experimental disconnection stiffness data are discussed. Chapter 5 introduces the second significant design project in this thesis which is a modular linear actuator based on magnetic lead screws. This chapter includes discussion regarding modular linear actuators in related work and the fundamental challenges involved with creating them. The design for the two primary parts of a new linear modular system: BLDC motor driven carts, and passive tracks are presented. Chapter 6 starts with a discussion of propriocptive actuators in robotics before introducing the design of a simple lattice assembler robot using proprioceptive actuators which is named Belty. This chapter covers the mechanical design of Belty which has three actuated degrees of freedom and uses large-diameter brushless motors paired with belt transmissions.

Motion algorithms and associated experimental data and are presented in Chapter 7. Details are provided for lattice reconfiguration moves including those integrating the system dynamics like hopping. Chapter 8 shows examples for systems integrating multiple modular

robots together. Tasks attempted include precisely relocating passive modules, relocating a track component from the modular linear actuator, creating a simple 2-axis gantry machine, and building a simple bridge. Chapter 9 will conclude the thesis with a focus on future work, lessons learned, and overall discussion regarding future paths to creating more effective systems.

Chapter 2

Related Work

This chapter will provide an overview of several broad categories of related work and attempt to make groupings and comparisons among them to give context to the new work presented in this thesis. It is difficult to be precise with the terminology regarding relevant related work since various systems attempt to solve different goals and are described using different language and labels. This chapter will begin by discussing the overlapping concepts of modular self-reconfigurable robotics (MSRR) and relative robots in Section 2.1. Next, Section 2.3 will discuss the concept of digital materials and list and compare several select systems which have the most similar system goals, functionality and architecture to the FrFlFuFa system. Next, in Section 2.4, we will discuss a few concepts for modular industrial systems, and modularity in machine tools more broadly. The chapter will conclude with a discussion of the M-Blocks robots in the context of these ideas in Section 2.5, of which the FrFlFuFa system is a descendant.

2.1 Modular Self-Reconfigurable and Relative Robots

Modular self-reconfigurable self-assembling machines are a promising class of systems which can adapt their shape and configuration by rearranging their internal structure of Lego-block like modules. Ultimately the goal of the research community is to create functional systems that will accomplish useful tasks, although as a whole the field is far from achieving this goal. In the short term a number of potential applications where self-assembling machines could prove useful exist, often focused on applications that have a high density of expensive similar sized components that sometimes benefit from rearrangement. One of the most relevant targeted application areas is re-configurable space systems [6] as well as to a lesser extent adaptive manufacturing applications. Additionally several other applications like educational toys and reconfigurable furniture [7], [8] have been proposed.

While an exact categorization is elusive, MSRR systems in general include those that have an ability to reconfigure their internal structure to match to different tasks. In practice this usually includes some type of modular connector, and some form of regular lattice or grid, as well as a method to move modules relative to each other. Many systems have been proposed throughout the last 30+ years in the MSRR field, with this seminal article [9] providing a comprehensive summary of this work up to 2007. Several more recent survey

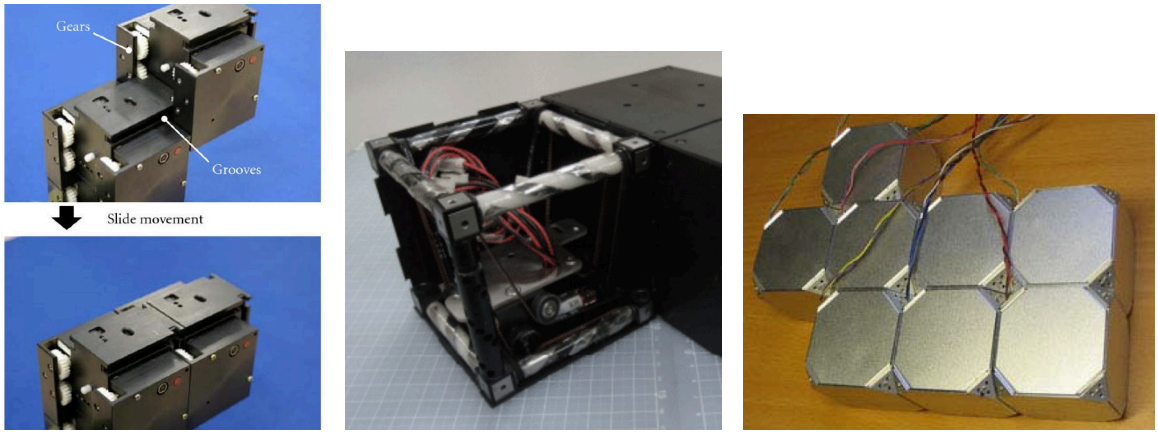

(a) (b) (c)

Figure 2.1: Selected modular linear actuators seen in MSRR related work. While the majority of MSRR systems use rotating joints more akin to little robotic arms, here we highlight several MSRR systems that use extendable linear motion to reconfigure. Modular linear actuators are challenging for several reasons, including aligning the linear bearing systems and managing the power transmission through the gap between modules. These systems include: (a) the Chobie system [13] which uses a rack and pinion to slide modules along each other, (b) a robot module using helically magnetized axes [14], and (c) the EM-Cubes [15] that uses switchable electromagnetic coils to act as a modular linear motor.

articles include [10] in 2017 and [11] which focuses on the hardware systems, as well as [12] in 2013 which provides an overview of algorithmic developments. However, few if any of these systems have demonstrated an ability to accomplish tasks beyond the laboratory, and there has been little progress developing standardized specifications that might allow for collaboration between different robots built by different groups of researchers.

While there is a large body of previous work regarding modular self-reconfigurable robotic systems, several aspects of the design space are holding back the effectiveness of existing systems. This thesis aims to generate progress towards these areas. The first focus area is actuation, or the mechanism used for generation of relative movements to rearrange the modules in the system. While many real-world machines use linear actuators to generate motion, designing high-performance modular linear actuators has proven to be difficult. Few existing modular robotic systems use linear actuation, with most using rotating joints similar to simple self-contained robot arms to latch onto and move other modules around.

Among the many fundamentally unique, creative and interesting technical approaches which have been developed in pursuit of robotic self-reconfiguration, there have been several designs incorporating linear motion. Several systems, including the EM-Cubes [15] and modular conveyors [16] have used or proposed to use arrays of electromagnets and permanent magnets to generate relative linear motion between modules, essentially acting as modular linear motors. While these approaches can move very quickly and require no moving components, they have a limited actuation force due to their low specific force which is a consequence of not having a mechanical transmission. Additional examples of modular linear actuation include a modular rack and pinion system shown by the robot Chobie [13]

presented in 2007, and show in Figure 2.1a. A system presented in 2017 and shown in Figure 2.1b uses helically magnetized rotating actuators [14] to slide modules relative to each other. While this is approach is novel and interesting the configuration of the magnets limits the maximum actuation force due to a large magnetic air gap.

In addition to developing new hardware, many works have focused on simulation, and on the challenge of controlling thousands or millions of independent agents to efficiently collaborate. Simulated algorithms and control hierarchies have been presented which accomplish distributed behaviors, e.g., [17]–[19], however most of these works abstract away various challenges that real-world applications face. Some examples of the significant challenges often sidestepped by simulations include ignoring the necessary torque and forces involved with lifting groups of modules and mechanical difficulties like binding caused by elastic structural deformation as well as error stack-up inevitable in large structures. There have been several works which present decentralized algorithms operating on actual hardware, including the UBot [20], the ATRON system [21], and several others, e.g., [22], [23]. However, few of these systems provide a clear path to being able to reconfigure according to a generalized 3D movement framework, which limits the future scalability of these systems.

2.2 Connectors in Modular Robots

Virtually every MSRR or digital material system presented in related work has a unique bespoke connector which allows modular elements to be attached and disconnected to form different structures. Despite a lack of compatibility between these different connectors, they aim to solve generally the same set of problems, and often use similar methods to do so. The following is a short summary of several of the key functional topics that these connectors are designed to solve drawn from the related work in general, and also guided from connector focused papers including [24].

These functionalities can be broken up into the four following areas:

1. Mechanical lattice attachment and alignment system: Section 2.2.1
2. Electrical communication and power distribution system: Section 2.2.2
3. Configuration identification system: Section 2.2.3
4. Temporary controllable mechanical gripping mechanisms: Section 2.2.4

Since the connector in a modular systems is the primary interface through which it is reconfigured, its importance cannot be overstated. Many attempts to 'solve' the connector problem have been presented, and there is a fascinating array of designs and technologies that have been published. The modular connector has been one of the most well-developed and studied areas of MSRR and digital materials research, with the following papers providing excellent overviews to the topic [25], [26]. However, despite this large body of work few if any of the existing connectors are suitable for creating practical modular industrial machines. In general the aspects of these connectors that need more development include improving their strength, robustness, mechanical accuracy and affordability.

2.2.1 Mechanical Lattice Attachment and Alignment Systems

A fundamental requirement for a lattice-based modular robot system is the presence of a repetitive structure with specific locations designated for mechanical connectors. Most systems use a simple cubic lattice, but alternatives exist, for example the cuboct lattice (i.e., cuboctahedron lattice) which 'is composed of vertex connected octahedrons' and is used in the Bill-E [27] system and derivatives like Solle-E [4]. The majority of systems that use permanent magnets, including Bill-E, the M-Blocks and Roombots Extended [8], use eight circular permanent magnets arranged in a four way symmetric pattern. This basic magnetic connector approach has the benefits of automatic and simple alignment, but has the significant downside that the energy stored by magnetic field must be overcome for every movement. Some systems like the M-Tran robots [28] and also the preceding Robot Molecule [29] avoid magnets altogether, and instead have an active mechanism with little arms that reach out and align and hook on to each connector during a connection, and then retract to disconnect. Mechanical approaches like this are enticing and avoid the burden of breaking the magnetic bonds during every move, but are mechanically and electrically complex, and lack the robustness and simplicity provided by permanent magnets.

Some systems, including the Electrovoxels [30], use electromagnets instead of permanent magnets in order to be able to 'turn off' the connector when desired. However these are not practical for a system with heavy modules due to the heat generated from the constant current required to drive the coils. An intriguing technology that appears to offer a perfect balance between permanent and electromagnets is a device creatively called an electro-permanant magnet (EPM), as described in detail by Marchese et al. in [31], and in [32]. These devices use a type of magnet called AlNiCo, which can be switched 'on' and 'off' while in the presence of a temporarily high magnetic field generated through a pulse of current flowing through a coil. Systems including the robot pebbles [33] and the SMORES robots [34] use EPMs, but EPMs have proven to be difficult to manufacture at scale, and require relatively sophisticated electronics in order to operate, which has limited their use.

2.2.2 Communication and Electrical Power Distribution Systems

While some systems rely solely on wireless or optical systems for communications, old fashioned physically touching metal connections have many advantages. Systems such as the most recent variants of the Bill-E [35] system use simple commercial off-the-shelf spring loaded connector arrays, and many others use off-the- shelf pogo-pin style electrical connectors. While this style of connector is readily available and easy to integrated into standard printed circuit boards, these components may have problems with robustness, and would likely fail the *hammer test* described in Section 4.2.

Power sharing has long been a goal for MSRR systems but it has practical challenges that prevent its widespread adoption. This paper [36] provides an overview of some of the challenges involved with sharing power between modular robots. One of the fundamental challenges is that in order to share power the bus voltage must be exposed, and in most implementations, at least one of the connector contacts needs to extend beyond the lattice cell boundary. Exposed potentially high-voltage electrical contacts risk the danger of a short circuit destroying either the internal power path, or any other external electrical system that

Table 2.1: Comparison of attributes for several tagging technologies utilized by MSRR systems in order to determine the configuration of assemblies of modules. This table is lightly edited from its original appearance in [39].

	RFID/NFC	Optical	Electrical	QR Codes	Inductive
Information Medium	Radio waves	Light or IR	electric	Light	magnetic
Tag cost	inexpensive	moderate	inexpensive	inexpensive	moderate
Reader cost	expensive	moderate	moderate	expensive	moderate
Passive	yes	no	possible	yes	difficult
2-Way Comms	possible	yes	yes	no	yes
Orientation	needs 2+ tags	possible	possible	yes	possible
Systems	[40]	CK-Bot [37]	Soldercubes[24], [42] UBot [41]		SMORES [34], Catoms [43]
Range	0-2 m	variable	0 m	0.01 - 1+ m	0-10 mm

it comes in contact with. There are several electrical methods that can help to mitigate these risks, with further discussion of this topic in Section 4.10, but making a truly robust power sharing system will likely take significant engineering efforts and entail non-trivial component costs.

2.2.3 Configuration Identification System

For effective self-assembly and reconfiguration, the system benefits from a mechanism that robustly identifies the location and orientation of each module's connections. This system should ideally be passive and inexpensive while reliably storing millions of unique identification tags. Active solutions like infrared LEDs, as seen in modular systems like [28] require every connector to be powered in order for modules to be identified, which is impractical for systems that aim to construct structures out of passive blocks. Many of the modular robotic systems proposed to date have either built very limited and error prone methods for solving the configuration detection problem, or have omitted implementation of such a system entirely. Any *connection* between modules in a modular system involves a minimum of three unique parameters (1) some form of identity or *ID* of the two modules in question, (2) the connector, or *face number* for each of the modules, and (3) the *orientation* of the connection, which in a cubic lattice is one of four possible 90-degree values. Much of the algorithmic work which concerns configuration discovery (e.g., [37] and [38]), assumes that this information is accurately determined. However, these works focus on the algorithmic challenges, abstracting away some of the details involved with implementing the algorithms on actual robots.

Connectors have been used in the literature to enable inter-module communication [44],

[34], and determine the presence and relative orientation of adjacent modules. However many of the solutions for gathering presence and orientation information in MSRR require active communication between two robots, e.g., the inductive links in the SMORES [34] and CATOMS [43] systems or IR optical links used in many of the early MSRR, including MTRAN [45]. An ideal neighbor detector works passively, essentially acting like a barcode paired with a scanner. This would increase the robustness and scalability of the modular system, since it would allow passive elements to interact with active elements. There is a rich potential array of technologies which might be used to implement neighbor detection mechanisms, several of which are summarized in Table 2.1.

While there are many potential solutions for neighbor detection that allow passive identification of modules, few of these are practical for MSRR systems. RFID and NFC tags are two of the more promising technologies, and are prevalent in robotics research, including in several fields related to MSRR (e.g., [46]). However, due to the size and cost of the reader electronics, without appreciable engineering labor, these methods are currently impractical for MSRR systems with small characteristic dimensions. NFC is a technology related to RFID that looks promising for this type of application, but it remains a proprietary standard, and is not easily accessible at the present time. Additional passive methods, such as QR tags or APRIL Tags [47] are effective in other fields of robotics, but require the use of a camera and sophisticated image processing techniques which at the moment are impractical to include in every active connector of a MSRR system. An interesting recent work [48], presents a system which uses an array of 42 Hall effect three-axis sensors and sensor fusion algorithms to detect the positions of a free-form spherical system, and this approach shares some similarities with the approach presented in Section 4.11. While there are many potential ways to passively embed information into connectors, the key features to consider include how to minimize the size and cost of the readers and tags, as well as how to guarantee detection even when there are misalignments between modules.

2.2.4 Mechanical Latching Mechanisms

In order to create systems which are useful and practical in the real world, a big challenge is to develop a method to *semi-permanently* attach modules together in order to form a true structural interface, defined as a connection that can transmit forces and torques while having a consistent stiffness and mechanical repeatability [49]. There has been an incredible diversity of different strategies to achieve this goal in related work. This section will further discuss connection mechanisms that most closely achieve proper structural interfaces, including those based on screw and screw-like mechanisms and those that involve various forms of welding-like behavior. There are several other types of latching methods worth noting that are not covered here in depth, including electrostatic forces [50], and fluid pressure [51].

Bolted connections are one of the primary methods for forming structural interfaces in the traditional machinery and non-modular robotics worlds. Bolts have many advantages:

1. Bolts generate high forces for a small input of power and torque required to tighten them and do not take up much volume.

2. They are universally standardized and are readily available commercially, and custom versions are easy to manufacture.

3. They only require energy input during connection and disconnection, and hold the connection with the full strength at all other times.

4. They are relatively mechanically robust, with the exception of the exact moment right before disconnection or connection.

In light of all of these advantages, it is curious that most modular lattice systems do not use bolts as their primary attachment mechanism. One reason is the challenges involved with automating the bolting operation itself, which is further discussed in Section 4.8. In addition to the auto bolting mechanism seen on automated collet changers in CNC mills, some robotic systems do use bolted connections. One such system is the SMAC modular system presented in [52]. This system uses a small spring loaded thread centered in the cubic blocks faces which can attach to blocks which have an exposed threaded connector. However there aren't many details presented about this mechanism. It seems it is a gendered mechanism, which limits its utility. The modular gantry system presented in [53] also includes a spring-loaded threaded mechanism in its Figure 19 that also appears to be gendered.

Many connectors are 'screw-like' but do not use traditional threaded fasteners. These designs include connectors like the worm-gear driven RoGenSiD connector [54], which has four widely spaced metal teeth that act as inclined planes in the same way as a screw. Additional connectors like the open-hardware RoFICoM [55] is able to retract the inclined planes behind the connection plane. Screw-like connectors are interesting and have advantages over traditional fasteners such as the ability to use the center of the connector (which is extremely valuable design real-estate) for other purposes. However the disadvantages include their complexity and the difficulty of standardisation. Additionally, many of the designs presented have components that permanently extend significantly past the connection plane, which constrains the freedom of motion for modules in regular lattice environments.

Another intriguing class of of semi-permanent bonding mechanisms are those that adhere or weld themselves together. This approach is attractive since it can produce very large forces in small volumes without any moving parts. However these systems are likely not very energy efficient - as the two systems discussed here both use electrical currents to heat up the material to the desired temperature, which requires significant unavoidable energy expenditure. The Soldercubes connectors presented in 2014 [56] and integrated into modules in 2016 [24], use several low temperature blobs of solder that are heated by adjacent power resistors in order to solder together. They report a force of 170 N for a 0.13kg module, resulting in a connection strength-to-weight ratio of 133 (i.e., 133 modules could theoretically be held by the top one against gravity). The fascinating FireAnt series of free-form (i.e., non-lattice) modular robots [57], [58] use the melting of a specially designed plastic component to effectively weld themselves together to form bonds. These bonds are reversible through softening of the plastic through heating. This systems is able to form bonds while climbing against the weight of gravity, which is a significant achievement in the context of the research field. The Fireant3D claims to support 250 N of force for a 1.2 Kg module, resulting in a force to weight ratio of 23. While these connections have many favorable characteristics, concerns relating to durability and contamination present obstacles to using them in industrial environments.

The final class of mechanisms considered here are variously called 'hook and latch' or 'key and lock' style connectors. This is perhaps the most common type of gripping connector

and has been used by many of the most developed modular robots, including the Atron system [59], the M-Tran series of robots[28], the Roombots[7], [60], and many others. While the specific designs of these mechanisms vary between systems, the basic idea is that some series of actuated arms moves into place and grips onto some receiving feature on the opposing connector. There are many benefits to these types of mechanisms, which is suggested by their widespread use. These benefits include the ability to fully retract the mechanism behind the connection plane, high strength to weight ratios, and with clever design, quick actuation and compactness. Of course there are also downsides, including that they are often *over-constrained* which sets a limit to the positioning repeatability, a fundamental problem for precision modular machines. Additionally, since they usually require more than one arm or latch they often require either multiple little motors, or a complex mechanism to actuate the arms from a single actuator. Finally, many of these designs are prone to mechanical damage due to the use of small highly geared motors, and often they struggle to unlock while under high load.

2.3 Digital Materials and Structure Assembling Robots Overview

A related field of research to MSRR is digital materials, which are materials that embody characteristics that allow for modular reconfiguration. The fundamental idea for such systems has been around for many years while physical systems which can implement these ideas have recently seen increasing development. Digital materials can be reconfigured by an assembler robot fixed to an external reference point, like a gantry system (e.g., the Bitblox digital electronics system presented by MacCurdy in 2014 [61]), or by assembler robots that traverse the modular structure being built, i.e., *relative assembly robots* [62].

As summarized from [62] and [63] these are several characteristics of digital materials:

- Contain physical features that align parts to a higher level of accuracy than the device which assembles them are capable of proscribing.
- Contain all of the information and features necessary to be disassembled and reused - therefore they produce little waste.
- Embody key physical characteristics such as the lattice size and other critical dimensions. Because of this, they do not need an outside reference source to guide their construction.

Gershenfeld in [3] describes how ribosomes assembling amino acids or people assembling Lego can be considered as examples of digital materials systems. Inherent in any digital material system are the concepts of an *assembler*, that rearranges pieces, and a *connector* which is the interface between potentially dissimilar but compatible modular elements. Digital materials can exist at many different size scales, and one of the challenges involved in creating physical systems is the need make a decision as to the length scale that best balances the costs associated with the connectors with the benefits obtained through modularity. Some systems [64] aim to make light-weight high-strength digital material for proposed use cases

including morphing airplane wing and body structures. One of the challenges faced by these systems is balancing the strength and functionality of the modules relative to the strength of the assembler robot's actuators and the strength of the connection points. The structure being assembled has to be able to handle all of the forces and moments imparted on it from the assembly robot while it moves on the structure. Moments caused by cantilevered long-armed assembler robots especially present difficulties, and conflict with the increased capability of assembly afforded by larger and longer robots.

While the parts that robot construction systems use to create structures can often be classified as digital materials, many systems use more traditional building materials. This 2019 review article [65] describes systems that use materials including fibers, beams, or non-smart (i.e., regular) bricks. Although these systems don't embody all of the features of digital materials, they perform similar tasks like locating assembler robots and manipulating structural materials. Another similar class of systems are large format 3D printing systems [66], some of which are optimized for creating entire buildings. While the materials used by printers are not digital materials since there are no connectors or digital information embodied in the material, these systems share similar goals to robotic digital material assembling systems. Ultimately it is worthwhile to attempt to compare digital material systems with more traditional automated construction systems to determine the most fruitful direction for future work.

An initial theoretical system proposing relative robotic assembly of digital materials is the AMAS (Automatic Modular Assembly System) system by Terada et al. in 2004 [63], [67] and shown in Figure 2.2g. More physical systems that assemble digital materials are shown in Figure 2.2, with some key parameters compared in Table 2.2. Many of these system include assembler robots that are similar in overall design to the AMAS system, with differing methods of balancing both walking on the structure with also carrying the new modules to be assembled. Examples of these systems include the SMAC system [52] from WPI which has a similar assembly robot that works on a standard cubic lattice. Additionally the Bill-E series of relative robots first presented in 2017 [27] and further extended in 2019 [62] all have shown impressive feats and operate on a cuboct lattice. A further ongoing extension of this work at NASA Ames called SOLL-E [4], [68] shares many important characteristics with the work in this thesis. The robots use very similar proprioceptive actuators to those shown in Chapter 6, and the robot is similar in form to the Bill-E robot. This project appears to be geared towards assembling very lightweight lattice structures, and does not focus on achieving high repeatability or rearranging heavy modules to the extent of the FrFlFuFa system. While this limits its utility for creating industrial automation equipment, it shows great promise towards creating space-based structures.

Additional digital materials assembly approaches include flying robots assembling structures with embedded magnetic connectors, presented in [69], and the use of mobile forklift-like robots called SRoCS [70]. The SRoCS robot itself does not connect directly to the lattice, instead driving on the ground. Driving approaches are interesting as these robots can carry heavy payloads, and can take advantage of the vast engineering knowledge base involving wheeled robots. However they have a fundamental limit in the height and complexity of structures they can assemble, and are not able to take advantage of the relative error-correcting nature of lattice traversing solutions. The Termes system [71] is a fascinating hybrid between mobile wheeled robots and relative robots. Termes robots can drive/crawl

Table 2.2: Robotically assembled digital materials structures system summary table. Data indicated by ∼ is estimated from the related work, with the remainder taken from the reference in the first column.

System	Axes (+gripers)	sec/move	mass (g)	H (lattice Size)	Lattice Type
Belty (Chapter 6)	3 (3)	0.5-2	2090	100 mm	Cubic
BILL-E [72]	5 (7)	∼5-15	510	80 mm	Cuboct
SMAC [52]	5 (7)	20-50		76.2 mm	Cubic
Termes [71]	4 (5)	∼5-10	810	110 mm	Rectangular
Quad Rotor [69]	4 (5)	∼1-10	710	∼ 400 mm	Truss
Soll-E [4]	5 (7)	20	4800	300 mm	Cuboct

over specially designed brick-like structures with wheel-like arms, but they can only climb up a single abbreviated height step. This design limits the structures able to be constructed (e.g., no cantilevered structures), but the system has been well-developed and has produced some impressive structures in experiments involving many modules and hundreds of steps.

2.4 Modular Manufacturing Systems

While general MSRR-style modular architectures are rare in industry, there are many examples of specialized modular interfaces. The machine tool industry has been increasing the extent of automation in high-end machine tools, which requires some level of modular interfaces to function. However these efforts seem to be focused on several specialized interfaces that don't include any attempt to develop deeply modular architectures. A common example of one of these modular interfaces is automatic tool changers [73] for CNC machining systems. Most tool changer mechanisms are optimized for high stiffness and concentricity, and achieve this through the use of collets and hardened steel conical mating surfaces. However there are some designs targeted at smaller machines [74] that use traditional kinematic couplings and magnetic preloads, which are similar in some ways to the work presented in this thesis. Additionally there are beginning to be automatic work-piece attachment mechanisms but these are less common and less standardized than tool changers. Several modular interfaces for industrial robots have also seen development including [75] for bases and [76] for wrists, but these do not aim to create a widely usable standardized interface.

The idea for large scale modular manufacturing systems has been presented before in various ways. One such system was presented in 2014 by Moses and Chirikjian [53], which shares several similarities to the work in this thesis. This system includes three-dimensional gantries constructed out of modular rack and pinion tiles, which can be seen in Figure 2.3a. An additional system along the same lines called the Factory Floor was presented by Yim et al. [77] in 2010. This system proposed a standardized modular work cell that is constructed by modular MSRR style robot arms that can manipulate truss structures that provide attachment points for specialized manufacturing hardware.

There have also been systems that aim to create functional CNC machines from modular

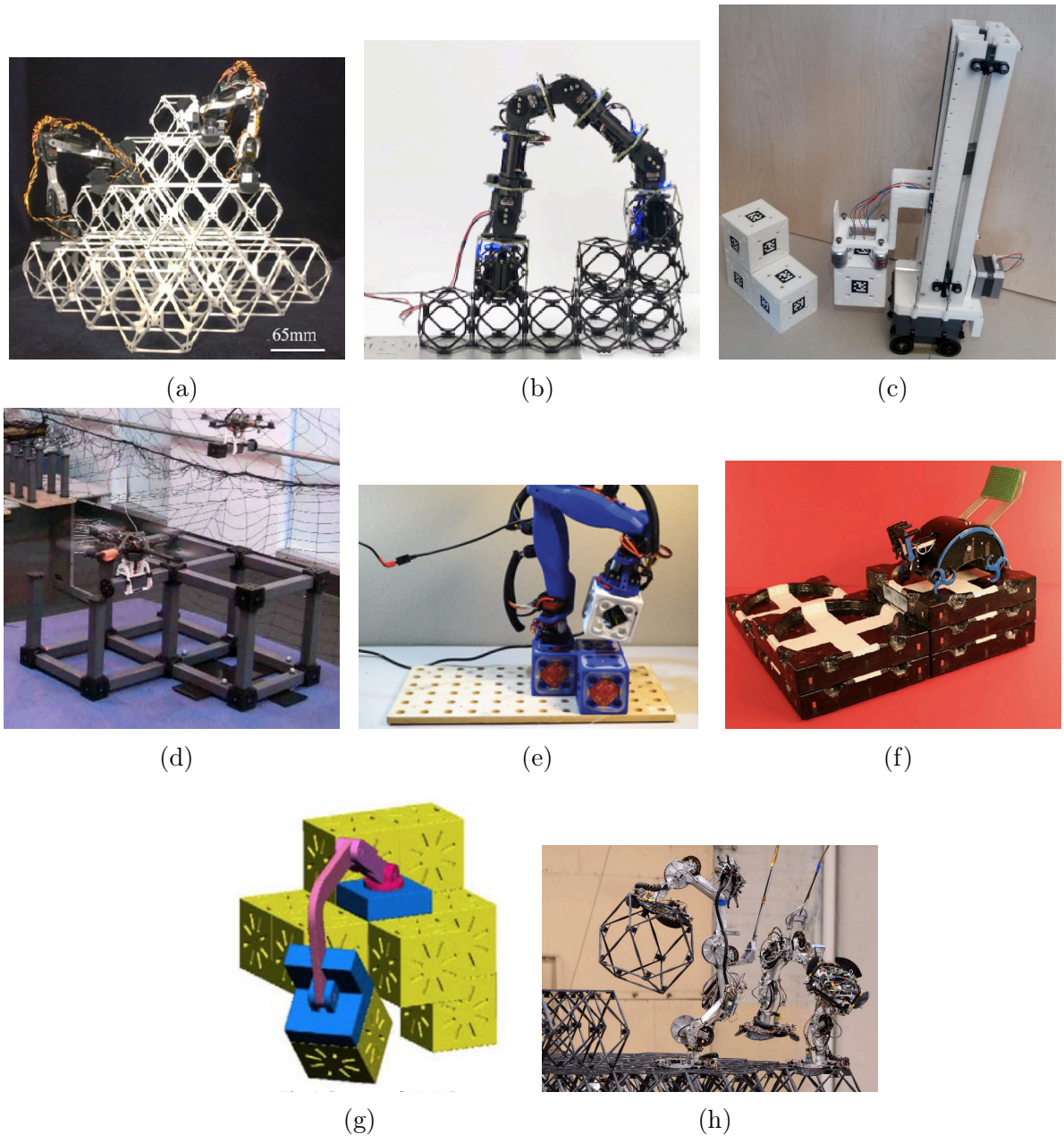

Figure 2.2: Related work systems that use assembler robots to create structures out of modular elements, including (a) The Bill-E system by Jennet et al. in 2017 and 2019 [27]. (b) Upgraded Bill-E robot built from modular cells [35] (c) The SRoCS mobile driving robot block assembly system [70] (d) The Mod Quad system which used quad rotors to assemble magnetically connected truss structures [69] (e) which shows the SMAC system from WPI which has a similar assembler robot as the Bill-E system. (f) The Termes robots which are able to climb and assemble structures using termite-inspired robots. (g) Shows one of the earliest digital materials assembly robot concepts [67] by Terada et al. in 2004. Finally (h) shows the SOLL-E [4] robot from NASA which is a large format relative robot geared towards space-based applications.

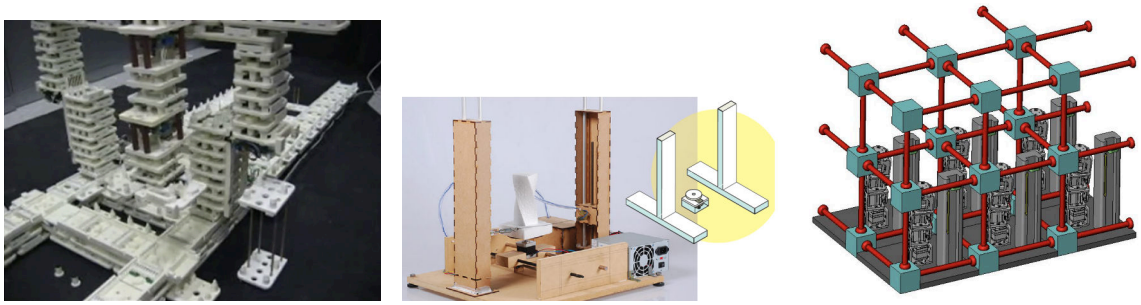

(a) (b) (c)

Figure 2.3: Modular industrial machine systems and concepts, including (a) Modular self-assembling gantry system presented by Moses and Chirikjian in 2014 [53], (b) Modular CNC machines created by N. Peek in 2017 [79], and (c) which shows the Factory Floor system [77] presented in 2010 by Galloway and Yim. These systems share the goal of helping to bring increased flexibility into manufacturing systems by introducing modularity.

linear axes, for example the work from N. Peek in 2016 [78]. However this work still uses linear axes that are of fixed length, and therefore does not allow the level of deep modularity required to create large scalable systems. Recently several commercial systems similar to this work have become available that include swappable machining axes, but each one appears to use a custom, often proprietary, connector to attach the axes. The connectors in these commercial systems often do not support many of the features necessary for applying them at large scale, like the configuration detection or distributed electrical systems seen in more deeply modular academic works.

2.5 M-Blocks Robots

The FrFlFuFa system described in this thesis has many aspects of its design that are extensions of the M-Blocks modular robotic project, which this masters thesis [1] discusses in depth. The 50 mm cubic lattice M-Blocks, shown in Figure 2.4, are traditional MSRR robots where the modules move themselves in order to form the structure instead of being assembled by a separate robot. The M-Blocks robots used a flywheel and band brake-based inertial actuator, which was originally introduced in 2013 [80] for one dimensional motion, and extended to three dimensions in 2015 in follow up work [81].

This project was unique among previous MSRR systems in that it reconfigured through bursts of high-power inertial forces. This made the actual motions themselves depend on the system dynamics, as opposed the vast majority of other MSRR systems which used only statically stable motions (i.e., you could 'pause' the motion at any point along their trajectory without disrupting the motion). The advantage of robots which operate with high-powered dynamic motions is that ultimately the average power output of a robot limits the assembly capabilities in terms of speed, and potentially also efficiency. In order to create practical real-world systems, high-speed motion and dynamic properties of the robots and the structural elements will become increasingly important.

Several autonomous behaviours to construct structures were implemented in simula-

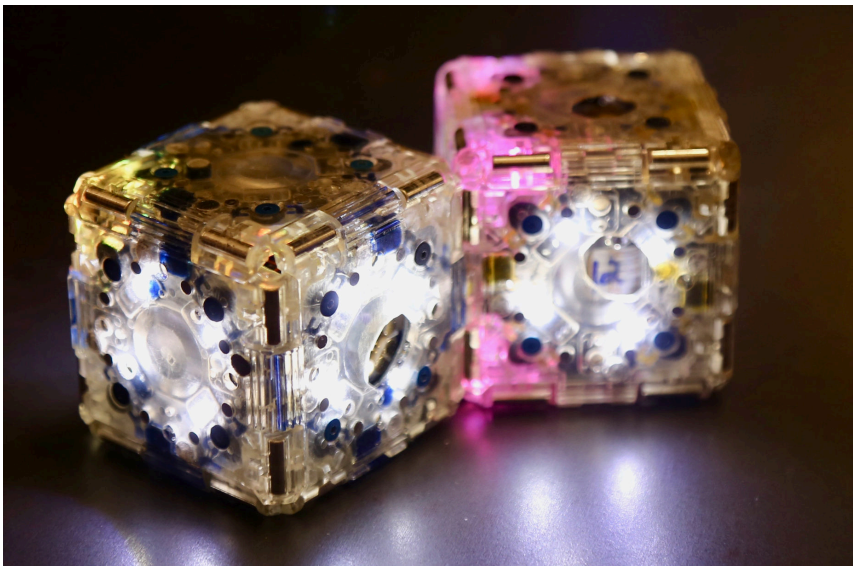

Figure 2.4: This figure shows the M-Blocks modular robots, which predated this work by the same author. These robots are lattice-based self-reconfigurable robots with a lattice size of 50 mm. They move on a lattice by rotating through bursts of angular momentum from an onboard inertial actuator. Many of the features in the FrFlFuFa system were guided by the challenges and lessons learned while developing this project.

tion [82], [83] and on the physical 3D M-Blocks in [84] and [39], which use light gradients and neighbor identification to guide the design of the structures. Non-modular swarm systems have constructed structures in similar ways, most notable the Kilobot system [85]. Additionally the M-Blocks were able to construct short cantilevered structures, but the lack of a semi-permanent connection mechanism like the AutoBolt mechanism (Section 4.8.1 prevented them from extending past one or two lattice cells.

There are several fundamental problems with the M-Blocks robots, which this thesis has attempted to address. The first problem was that the structures were held together only through the standard permanent magnet array. Attempts to implement an electropermanent magnetic connector along the lines of the SMORES System [86] were found to be impractical given that the inertial actuator took up most of the space inside of the module. Secondly, these robots were very expensive to manufacture, and could only manipulate other passive modules in a very limited fashion. This helped to reinforce the lesson that if the goal is to actually build structures that accomplish something useful, it is not practical to have the modules embedded with a full suite of actuators, batteries, etc. To achieve this goal, assembling passive or mostly passive modules by teams of assembly robots makes more sense, and the rest of this thesis attempts to demonstrate a system that can do this.

Chapter 3

Flexible Manufacturing System Overview

To advance the concept of modular industrial machines, this thesis introduces a small-scale prototype system. This system is comprised of various modules that test and demonstrate the functionalities necessary for larger-scale future systems. A full list of the modules created and used in this thesis is shown in Table 3.1. The system has gone through several iterations of prototypes and hardware development over the course of this PhD research. We are calling the system, FrFlFuFa, which is intentionally goofy and difficult to pronounce, and which stands for a Framework for Flexible Future Factories. This system is not intended to be an actual practical solution to any actual problems - it is a means of prototyping and testing hardware and algorithms towards that goal. Various aspects need to be improved and reconsidered before we reach a practical solution that works outside of the laboratory. Many of these aspects are proposed as future work and are discussed in Chapter 9.

The FrFlFuFa system comprises a set of modules built around a 100 mm cubic lattice. Each compatible device must contain at least one standardized connector, which is described in detail in Chapter 4. The system is composed of several broad classes of modules including (1) active modules that have a power source and some form of motion capability, (2) structural blocks, some of which have smart functionality that needs to be powered from an active module to utilize, and (3) special function blocks which include sensors or end-effectors, and fixtures, or other task specific features. Section 3.3 explains how these modules can be combined into useful groupings, termed metamodules. Metamodules are a collective of a specific set of modular parts connected in a specific way that performs functions as one system. These are used as an abstraction layer for developing higher level controllers, and can involve as few as two individual modules.

3.1 Flexible Future Factories: A Framework for Modular Machines

This thesis presents a new system, called FrFlFuFa which stands for a Framework for Flexible Future Factories. The system is based on a 100mm side length simple cubic lattice. This system has been created as a testbed to investigate several specific technical contributions, as further detailed in Section 1.5. The existing system includes all of the elements necessary for autonomous operation, including both wired (CAN bus) and wireless (UWB Decawave) dis-

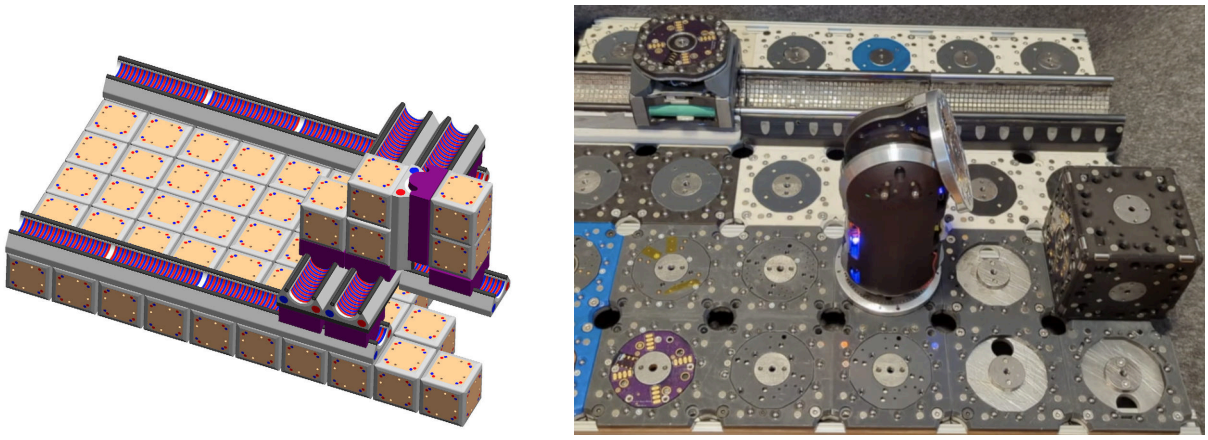

(a) (b)

Figure 3.1: (a) Rendering of a 3D gantry system created out of many MagnaCarta linear actuators and structural blocks that is capable of extending itself given enough new materials. (b) An example showing the core parts of the prototype system. The *Assembly Robots* are like small three-DOF robot arms that can crawl and hop around the lattice assembling and manipulating other modules. The *carts* and *tracks* form the modular linear actuator system MagnaCarta. These devices are able to create extensible high force linear actuators that can perform linear motion general tasks as well as help transport pieces. Finally on the far-right of (b) is an example of a structural block - which is a passive block like a lego-brick that can be used to create structures.

tributed communication networks. Additionally, it includes a customized software command format, onboard energy storage and distributed power management capability, configuration detection sensors, as well as the ability for special connectors to be able to safely share up to 100 watts of power through the connector.

This work is driven by two central theses within the overarching thesis, each of which is explored through a specific physical system. The first thesis posits that kinematic couplings—an extensively researched sub-field of mechanical engineering—serve as an ideal basis for creating modular connectors in robotically assembled systems [49]. These couplings can be fabricated from low-cost, readily available components and offer connectors with a large area of acceptance, exceptional positional repeatability, and predictable, analytically tractable stiffness.

The second hypothesis suggests that high-speed, robust, and energy-efficient assembly is best accomplished using high-power, efficient, force-sensing actuators. Examples of these actuators include the quasi-direct-drive proprioceptive actuators found in legged robots like the MIT Mini Cheetah, or efficient series elastic magnetic power transmissions such as magnetic lead screws. The former are implemented in the assembler robot Belty (Chapter 6), and latter forms the foundation of a modular linear actuator presented in Chapter 5 included in the FrFlFuFa system.

The research goals for this system includes (1) the ability to self-reconfigure its components and (2) creating useful machines from a library of modular components. A complete library of the components which are included in this thesis are shown in Table 3.1. The sys-

tem includes different elements that are common in related work modular robotic systems like structural blocks, assembler robots, and 2D plates. However, this system is intended to support increasing the scope of modular machine concepts to also include traditional industrial elements like linear actuators and components like force and torque sensors.

While significant work remains to be completed to form a complete high level software control system for managing large assemblies of modules, the insights discussed and the existing hardware demonstrate several system examples that break new ground in robotically assembled systems. One example demonstration that the FrFlFuFa system is able to accomplish that has not been convincingly demonstrated previously is the assembly of a high strength (defined as holding 100x the weight of the average module weight) cantilevered beam which is assembled and attached by relative assembly robots. Additionally there have been few examples of similar systems creating structures which accomplish actual tasks beyond the assembly of the structure itself. Chapter 8 presents a prototype pick-and-place system created out of basic components that has the capability to move and pick up blocks.

3.2 Basic System Elements

Images showing the four core types of modules in the prototype system are shown in Figure 3.2. This non-exhaustive listing of module types can combine to form larger integrated systems. *Assembly robots* resemble compact, three-degree-of-freedom (DOF) arms, capable of crawling and hopping around a lattice to assemble and manipulate other modules.The *carts* and *tracks* form the modular linear actuator system named MagnaCarta. These devices are able to create extensible high force linear actuators that can perform general linear motion tasks as well as help transport pieces throughout the machine, analogous to little railroads.

There are four primary classes of modules that have been created as part of the current FrFlFuFa system. The four categories of modules are included in the following enumeration and are shown in Figure 3.2.

1. The **assembly robots** are like small multi-actuator robot arms that can crawl and hop around the lattice assembling and manipulating other modules. (Chapter 6)

2. The **MagnaCarta** is a modular linear actuator that is able to create extensible high force linear actuators that can perform general linear motion tasks as well as help transport pieces. It uses a magnetic lead screw transmission and has two parts, passive tracks, and active motor-drive carts. (Chapter 5)

3. **Structural blocks** are passive Lego-like bricks that can be used to create structures. These modules can be passive, or can have active connectors and the ability to share the wired network through its connectors. (Section 3.4)

4. **Function modules** are like robot end-effectors, and can contain any relevant electronics and mechanical components that are needed by the system. Examples that have been constructed include a calibration sphere, a simple universal testing machine force testing block, and a dial-indicator holder. (Section 3.5)

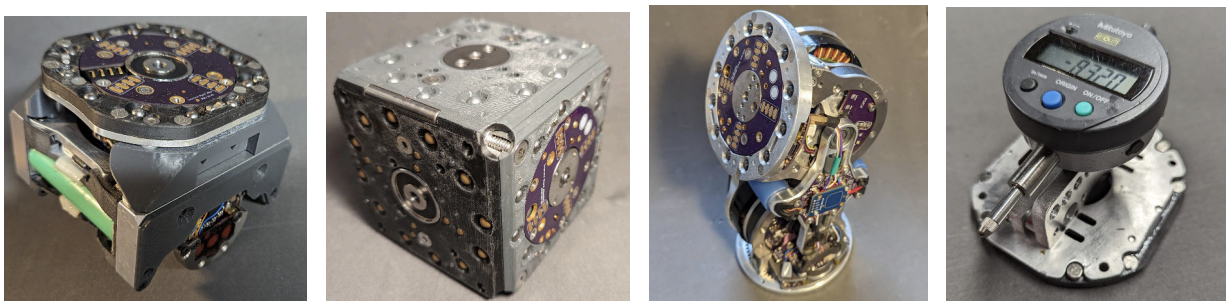

(a) (b) (c) (d)

Figure 3.2: Selected images of the core parts of the FrFlFuFa system. Subfigure (a) shows the cart part of the modular linear actuator system, (b) shows a smart structural block with a prototype automatic bolting connector, (c) shows Belty the assembler robot, and (d) shows an example of a special function module which can accurately measure distances.

Table 3.1: Table of the FrFlFuFa system elements. These components are like industrial Lego bricks that can be mixed and matched to create useful reconfigurable machines. This list includes the full set of elements that are discussed in this thesis, although there are many more possible interesting and useful modules that would be part of any future system that are not listed here.

Module name	X	Y	Z	Mass (g)	Connectors	Est. cost
Belty	99	99	200	2190	2	$ 3000
Cart	99	96	70	1210	1	$ 800
Track	199	90	60	980	2	$ 400
Structural Block	100	100	100	1237	6	$ 300
Structural 1x3	300	100	100	2914	14	$ 1000
Force Sensor Block	99	99	100	968	2	$ 1000
Dial Indicator	99	99	70	460	1.5	$ 300
90 Degree Bracket	100	100	70	400	1.5	$ 200

A topic that is often challenging for lattice-based systems is managing the clearance between modules. If every module is exactly the size of the lattice cell, then there is no clearance when modules are moving next to each other, which will in practice cause collisions between adjacent modules. This problem is in some ways unsolvable without exotic strategies like making each connector extend, and in general the clearance between some modules will limit practical motions possible with such a system. The approach taken in this system is to have each dimension that contains a *connector* to be as close as possible to being on the exact plane between the lattice cells. However, every lattice cell that does not have a connector is set back at least half of a millimeter, and more if possible. An example of these dimensions can be seen in Table 3.1, where the cart module is 96mm wide, this allows a cart to drive adjacent to a full lattice cell without any collisions.

Table 3.2: Individual modules can be combined into groupings called metamodules. This table lists several of the useful meta-module combinations that have been realized using the experimental hardware.

Name	Modules	Mass (g)	Actuator DOF
RoombaCat	2	3097	4
TrackBot	3	4310	5
XZ Gantry	3	3415	2

3.3 FrFlFuFa Metamodules

In the modular robotics field the term *metamodules* refers to specific groupings of modules that connect to each other and function temporarily as a single robot. Table 3.2 gives an overview of several different metamodules that have been developed in this work, although it is by no means an exhaustive list. Metamodules serve as an abstraction layer for the development of higher-level algorithms and attempt to create meaningful cohesive groupings of modules that can execute specific functional algorithms.

1. The **RoombaCat** metamodule consists of one Belty assembler robot connected through its rotating face to a single cart module. It is named after a video of a cat riding a Roomba vacuum around while grabbing and hitting things. This robot is able to move along a single track of any length, and can pick and place components with a work space that extends up to two lattice cells to each side.

2. The **TrackBot** consists of one Belty robot with cart modules on both modular feet. This module can pick up and relocate track segments, as well as transfer from perpendicular tracks under some circumstances. This robot is relatively heavy, and is over 4 kg in total without counting the weight of the tracks. An experiment where a TrackBot rearranges one of the tracks is described in Section 8.2.

3. The **XZ Gantry** metamodule includes a cart, structural cube, and the linear force stepper module. This metamodule can drive along a track and pick up and place down adjacent modules that have a connector on their top face. An experiment showing a proof of concept of this system is shown in Section 8.3. In the future, these could be expanded to include a third axis, which could create small pick-and-place machines or 3D printers that are able to operate as a traditional gantry machines.

3.4 Structural Blocks and Plates

Structural modules are perhaps the most basic of any system's modular components, analogous to the basic bricks in Lego. Structural modules help to create the frame for the active parts of the modular machines to connect to, and some of them have bonus features, such as bolt-on connectors, extra sensors, or actuators that can be temporarily activated through the network, assuming they can receive power through the network.

(a) (b) (c)

Figure 3.3: Images of three FrFlFuFa metamodules. Each of these robots is composed of several different constituent modules in order to accomplish specific tasks for the system. The modules all share a power and a CAN communication network through their connectors, so they are able to operate as a single robot. The three metamodules include: (a) RoombaCat, (b) TrackBot, and (c) the XZ Gantry metamodules.

In addition to structure cubes and lines, structural plates consist of a planar implementation of the modular connector, and are held together on the bottom through a 80-20 frame in order to provide a solid base, or substrate, for performing experiments. An image of one of these can be seen in Figure 3.4b. Some of the connectors have active elements, such as electromagnetic attachment mechanisms, etc. These plates are designed to be very inexpensive to manufacture. They are built out of a 2D-cut plate and a 3D-printed top plate which are then epoxied together.

3.5 Instrumentation and other Special Function Modules

The assembler robots can create gantry machines out of MagnaCarta and structural modules, but these machines require specialized modules to accomplish useful tasks. By using gantry machines as a sort of 'mechanical operating system' to which various special function modules can be attached, the benefits of a modular modular architecture really begin to shine. This section discusses two example function modules which have been developed and integrated into the FrFlFuFa system. These particular modules were built in order to aid in the collection of experimental data and to verify and measure properties of the system. The first function module (Subsection 3.5.1) consists of a dial indicator module which reads a commercial off-the-shelf Mititoyo dial indicator to measure connector repeatability. The second module (Subsection 3.5.1) act as a crude 'Instron' universal testing machine module which integrates a force sensor and a high-stiffness stepper motor driven linear stage.

The short-term motivation for developing this hardware, and taking the engineering effort to integrate them into the existing communication bus to is help solve the problem

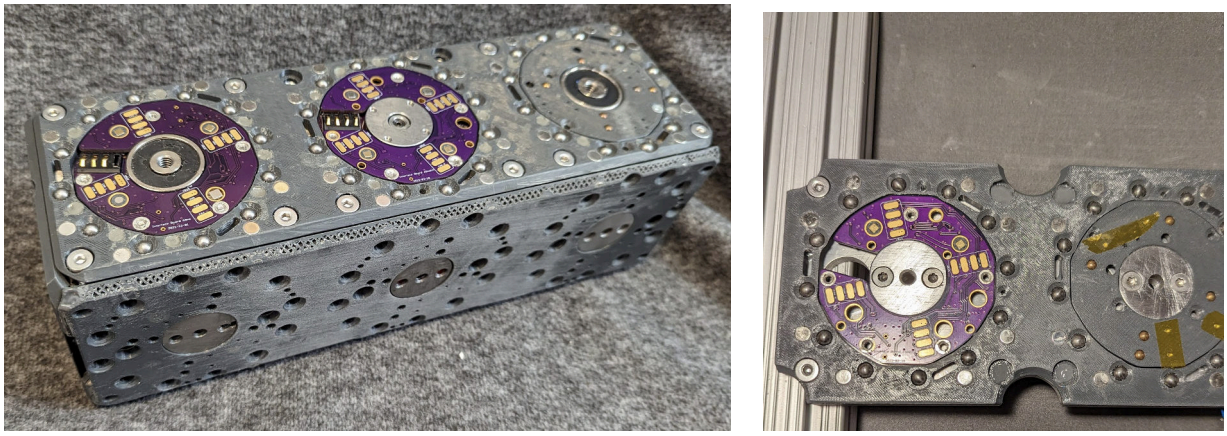

(a) (b)

Figure 3.4: This figure shows (a) a 1x3 single structural block which has the first AutoBolt connector (Top center connector). This module has active circuitry inside, but similar blocks could be built that are entirely passive to provide cost effective frames for larger structures. Structural plates (b) are simple and inexpensive 2D plates that can be combined with aluminum extrusions to build large base plates for custom machines.

of synchronizing experimental data. The existing hardware, like Belty, or the MagnaCarta robots generate high bandwidth data including current draw, kinematic position readings, and IMU readings, but it can be challenging to synchronize this data with external measurement tools, such as an actual Instron machine. By integrating all of this hardware together the system can generate more comprehensive time-synchronized data. An example of such a practical measurement system is the motor testing apparatus created out of a structural cube and the Universal Testing Module which is used in Section 5.4 to help characterize the force and torque to current measurements for Belty's actuators.

Long-term, special function blocks can be constructed that accomplish many of the steps involved with industrial manufacturing or measurement applications. These blocks can be considered as analogous to the 'end-effectors' used in industrial robots today. They should ideally have at least two modular connectors to allow them to attach to the machine and function, while leaving one connector for an assembler robot to be able to grab onto for relocation. In future systems it is imagined that function modules could accomplish functions such as the following tasks:

1. Measurement and instrumentation devices. This could range anywhere from dial indicators, to camera modules to various actuated testing machines, like the Universal Testing Machine module described below.

2. Work-Piece holding mechanisms. These modules could include vices, special plates, or other grippers that hold work-pieces or samples that can move around a modular industrial machine and have actions performed on them by the other functional modules on the machine.

3. Active industrial tooling. These types of modules could include devices that cut, add or

re-arrange materials. Examples of these include spindles, 3D-Printer extruder nozzles and pick-and-place vacuum nozzles.

4. Miscellaneous function specific blocks. These could included specialized hardware, like mirrors, lenses and lasers for an optical setup, or specialized calibration shapes, or additional mechanical parts like bearings, linkages, or extra linear or rotary axes.

3.5.1 Distance Measuring Dial Indicator Module

Figure 3.5 shows a block which has been instrumented with a high quality commercially available dial indicator which can be read through its serial connection, and translated by a dedicated microcontroller into the shared CAN communication bus. While companies like Mititoyo do offer systems to communicate with their devices including their dial indicators, these systems involve the use of a computer, proprietary software and expensive cables.

Integrating high performance measurement equipment into a modular machine system is one of the promising new capabilities that are possible in a system that contains highly repeatably located connection points. Custom robotic testing cells can be created with two of these modules paired with a RoomaCat metamodule to measure the connector repeatability. These modules were used to test the repeatability of different assembly operations and are just one example of what a special function module can accomplish.

Figure 3.5: This module integrates a Mititoyo dial indicator onto a connector plate which includes the necessary kinematic teeth to repeatably locate it. The dial indicator can be read through a small Teensy-based microcontroller with the data being sent through the CAN bus network. While Mititoyo dial indicators are very precise (resolution down to 1 um, they have a low data update rate, with the maximum update frequency of roughly 10 Hz.

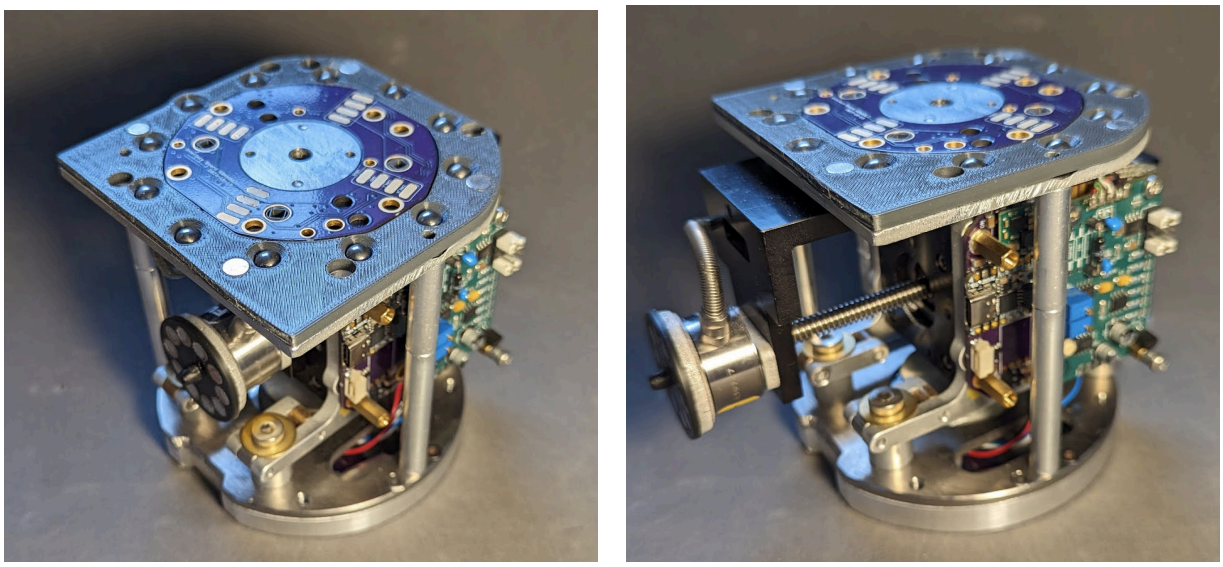

(a) (b)

Figure 3.6: This image shows the actuated force-distance measurement module. This module has a stepper motor driven linear stage combined with a Futek industrial load cell and amplifier stage which is read by a custom CAN enabled SAMD21 QTPY based circuit board, which integrates a custom stepper motor driver (behind the green PCBa). The device can be seen in retracted (a) and extended (b) states.

3.5.2 Universal Testing Machine Function Module

One of the challenges in working with high performance mechatronics is that high-quality instrumentation is expensive, and difficult and time consuming to implement on systems working in non-laboratory environments. Traditionally, accurately measuring forces and torques for experimental robots either involves using a dedicated force-distance testing machine, like an Instron machine, or integrating specialized force/torque sensors into the design or testing environment.

Here we introduce a preliminary design for a single modular block which can act as a mini Instron machine. This device utilizes a FUTEK LCM300 load cell, which is coupled with a CSG110 amplifier to measure force data which is read by a 12-bit SPI ADC, capable of sampling at rates up to 10 kHz. This device can extend its lead-screw stepper motor driven axis up to 40 mm, as shown in Figure 3.6b. The module has been used as a force sensor, a force-distance testing machine, and also as a actuated gripper for the gantry machine shown in Section 8.3.

Chapter 4

The Connector Problem

Since the connector in a modular systems is the primary interface between the various components, its importance cannot be overstated. A fascinating array of designs and technologies have been published related to connectors for modular robots, as discussed in Section 2.2. This chapter will present a new design for a connector as well as initial characterization of its strength and mechanical repeatability. The design borrows elements from previously published MSRR connectors, for example, the traditional eight four-way symmetric permanent magnet array (i.e., the passive magnetic lattice) which is discussed further in Section 7.1. This new connector is intended for 100 mm cell-sized lattice systems, and all of the active elements are fit inside of a 99 mm circle, in order to accommodate collision free rotating connections. This chapter begins with a description of the high-level design overview of the connector subsystems in Section 4.1, before detailing the technical parameters of each of these systems in the following sections.

In many connection mechanisms, there is a trade-off between what is termed the *area of acceptance* [87] of a connector (how far off the connector can be placed while still snapping into alignment to form a valid connection) and the accuracy and repeatability of the connector. However, a special mechanism called a kinematic coupling is well suited to both high repeatability and large area of acceptance and is reviewed in Section 4.5. While kinematic couplings have been used extensively in industries that require high precision (e.g., semiconductors, optics), there are a few design modifications that need to be undertaken to adapt them to a 3D lattice cell connector. The description of these modifications and the characterization and design challenges involved with kinematic couplings are discussed in Section 4.6.

CNC machines are often designed as a single rigid monolithic structure in order to maximize performance characteristics like stiffness and accuracy while conforming to the desired constraints for size, weight and cost. Therefore, careful budgeting for error tolerances of the machine elements is traditionally undertaken during the design phase in order to achieve the desired precision and stiffness [88]. Reconfigurable and self-assembling robotic gantry machines face a more complicated problem due to the need to make potentially hundreds of modular connections. Each connection introduces some level of positional error and undesired mechanical compliance. Therefore the primary design requirements for a modular connector for reconfigurable robotic gantry systems is to maximize stiffness and positional repeatability, while being conscious of size and cost. Experimental data characterizing the

repeatability of modular robot connectors is rarely presented in related work. However, we estimate that common MSRR systems have mechanical repeatability on the order of 100's or 1000's of microns (um). It is easy to imagine how errors will combine through multiple connectors along the structural loop of a modular machine. Unless error is accounted for through calibration each time a component is reconfigured, the performance of modular systems compared with monolithic machines will be limited.

One additional challenging aspect of modular connectors is how to provide switchable strength to the connector in a robust, cost- and size-efficient manner. Ideally, the system's connections will retain all of their strength after power is removed, although temporary connections can still be useful for moving elements around a lattice. Two methods of generating these connector attachment forces are presented here, with Section 4.9 introducing a simple electromagnetic based approach for temporary gripping connections, and Section 4.8 introducing an initial design for an automatic bolting connector. The chapter concludes with a description of the electrical network which accomplishes both a CAN network system and a power sharing bus architecture in Section 4.10. Finally, the electronics and algorithms supporting a magnetic bar-code like system based on permanent magnet tags for embedding and reading the identity and orientation of each connector is presented in Section 4.11. This system is an extension of the system previously presented on the M-Blocks robots in 2019 [39].

Throughout this chapter the following definitions will be used:

- the **connection plane** is the nominal plane that lies between adjacent lattice cells. This plane lies on the boundaries of the 100mm lattice cells and should be parallel to the plane on the opposite side of the unit cell, and perpendicular to the four sides.
- a **non-gendered** connector in the context of modular connectors specifies that the connector is able to be matched with an identical connector, as opposed to requiring a different matching connector in order to achieve a proper connection.
- the **area of acceptance** of a connector is the set of physical offsets in X, Y, and θ directions where a connector is still able to 'snap' into place and form a valid connection. While this is usually considered as a qualitative metric due to difficulties measuring it and due the challenge of capturing all of the other relevant parameters (e.g., the tilt, momentum, and mass of the mating parts).

4.1 FrFlFuFa Modular Connector Design Overview

Trying to fit all of the potentially required functionality into every connector of a modular system is not tractable due to performance, weight, and volume considerations. An alternative approach is to design a variety of connectors, all supporting a small set of *basic functionalities* including mechanical connection and connector identification. The goal is to find a middle ground between using a completely bespoke connector for each type of module–which would likely prove inflexible–and employing a single standardized connector everywhere, which could become cumbersome and expensive. Because of their shared basic

functionalities, any pair of connectors *can* work together, but not all of the functionalities will *have* to work together.

The connectors have several subsystems which operate in parallel to each other, each with with multiple complementary options, i.e., part A, B, or C. The following lists the three mechanical subsystems and describes each of their functionalities.

1. **Lattice alignment** subsystem consists of a nominal array of eight 6.3 mm diameter cylindrical permanent magnets arranged in a four way symmetric pattern. This subsystem has no A or B parts, and all connectors are expected to have all eight magnets for a full connector, with fewer acceptable for partial connectors.

2. The **kinematic coupling** subsystem provides highly repeatable alignment capabilities and prevents bolt connectors from unscrewing. It includes part A, which consists of twelve 6.3 mm diameter hardened metal or ceramic spheres arranged in a circle with a diameter of 80 mm, and which is expected to be present on most connectors, and part B which consists of the three hardened kinematic teeth that slightly protrude beyond the connector plane. Kinematic part B is only expected to be present for modules that need the increased accuracy and stiffness provided by the coupling.

3. the **center preload circle** subsystem is the center 30 mm diameter ring which is designed to provide a secure centered attachment point for either 1/4-20 bolts, or various magnetic attachment mechanisms. The surface of the center preload circle should be precision ground magnetic steel with a 1/4-20 tapped hole in the center with a thread depth of at least 3 mm. There have been three different versions of this central plate that have been built in a way that maintains as much cross-compatibility as possible. The first is called the base level (a), which is a simple precision ground steel plate co-planer with the connection plane with a tapped 1/4-20 hole in the center. The second option (b) includes a 30 mm off-the-shelf electromagnetic gripping coil which has a tapped hole added to the center. This can be built with a bit of compliance and set slightly below (0.1 mm) the connection plane in order to provide a preload for the kinematic coupling. The third version (c) is a self-bolting connection mechanism, which is described in 4.8. While this mechanism is in the retracted state, the connector should be functionally equivalent to a type (a) connector. While in the extended state it is able to thread into a matching tapped hole on the mating connector in order to provide a high strength preloaded structural interface connection.

In addition to the mechanical system, the middle ring between 30 mm and 70 mm and up to 6.3 mm deep is dedicated to the electronic and configuration identification sub systems as described below:

1. The **electrical** subsystem is the annular ring-shaped region that is between two circles with diameters of 30 mm and 70 mm. This region consists of contacts for up to four electrically independent wires (CAN high, CAN low, ground, and bus voltage) and supports distributed communication through the CAN layer, and optionally can share power through the bus voltage of up to 100 W (24 V max). The electrical contacts have two matching parts: part (a) is four 90-degree rotational symmetric sets of four pads set up to 0.25mm below the connection plane. Part (b) consists of four spring-loaded

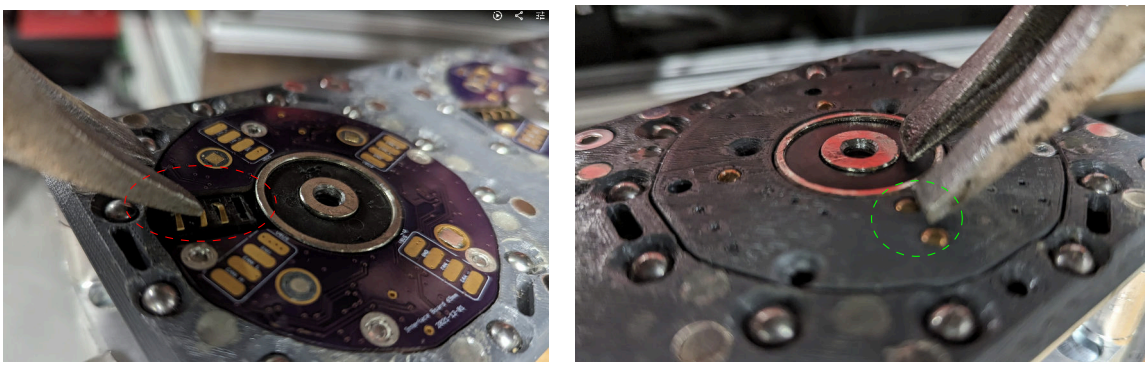

(a) (b)

Figure 4.1: Visual illustration of two versions of the connector that (a) fails the hammer test due to an easily damaged spring loaded connector (*red oval*), and the improved version (b) that uses spring-loaded electrically conductive spheres (*green oval*) that passes it. These spheres are held in by a small lip on the plastic part, and are effective since there is no place to hook onto them, as there is for the blade-style connector shown in (a).

electrical contacts that extend beyond the connection plane by at least 0.5 mm, and match up with the pads from part (a).

2. the **Magnetic ID bar-code system** is a passive barcode-like system for embedding unique barcode-like tags into each connector. This system consists of the tag, part (a) which contains up to four specifically located permanent magnets which encode information in the direction of each of their magnetic field vectors, and a part (b) which consists of four three-axis magnetic field measurement sensors which sit directly over the magnets from part (a) and read off the identity information from a matched tag.

4.2 Robustness: Passing the Hammer Test

While meeting the existing connector functional requirements is difficult enough, for practical systems *robustness* is of paramount importance. Since there will be many tens or hundreds of connection events over even a single reconfiguration of a system, each connector needs to be able to stand up to abuse and potential damage during assembly and operation. Sometimes the connectors will connect poorly, parts will slide over each other, or robots will accidently slam and scrape into each other. This system experiences high forces during magnet driven automatic connector alignment events, and especially during the hopping motion primitive 7.3.2, but also during moves as simple as placing a module on a connector.

Despite being such an important characteristic there is no clear way to measure or characterize robustness for connectors that has been presented in related work literature. Connectors like the USB connector [89] list the number of expected plug and un-plug cycles, but for a robotic system involving mechanical contact of an unpredictable manner this metric is not particularly relevant.

In order to attempt to create a standard that can determine if a connector is likely to be robust in practical use we define the *hammer test*. The hammer test states that the for a connector to pass it must be able to withstand the claw part of a hammer being dragged over its surface in any direction with only the weight of the hammer pushing down. This test is admittedly qualitative and arbitrary, but any connector that can pass this test is likely to be robust. From anecdotal experience the aspect of a connector that fails this test is any physical part of the connector that 'sticks out' from the interface plane that the hammer can hook onto. While the connector presented in this section is generally quite robust, and the versions of the connector that do not have electrical contacts all pass the test, the first version of the electrical contact fails the test. Figure 4.1 shows two versions of the FrFlFuFa connector's protruding electrical contacts, with the first being an off the shelf spring loaded blade-style array (Bourns part number: 70ADJ-4-ML1).

4.3 Connector Definition and Overview

This section defines a new precise modular connector based on kinematic couplings as one of the core enabling technologies for the FrFlFuFa system of self-assembling machines. Kinematic couplings have been used in robotic applications as interface plates between elements, usually in the context of modular end effector connections [90], or machine mounting platforms [49], and are in use for many industrial machines across several orders of magnitude of size scales. The contribution in this thesis is to apply and adapt the traditional kinematic coupling design to modular robotic connectors by specifically (1) presenting the design for a 4-way symmetric, quasi-non-gendered kinematic coupling connector, and (2) experimentally validating the repeatability and functionality of these connectors. Modular robotic connectors must be capable of repeatable and precise alignment, and must be able to align themselves to a higher level of precision than the robot which assembles them, analogous to how Lego connectors allows toddlers to assemble very repeatable structures despite having imprecise actuators.

Figure 4.2 shows a diagram that specifies the design of various elements of the proposed connector. Moving outwards from the center, the first element is a threaded 1/4-20 hole that allows for modules to be securely bolted together. Outside of this the circle area up to 30 mm is a flat plate of magnetic steel which is as flat as possible and is aligned as precisely to the connector interface plane as possible. This area allows for additional gripping forces using either permanent magnets or electromagnets. The following area between a 30 mm circle, and the almost-circular 70 mm ring is dedicated to the electronics. More detail of the specifications for the electronics section can be found in Section 4.10. The final area further than a 70 mm diameter ring holds the eight alignment and attachment magnets as well as the kinematic coupling.

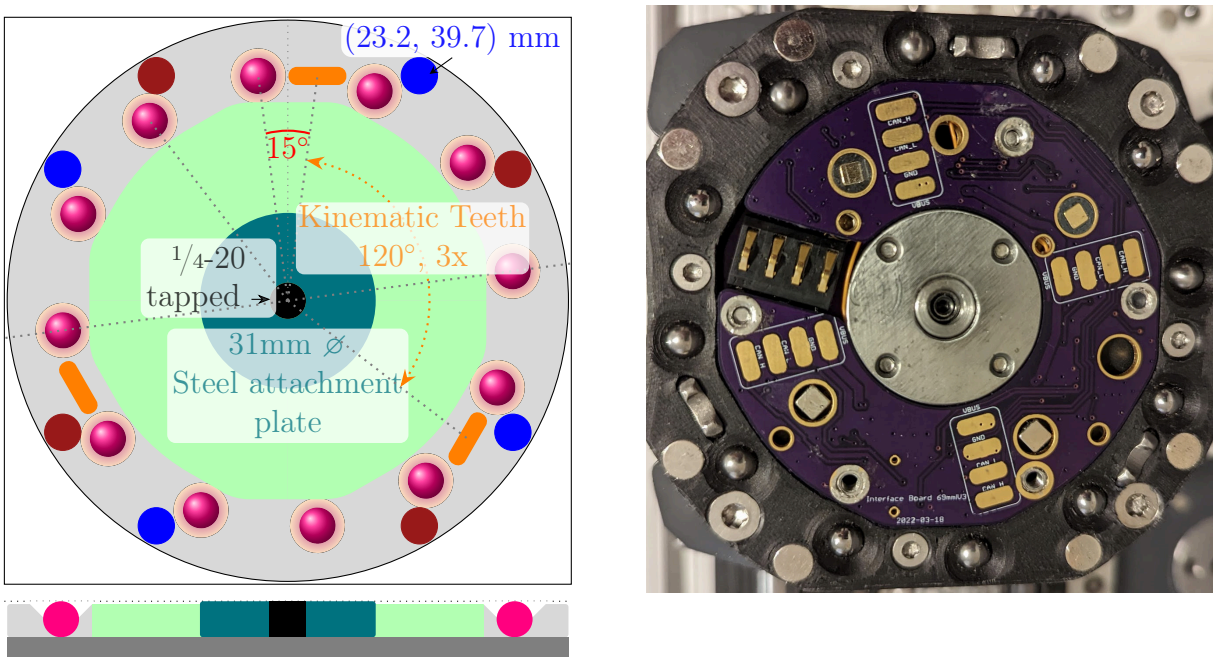

Figure 4.2: Connector diagram and image. This 100 mm round connector has multiple parallel systems with the core feature allowing basic connection is a relatively standard 8x permanent magnet lattice attachment system, shown in *red and blue* on the left, and *silver* on the right image. The novel aspect of this connector is a low-cost non-gendered kinematic coupling alignment system which can repeatably position modular elements to sub 10 um repeatability. This systems includes 12x 6.35 mm diameter hardened steel spheres arrayed on an 80mm circle in 30° rotationally symmetric increments. These spheres are offset by 7.5 degrees from the Y-axis in order to allow for non-gendered connections. The electronics and ID detection system fit in the *light green* area in the left image and are detailed further in Section 4.10.

4.4 Repeatability and Precision in Modular Robot Connectors

The tendency for modular connectors to introduce significant positioning errors is one of the significant problems with machines constructed out of modular components. In addition to being able to efficiently move modules around a lattice structure, being able to place them accurately relative to the rest of the structure increases the practical usefulness of modular machines since it lessens the need to perform extensive calibration and error registration after every reconfiguration. In order to begin to systematically compare this aspect of modular assembly we introduce the *Lattice Repeatability Factor* metric in Equation 4.1, which is intended to provide a statistical estimate of how far any two lattice elements will be from their nominal grid positions after being assembled, or to think of it another way, it represents the expected error per distance of assembled structure.

$$LRF = \sqrt{(\sigma_{rep})^2 + (\sigma_{acc})^2} \tag{4.1}$$

where:

- LRF is the proposed benchmark, the modular lattice repeatability factor
- σ_{rep} is the standard deviation of experimentally measured repeatability of a single connector using a CMM or dial indicator.
- σ_{acc} is the standard deviation of experimentally measured accuracy of the center of a representative subset of adjacent pair of connectors in the system.

In order to calculate the LRF metric for this system we have performed two preliminary experiments. The first involved manually moving and measuring a single connector with 1 um resolution using a Mititoyo dial indicator modular block multiple times, with the results shown in Figure 4.7. The second experiment which uses a RoombaCat metamodule to move a calibration test module repeatedly to the same lattice cell is shown in Figure 8.1. The result from five similar experiments and measurement of various grid pairs performed manually result in a standard deviation of $\sigma_{rep} = 21$ um. Additionally, to calculate σ_{acc} the offset from 100 mm was measured with calipers for various module pairs with a resulting standard deviation of around 900 um. After dividing by the H final LRF metric is dominated by σ_{acc} and is estimated to be 0.9 mm.

While the nominal dimensions for this system involve modules being located on a perfect 100 mm lattice, in reality there are many points where errors are introduced, including (1) the inaccuracies of the physical dimensions of the constituent modules, and (2) the inaccuracies introduced by the location of each connector relative to the adjacent faces. The dimensional accuracy metric (σ_{acc}) is several orders of magnitude worse than the repeatability metric. This points to two conclusions, (1) the effectiveness of kinematic couplings for repeatable alignments, and (2) the need to develop specialized manufacturing fixtures to make modules with more accurate dimensions.

4.5 Kinematic Coupling Overview and Discussion

A *kinematic coupling* encompasses physical interfaces that implement the concept of exact constraint [49] in order to repeatedly locate and constrain two parts. The 'exact' means the number of independent constraint forces is equal to the number of degrees of freedom that are constrained between two objects, which is usually six. Figure 4.3 illustrates some of the important concepts related to the balance of forces in a kinematic coupling. This figure shows the two parts of the connector with the bottom assembly consisting of the three *purple* kinematic *V*'s which are part of the *dark gray* bottom connector. The *transparent gray* part on top is intended to represent the second connector that mates with it. As a

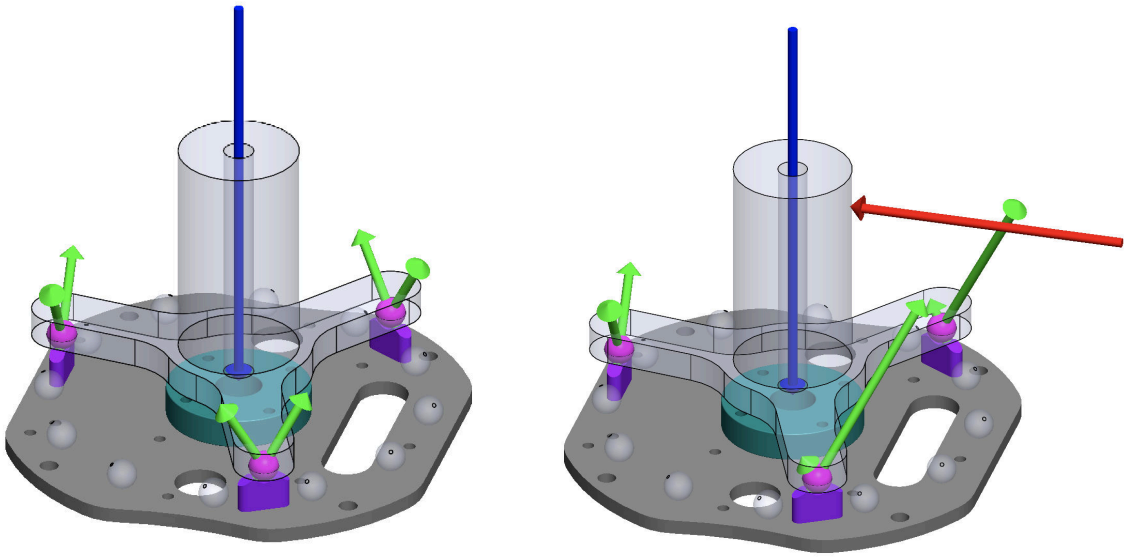

(a) (b)

Figure 4.3: Diagram showing a visual representation of the 3D force balance within a traditional three grove kinematic coupling. Subfigure (a) represents the force balance of a kinematic coupling with only a preload force (shown in *blue*). Assuming this preload force is vertical and centered between the three spheres, the magnitude of the six reaction forces (*green*) are equal to each other due to arguments of symmetry, and the total magnitude can be found through basic trigonometry. Subfigure (b) qualitatively shows how these reaction forces vary under the influence of a disturbance force. The forces still need to balance, and the magnitudes of the six reaction forces will vary until one of the constrain forces reaches zero, which leads to disconnection.

comparison a common alignment feature in precision machines is to use two pins and two holes for alignment. While this type of solution can achieve impressive alignment capabilities, as the tolerance between the diameter of the holes and the pins decreases (therefore increasing repeatability), the ease of automatic connection dramatically decreases due to the introduction of the phenomenon of *jamming*. Ideally, the connection process should be automatic (i.e., you bring two connectors moderately close to each other together and they automatically 'snap' into alignment by themselves). This is difficult for pin-based alignment

methods, but comes naturally for kinematic couplings.

The forces involved with a kinematic coupling have several notable properties. Since there are no interlocking features, there needs to be a *preload* force, which holds the connector together, (shown in 4.3 as the *blue* arrow pointing downward in the center). The preload force is usually generated through some combination of the weight of top component combined with either magnetic forces and/or a bolted connection. The preload is balanced by six contact forces (*green arrows*) which are each formed by a hardened sphere shown in *pink*, that touches the two flat surfaces that are parts of the purple vees, and therefore are always (disregarding friction) perpendicular to the surface of the vee. This means that the directions of the six forces effectively cannot be changed. Therefore in order to achieve static force balance, the magnitude of the forces change in order to adapt to any external disturbance forces.

Kinematic couplings resist external forces through a deterministic combination of the magnitude of the six reaction forces, as illustrated in Figure 4.3a. In a traditional coupling the three vees are traditionally 120 degrees rotationally copied around the center. The angle of the teeth can be varied, as shown in Figure 4.4, but in this systems they have been arbitrarily chosen to be either 45, 35, or 30 degrees. The primary trade-offs involved with this angle is that steeper angles are stiffer in the horizontal direction, but also have to extend further past the connection plane. The further the teeth extend beyond the connection plane the more difficult assembling adjacent blocks becomes, and also it will more likely to fail the hammer test. As long as the distance between the base of the tooth and the center of the sphere is the same, all teeth geometries are compatible with each other assuming there is clearance for the vee next to the matching sphere.

Figure 4.4: Kinematic vee illustration, showing an example cross-section of two of the vee shaped kinematic 'teeth' with two separate vee contact angles with (a) showing a 25 degree angle, and (b) showing 45 degrees. The *dotted red* line shows the interface plane, and the section of grey above that is the part of the vee that permanently extends past this plane. This distance is less the more shallow the angle, but the coupling is also less effective in countering disturbance forces.

4.5.1 Multi-Tile Rectangular Kinematic Couplings

A single properly functioning kinematic coupling perfect constrains two objects to each other. However, this causes the problem of overconstraint when two objects are connected to each other with two or more kinematic couplings. A device that is theoretically overconstrained can often turn into an elastically-averaged design that functions adequately in many circumstances, though at a cost of repeatability, and analytical stiffness predictability. There are several different ways to solve this. One solution is to have a single coupling that spans multiple grid cells. This has the advantage that the coupling better supports the two objects. The downside is that a tile-spanning couplings requires the multiple tiles to always be connected at the same time, therefore precluding actions like holding the module by a single lattice cell.

Figure 4.5 shows a coupling that spans across two connectors that is used on the bottom of the track modules. While kinematic couplings are often made in a rotationally-symmetric manner where each interface point is the same distance from the center, this is not required. As long as the reaction forces are oriented in such a way that at least one of their decomposed vector components can point in any possible 3D direction (analogous to a 3D matrix having linearly independent eigenvectors) then *any* three non-collinear points will work. The danger is that if the shape of the coupling becomes too distorted certain directions of forces will require ever higher preload forces to remain connected.

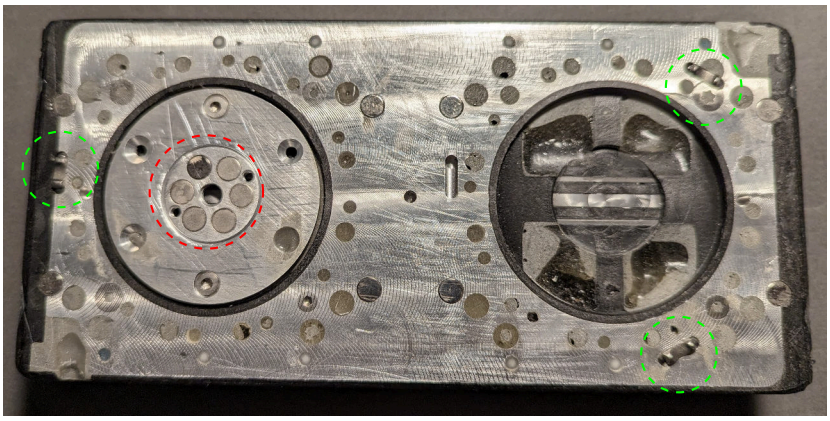

Figure 4.5: In order to avoid overconstraint it is possible to have single kinematic couplings that span multiple grid cells. This example shows the bottom of one of the 2-cell long tracks. The three kinematic teeth are shown with *green circles*. The coupling can be held in place with a preload force from either of the center points of the lattice cells. The section shown in *red* shows a magnetic connector that is embedded in a large threaded hole so that the strength of the bond can be adjusted by rotating it, which moves it either closer or further from the connection plane.

4.6 Kinematic Coupling Design and Analysis

Most kinematic couplings presented in related work consist of three vees and three matching spheres, and are designed to only connect in a single orientation. The first challenge to

apply this design to the problem of a cubic lattice MSRR connector is to rotate copy one of the two elements at 90-degree increments. Choosing to rotationally copy the spheres makes more sense than the vees since they are easier to embed, are inexpensive, and are harder and smoother. The end result is 12x spheres which are each 30 degrees apart, with three different spheres touching the three vees for each 90 degree increment rotation of the two connectors. While kinematic couplings are inherently gendered, this implementation can be described as 'quasi-non-gendered' in that the full functionality of the coupling is only present when an 'A' connector (spheres inset below the connection interface plane) is connected to a 'B' connector which includes the kinematic vees. In the case that two 'A' connections are matched (only 12x spheres) it will provide no kinematic alignment or interact with each other at all. Two connectors which each have both 'A' and 'B' hardware will connect together, but the connection will be over-constrained and while it will gain some increased stiffness, its exact location accuracy and stiffness will be non-deterministic.

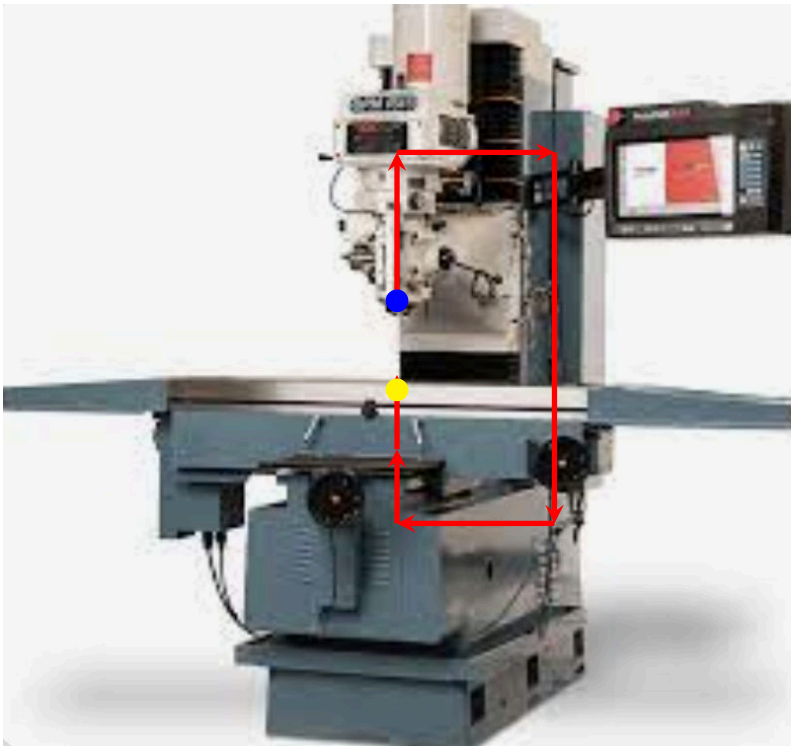

Figure 4.6: Diagram showing an example of structural loop analysis superimposed on a prototrak CNC mill. In this case the structural loop, shown in red, goes between the milling machine's spindle (*blue circle*) and the place where the work-piece is fixtured (*yellow circle*). In the full analysis, each arrow would include the stiffness of that particular element and a matrix representing its kinematics, for example there are at least 4 sets of bearings, as well as structural members which all contribute to the stiffness of the overall structural loop. In traditional machine design applications, one of the primary goals of the machine is to make this loop as compact and stiff as possible. Likewise for the FrFlFuFa system the structural loop 'flows' through a connected set of modules by way of the connectors and structural elements in-between, and can be analyzed using the same conceptual tools.

Structural loop analysis is a method of analyzing the performance of machines in regards to the stiffness between different parts of a machine. Figure 4.6 illustrates the core idea of structural loop analysis. In order to know the stiffness between the two relevant parts of the structure, usually referred to as the workplace and the tool, a mathematical model which accounts for the stiffnesses of each item and the kinematics of the structure needs to be developed. Chapter 6 of Slocum's Precision Machine Design textbook [88] describes in detail the way to implement this approach. This approach uses homogeneous transform matrices (HTM) to represent the kinematics, and with further work this approach should apply in a relatively straightforward manner to a modular machine framework.

To achieve automatic, repeatable, precise alignment, we begin with a magnetic connection mechanism consisting of a non-gendered, 4-fold rotation-symmetric pattern of permanent magnets, similar to that of many modular robotic systems, (e.g., [80], [62]) that automatically snap modules into place but do not provide accuracy or significant mechanical strength by themselves. To achieve repeatable, precise alignment, we use a kinematic coupling interface similar to the type presented in [49]. We add a pattern of 3 V-shaped extrusions, which match with 3 of the 12 matching spheres on the opposite connector. This kinematic pattern is 12-fold rotational-symmetric, which includes the four primary grid directions already achieved with the basic 8 magnet connection. The overall mechanical connection is shown in 4.2, and we demonstrate its repeatability in 4.7 by showing the measured x and y error for a human arm disconnecting and then connecting connection over 25 times. The results had a maximum deviation in either axis of 7 um, and a standard deviation of less than 3 um.

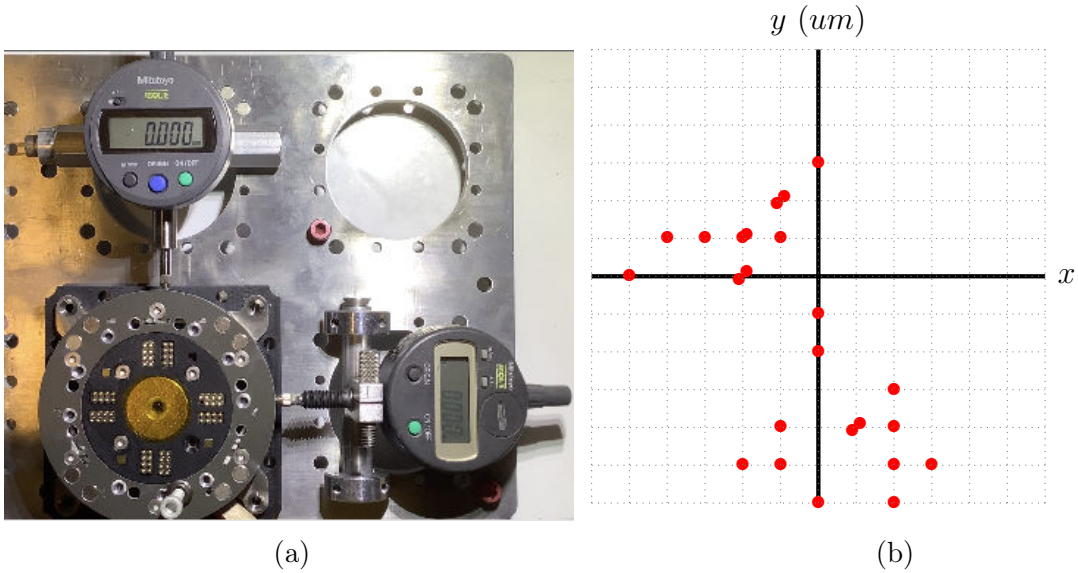

Figure 4.7: Connector characterization experiment (a) uses two digital Mitutoyo dial indicators to graph the x and y offsets (b) from the connector being repeatably connected and disconnected through a very low precision compliant actuator (i.e., a human arm). Note that the indicators give readings to the nearest micron. Overlapping data points are offset slightly for visualization purposes, but all readings in actuality lie on the grid (1 box = 1 um). The kinematic coupling provides for a connection repeatability that exceeds any existing modular self-reconfigurable robotic connectors that we are aware of.

Some of the characteristics of kinematic couplings that make them the ideal for use in modular robot connectors for modular industrial machines include:

1. Can obtain closed form equations for stiffness/deformation of the interface, acting as a structural interface [88].

2. Ability to handle thermal expansion without overconstraint. They expand evenly about their center point when heated or cooled.

3. Use inexpensive and easy to source components, including hardened spheres (i.e., bearing balls) and simple 2D components for the vees. This results in a robust mechanism with few sharp edges, therefore increasing connector robustness.

4. Require only a single additional force referred to as the *preload force* which acts in the center to connect. This allows a decoupling of the preload force from the the primary structural load path which passes through the spheres and vees. This creates predictable and consistent performance even when different methods of generating preloads are employed.

4.6.1 Kinematic Coupling Hertz Contact Force Analysis

The kinematic coupling achieves its repeatability through focusing the entirety of the forces for the connection to six specific points of contact. Specifying exactly which points make contact helps to guarantee the repeatability of the connector. However, the downside is that a sphere-on-plane contact has lower stiffness than other types of interfaces and this can lead to potential permanent plastic deformation of the mating surfaces when exposed to high forces. This section will attempt to estimate the maximum force that this connector is capable of sustaining before plastic deformation in the kinematic features occurs. Hertz contact theory is used to model the stresses and deformations when two curved surfaces (or in this case a curved surface and a flat surface) come into contact under an applied load. Equation 4.2 relates the contact patch radius to several variables which include the applied force, and geometric and material properties of the two bodies.

$$a = \left(\frac{3FR}{4E^*}\right)^{\frac{1}{3}} \tag{4.2}$$

Where:

- a is the contact area radius between the sphere and the plate, measured in meters (m).
- F is the applied force, measured in Newtons (N).
- R is the radius of the sphere, measured in meters (m).
- E^* is the effective modulus of the two contacting bodies, given by:

$$\frac{1}{E^*} = \frac{1-\nu_1^2}{E_1} + \frac{1-\nu_2^2}{E_2} \tag{4.3}$$

While there are already many simplifications built into this model, it can be further simplified by assuming both components are made out of the same material, which reduces Equation 4.3 to simply E/1.8.

The maximum hertzian contact stress ($\sigma_{\max}$) is concentrated below the center of the contact patch ($\sigma_{\max}$), and can be calculated through Equation 4.4. The condition in order to ensure no plastic deformation is for the $\sigma_{\max}$ to be lower than the σ_{yield} of the material.

Where:

- E_1 and ν_1 are the Young's modulus and Poisson's ratio of the first body (sphere).
- E_2 and ν_2 are those of the second body (kinematic teeth).

$$\sigma_{\max} = \left(\frac{3F}{2\pi a^2}\right)^{\frac{1}{2}} \tag{4.4}$$

A full solution to this coupled pair of equations is not necessary to provide the approximate estimate necessary to calculate the number of module mass that can be sustained by a structure. A preliminary estimate can be achieved through picking a value for F, plugging it into Equation 4.2, and then plugging the resulting value for a into Equation 4.4. Using commonly available values for the E, ν, and a sphere radius of 0.003 m, and several guess and check points we end up with a rough estimate of about 20000 N of force before plastic deformation, which is far beyond what the rest of the structure of the modules can handle.

4.7 Connector Forces Characterization

Given the variety of connector hardware designs even in this prototype system, there are numerous unique combinations of mechanical connector interfaces available. These different pairings of connectors might produce different attachment stiffness results. While connectors that are bolted together (see Section 4.8) can be considered as proper structural interfaces, connectors that are held together purely by magnetic forces have lower limits to the maximum forces they can sustain. This maximum connection force varies depending on the direction of the applied forces or moments, with pulling directly apart being the strongest direction. In a result that will be somewhat intuitive for anyone who has played with magnets, applying sheer forces and twisting moments, make separating two connectors much easier.

Figure 4.8 shows a graph of the forces required to slide a structural module which is attached to a connector on a structural plate. The module is preloaded with the basic eight magnetic connector in addition to its weight, and the experiment is run both with (*red line*) and without (*blue line*) the kinematic teeth. The most important takeaway from this experiment is that the stiffness of the connection with the kinematic coupling is almost twice as high as without it. Additionally, as can be seen by the slope change in the graph for the coupling-enabled experiment in Figure 4.8 at around 0.5 mm, this higher stiffness is only there until the teeth from the coupling disengage from the spheres.

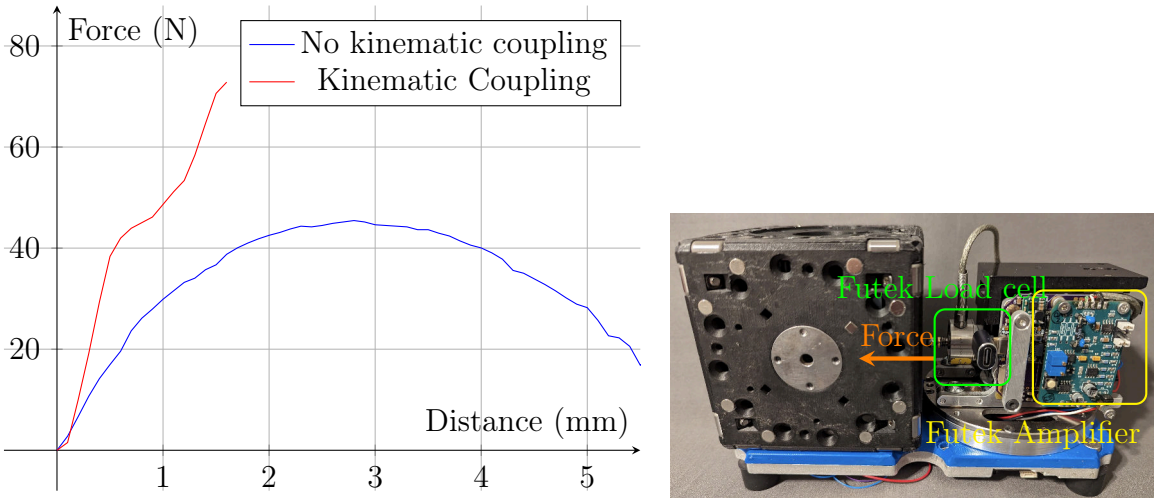

(a) (b)

Figure 4.8: This figure shows a graph of the force required to slide two different connectors horizontally. The X axis shows the distance displaced from the zero position, while the Y axis shows the force as measured by a special module that includes a force sensor and a linear actuator. The change in the stiffness of the *red* line near x = 0.5 mm is likely caused by the sphere sliding past the matching kinematic vee tooth.

4.8 Automatic Bolting Mechanism Design

Despite bolted connections being ubiquitous in everyday life and part of the design of traditional machinery, few modular robots or digital materials in the related works use them as switchable connectors. While there are several MSRR connector mechanisms that are screw-like (e.g., the RoFi Connector [55]) one of the only MSRR connectors that is able to bolt blocks together is the connector from the SMAC [52] smart blocks. This connector is used to bolt blocks together, but is gendered - meaning that if two of the connectors are placed together they cannot form a connection. In the SMAC system, each block has 5 concave threaded connectors, and a single convex threaded connector, so the orientation of the parts needs to be considered when bolting. The rest of this section will present the design of a novel cost-effective and simple self-screwing connector mechanism implemented into the connector design already described in this chapter.

$$F = \frac{T_{in} \cdot 2\pi \cdot \eta}{l} \tag{4.5}$$

1. F : Axial force or preload generated by the bolt.
2. T_{in} : Applied torque.
3. η : Overall friction coefficient.
4. l : Lead of the screw.

Consider the basic screw equation which relates the torque applied to a screw to the force pulling up on the nut, Equation 4.5 shows the force that can be expected from a simple screw. This force obtains a high mechanical advantage due to the geometry of the screw itself due to relatively fine pitch of the 1/4-20 thread used in this connector. However, for calculating the final clamping force, the coefficient of friction is an important factor that reduces the effective clamping force that should be experimentally measured.

Creating a self-bolting connection presents several difficulties that have to be overcome carefully. While (most) humans have little trouble using a screw driver to tighten a bolt, the physical forces and motions involved with accomplishing this task in an automated manner are non-trivial. Here is a rough description of the various steps required to tightening a screw and the difficulties involved in automating this action.

- while the screw connector is not engaged, some mechanism needs to hold the screw in the retracted position.
- A force needs to push the bolt into the threaded nut, and this needs needs to be uncoupled to any other degrees of motion. The point where the force is applied must be able to freely translate up and down in the direction of the axis of the bolt.
- While maintaining the previous downwards force, a clockwise torque needs to be applied for an unknown angle. This torque either needs to be controlled through a feedback loop, or have some mechanism for safely limiting its maximum magnitude when the bolt is fully bolted to prevent damage to the mechanism.
- In order to unbolt the connections, a torque, likely higher than that applied in the previous step, needs to be applied in the reverse direction, until the threads fully disengage.

There are several design challenges with attempting to create an automated screw connector, involving both the linear force mechanism and the torque application mechanism. The first issue is the linear force that pushes the bolt into the threads of the nut. The mechanism applying this force needs to be capable of continuous (i.e., more than 360 degree) rotational motion and linear travel at the same time. There is a standard machine component called the ballspline, which accomplishes the basic requirements of this motion. However, most ballsplines are long, cannot easily be machined due to the use of hardened steel, and are prohibitively expensive. The design presented in figure 4.10 accomplishes the same motion, but using a single 3D printed component and three $1 bearings to approximate a ball spline.

4.8.1 AutoBolt Mechanism Design

This section presents a design for a self-bolting connector that can optionally be integrated into FrFlFuFa designs assuming space is available. In particular several prototypes of this connector have been created and have been integrated into two of the carts (Chapter 5) and one of the faces in both the single and triple structural blocks. There are three main challenges with this design. The first challenge is how to make sure that the linear spring force is turned off while the screw is in the retracted position. This is effectively the same as how to make the device non-gendered. The second challenge is how to transfer the torque

from the actuator to the screw while it is free to translate up and down. The final challenge is how to make sure that the force generated when the screw is spun in reverse does not destroy the mechanism.

The first challenge is how to make the connector non-gendered, while not exceeding the simplicity of a single rotational actuator as the control device. This is accomplished through the use of a threaded steel nut shown in *bright green* in the center of Figure 4.10 in combination with a thrust bearing, which is shown in pink, and is immediately below the nut. When clockwise torque is applied to the large 3D-printed component that functions as the ball spline the nut travels down the screw until the thrust bearing makes contact. Once this occurs, the green nut and all of the rest of the parts of the *screw assembly* shown in Figure 4.9, spin as a single screw-like component that is pushed outwards by the cantilevered spring shown in the bottom of the figure. Torque is transferred from the thread *through* the thrust bearing to the bright green nut, thereby coupling these two as a single assembly. A clockwise torque can be applied indefinitely until the screw 'catches' onto and engages with a matching threaded hole, thereby bolting the two connectors together.

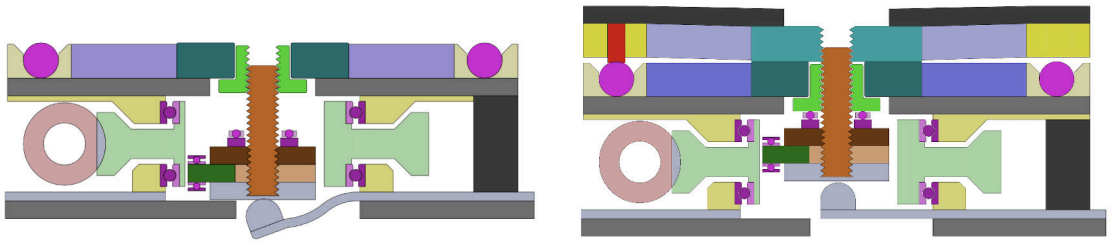

(a) (b)

Figure 4.9: Cross sectional view of the AutoBolt connector mechanism. (a) shows an AutoBolt connector in the retracted state, with the flexural spring at maximum deflection. In this state, no parts of the mechanism extend past the connection plane. (b) shows the connector while it is attached to an adjacent module. The angle shown between the two shades of purple is an exaggeration of the slight flexing (nominally 0.05 mm) of the connector when bolted at full strength. This preloads the kinematic coupling and effectively turns it into a quasi-kinematic coupling [91], as it is constrained by both the interface between the two steel plates (*teal, lighter teal*) as well as the kinematic coupling teeth. This is an optional design feature, as if the top steel plate and structure are stiff enough, it will behave as a traditional kinematic coupling where all of the compressive forces are transmitted through the six points of contact of the kinematic elements.

The magic happens when a counter-clockwise torque is applied to the 3D printed ball-spline gear. The thrust bearing now allows the bright green nut to become disconnected from the rest of the screw assembly, and as long as the friction between the green nut and the blue steel plate is higher than that of the threads between the screw and the green nut. Images of these parts can be found in Figure 4.11. In this case, the green nut effectively becomes joined to the teal steel plate instead of the screw assembly. Now as CCW torque is continually applied to the screw assembly, the entire assembly minus the green nut retracts downward, first disengaging the exposed thread from the mating connector, compressing the cantilevered spring and pushing the bright green nut further into the teal plate. Once the

screw spins CCW as far as it can travel, the concave thread at the top of the green nut is exposed and can accept a screw thread from a connector just as any regular connector plate, thereby allowing non-gendered operation.

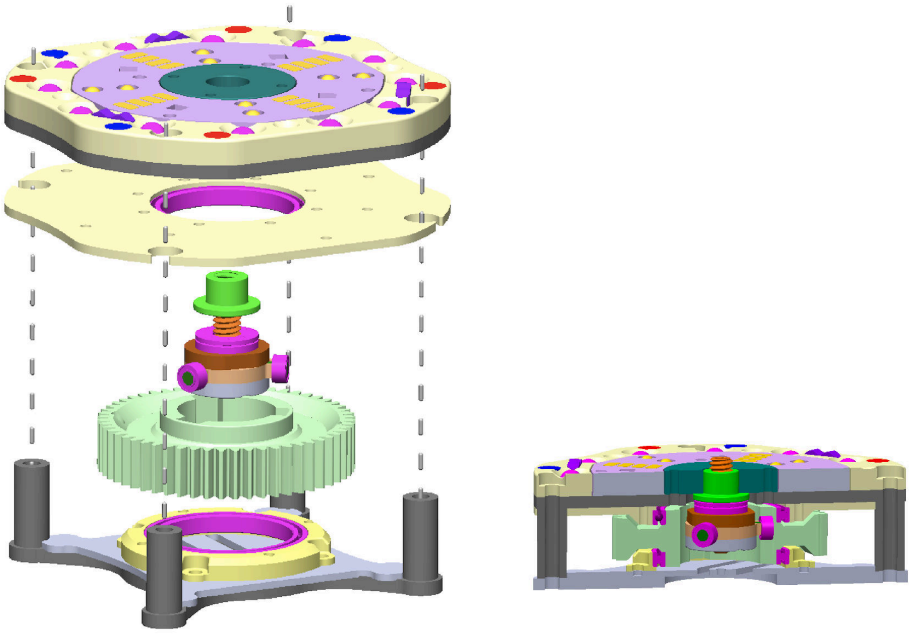

(a) (b)

Figure 4.10: This diagram shows two CAD views of the AutoBolt novel low-cost ungendered automatic bolting system for modular robots. Three ball bearings (*pink rings*, only 2 visible) roll along the a *light green* three-way symmetric 3D-printed geared spline ring, which is supported by two thin section large diameter ball bearings shown in *pink*. The structure is held by the 2D precision ground steel plate in the center, shown in *dark green*, which has a 10 mm clearance fit hole located in its center.

This design is effective for high-force connections since the structural loop of the connector is effectively isolated from the mechanism used to apply torques to the connector. This primary structural loop is stiff since it only goes through steel or a thick aluminum plate. While this connector has not been tested to failure, it should have effectively the same strength as a single 1/4-20 threaded bolt, which according to standard tables can be upwards of a thousand pounds.

4.8.2 AutoBolt Performance Overview

The ultimate goal for an active connector is to be able to switch a high-strength bond on and off as quickly as possible. The time and estimated performance of the three different variants of the screw connectors are shown in Table 4.1. The mechanism which holds the bolt and acts as the ballspline transmission was designed to be separate from the method of applying torque. Separating these parts of the mechanism allows for the performance, cost, and size of several types of driving mechanisms to be evaluated. The brushless motor

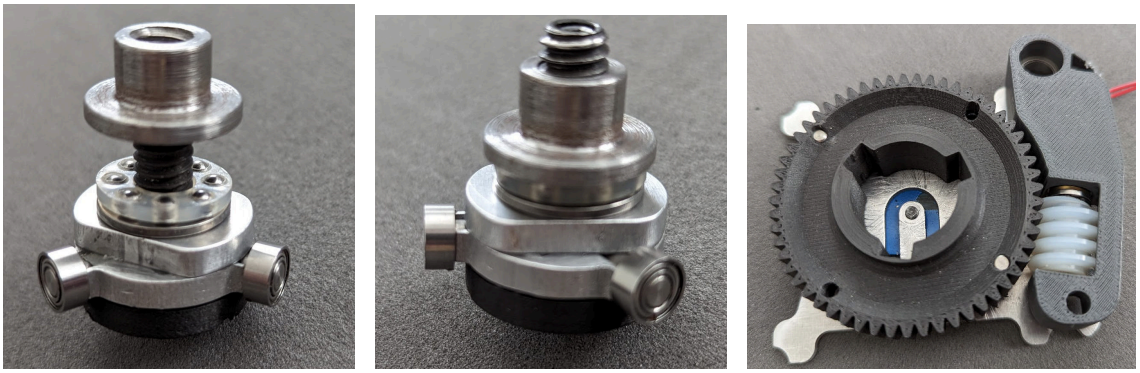

(a) (b) (c)

Figure 4.11: Images of the AutoBolt internal screw assembly, including the internal both in the retracted (a), and extended (b) positions. The third image (c) shows the 3D printed spline shaft, the cantilevered flexural spring, and a spring-loaded worm gear drive.

Table 4.1: AutoBolt actuation methods performance results table showing results for different types of motor drives which have been developed. The highest performance method is to use a dedicated BLDC motor, as it is faster and better able to detect its own state through current sensing than the other approaches. A method for detecting when the connector is fully tightened proved to be important feature in order to protect the gearing and motor.

Variant	Time (s)	Bounding Box	est. cost
Manual - Base	5-10	Compact	$20
BLDC geared	0.5	Large	$60
DC Worm Gear	5	Compact	$30
Friction drive	1	Medium	$30

driven versions are both faster and easier to safely control, but take up more space and are more expensive. The worm gear driven approach is shown in Figure 4.11c, and implements a safe torque limiting feature by pushing the worm into the large gear with a spring. This approach is a typical method used in precision machines to limit backlash, but it also leads to the worm being pushed away when the torque is too large.

The autobolt mechanism spins in reverse to retract and hold the bolt against the bottom of the mechanism, therefore presenting a threaded hole to the outside. However, since screws have such a high mechanical advantage, care must be take to limit the maximum torque applied in the reverse direction. If the mechanism is run in reverse with a high torque after the nut has fully reached the bottom of its travel range, it generates a high force that is difficult to counter with the structure of the current mechanism. In order to safely retract the mechanism, some method of limiting this torque, or increasing the strength of the frame of the entire device is necessary.

4.9 Active Electromagnet Connectors

Many modular robots use 8x passive permanent magnets as the primary method of forming connections between modules. However, there are many problems with this approach in practical use. The uncertainty of making sure the correct connector disconnects when intended is exacerbated by the potential variations in the magnetic forces due to manufacturing and component tolerances. Many modular robots have used different types of electromagnets in order to help form temporarily higher local bond strengths [43]. Electromagnets have many advantages, they are inexpensive and easily available commercially, they enable and disable quickly, they require only a single small brushed motor driver to actuate, and they disconnect gracefully under load. However, there is a single glaring problem, they require continuous power application, which limits their possible duty cycle at high currents.

This problem has lead several groups to implement a close cousin of the electromagnet called electro-permanent magnets (EPM), as notable in the SMORES robots [86], and the MICHE dissembling cubes [32]. These devices have most of the benefits of electromagnets, but with the ability to sustain the actuation force indefinitely without power. The downside is that extremely large currents are needed to 'switch' the EPM between on and off states, requiring moderately sophisticated power electronics circuitry. Additionally at present, there are few if any available commercial sources for these, requiring hand fabrication in most situations. While these certainly have a promising future for MSRR connectors, they are not practical yet.

In a system which has high-power and fast-moving dynamic motions, large connections forces are mostly required for short bursts of time, as are required for pulling a passive block away from a lattice position. In this case an electromagnet switchable connector can be run at high power, but only for a short period of time, therefore allowing for high peak connection strength, at the cost of limited duty cycle. In the existing system presented in this thesis, these electromagnet connectors were too bulky to include directly in the assembler robot Belty, but have been tested as the connector payload in one of the carts (Figure 3.2a), as well as in passive blocks and select structural lattice plates.

4.10 Interface Electronics Controllers

The two external connectors based on a custom layout of the Teensy 3.2 chipset [92], one for the rotating foot, and one on the fixed foot, have special circuit boards that are designed to safely manage the connector. The connector has three main goals: (1) acting as the physical layer for the shared CAN bus communication network, (2) acting as switchable current limited power supplies to share power with other elements in the system and (3) to read information which is magnetically embedded in the attached connector using the magnetic barcode system described in 4.11. Safe power distribution is handled by an electronic fuse, the TPS26633 that has an adjustable current limit up to 6A as shown in Figure 4.13. A I2C controllable digital resistor connected to the current limit pin on the eFuse allows for the output current level to be set in the range of 0.6 to 6A. This eFuse chip is able to quickly detect and disconnect during a large array of electrical faults including short circuits and overcurrent events. Additionally the connector power path is protected by several diodes

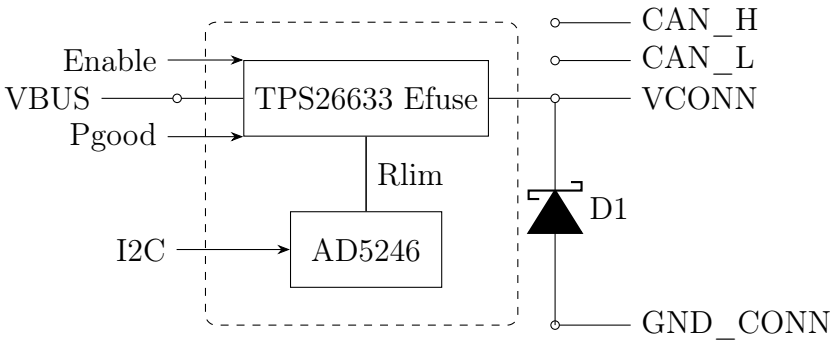

Figure 4.12: Output protection circuit schematic. This shows how the power path that is exposed through the connectors is protected. The CAN low and CAN high wires are naturally protected by the circuitry in the transceivers up to ± 36 volts, and often up to ± 70V. The TPS26633 is a switchable electronic fuse from Texas Instruments that can set a current limit from between 600 to 6000 mA. A diode *D1* handles the case where a bus voltage is applied in the reverse direction (i.e., GND_{conn} to $VBUS_{external}$ vice versa). The diode effectively shorts out this source, so if the power source can source more current than the diode's rating the circuit will fail.

that allow *any* shorting of the four output wires to each other up to -6A of current up to plus or minus 36 Volts.

The interface board for Belty's non-rotating foot has a magnetic ID barcode reader based on four ALS31313 3-axis magnetic field sensors, an IMU, as well as an 8x8 grid lidar sensor provided by the ST VL53L5CX in order to remotely track local lattice positions. The magnetic ID reading system reads three components of magnetic field from four magnets embedded in the attached connector to generate a vector of 12x single byte values. These values are compared using a least squares difference sum against an internal list of known connectors. This system allows the connector to identify possible millions of unique magnetic tags, as described in further detail in 4.11. The lidar sensor can be used by the robot to identify if lattice positions are occupied before trying to move into them or manipulate components into specific lattice cells.

4.11 Connector Magnetic ID Tags

This section introduces a refined implementation of the magnetic fiducial tags, which were initially introduced on the 3D M-Block modules in 2019 [39]. The goal of these tags is to support the ability for connected groupings of modules to determine their configuration. This is a problem that has seen much development in related work, some of which is discussed in Section 2.2.3. These tags can be considered as a form of a magnetic barcode that embeds a specific identity into the physical connector that can be read by a *tag reader*. The reader is an I2C based peripheral consisting of four 3-axis magnetic field sensors, which are not visible, but are on the bottom of the circuit board in Figure 4.13a.

Our system uses a 'tag' of 4x specifically placed permanent magnets which are on a 50 mm diameter circle, and four 3D-Hall-effect sensors which are mirrored along the plane

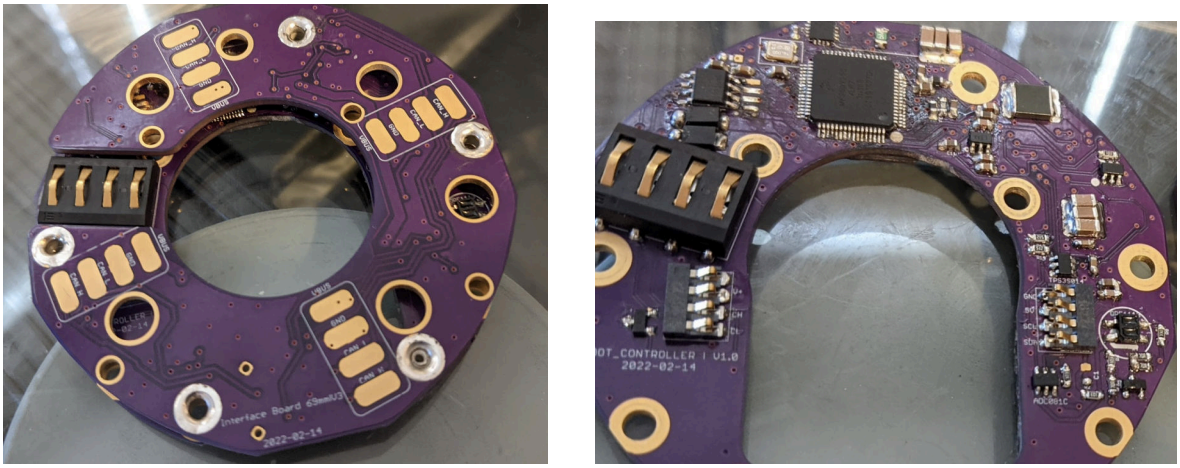

(a) (b)

Figure 4.13: This figure shows a close up of a complete interface circuit board which is integrated into Belty's non-rotating foot as well as other modules like the carts and structural modules. This board is based on a custom implementation of the Teensy 3.2 microcontroller, and has a power sharing protection circuit based on the TPS26633 eFuse chip which is combined with a digital potentiometer to be able to output a bus voltage with a controllable maximum current, effectively acting as a miniature power supply.

of symmetry of the connector to read them.

This system should be able to support millions of unique ID's with very low cost/weight tags with each tag costing on the order of 10 cents, and a moderately priced tag reading electronic components (approaching $4 per reader in high quantities). The connections between modules in a modular system involves a minimum of three unique parameters:

1. Some form of identity or *ID* of the two modules in question.
2. The connector number, or *face number* for each of the modules.
3. The *orientation* of the connection, which in a cubic lattice is one of four possible 90-degree values.

The MFTags fiducial tag system allows modules to detect information about their neighbors through local magnetic fields, and an overview of their design is shown in Figure 4.14. The following design criteria were taken into consideration while creating MFTags, specifically that they should be able to:

- *Be read passively* - information can be read even when the module is inactive. This greatly improves the reliability of a large system and facilitates the inclusion of non-powered passive modules into the system.
- *Be fabricated inexpensively* - necessary for systems with many connectors.
- *Identify many unique ID's* - needs to provide unique ID for many tags in large systems.

- *Detect connector orientations* - the tag needs to determine the 90-degree angle of the tag relative to the reader.
- *Robustness* - the tag should be able to be immune to damage or disruption from environmental factors that might be present in industrial environments, such as differing lighting, liquids like cutting fluid, or RF interference.

The exact performance of the MFTag system is implementation dependent (i.e., different size/shape magnets, sensors). In preliminary experiments any reader was able to correctly identify almost every tag after being programmed with a table of measured magnetic field data. The resolution of the magnetic sensors that are used (Allegro Microsystems ALS31313) is 12 bits per axis, but this is down-sampled to 8 bits per each X-Y-Z axis, resulting in 12 bytes of information for each tag. There are many factors which influence the accuracy of the sensor readings in the context of the MFTags. The following factors contribute to potential identification errors:

1. The relative alignment of the face containing the tag to the face containing the reader. The kinematic couplings help minimize this, but it is more of a concern for a pair of connectors without the kinematic teeth.
2. Alignment of the magnetic sensor relative to the face of the reader module.
3. Variability or changes over time of the magnetic field direction in the magnets themselves.
4. Effects of interference from nearby external magnetic fields, including most notably, the embedded magnets that encode the reader's tag.

Factors 2 and 4 appear to be the most significant contributors to the errors seen in this system. Much of the error from point 2 is due to the inaccurate, hand-soldered nature of this prototype system. For the errors from point 4, the offset distance from the magnets to the readers should possibly be increased in future implementations of this system.

The underlying hypothesis behind this tagging solution is that low cost and lack of radio transmissions make magnets an attractive choice for a technology that may have to be

Table 4.2: Information content in the MFTags encoding specification. The initial prototype system was limited to 2 angle sensors due to practical considerations of the physical dimensions of the PCBa's in the 3D M-Blocks. The system for this project has been extended with the use of four 3-axis magnetic field sensors (ALS31313), and a more open digitization system.

	M-Blocks [39]	Current System	Future
Magnets	4	4	4
Digits	30	N/A	48
# Of Sensors	2	4	4
Unique Tags	900	100,000	5,000,000

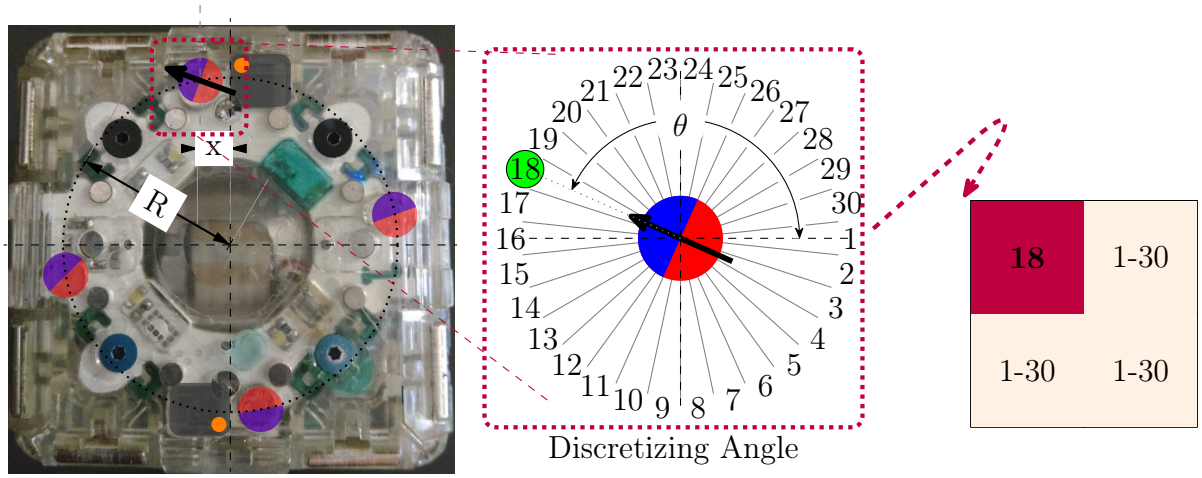

Figure 4.14: Figure illustrating the MFTags system. A tag consists of four permanent magnets placed according to two dimensions, (R) is the circle diameter, and (x) is the offset from the y axis. The left half shows a photo of one of the m-blocks from the previous implementation superimposed with the magnets and sensors. The magnetic field relative to a line extending from the center of the face is then digitized by a 3D Hall effect sensor (represented by the rounded black rectangle with an orange dot).

implemented thousands of times in a set of reconfigurable modules. The strength of magnetic fields drops extremely quickly versus distance. This allows the ability to use several sensors at close proximity prevents interference between reading faces while still providing enough information to read tag orientation and determine a unique tag identity. This is in contrast to solutions like NFC or RFID, where it might be difficult to disambiguate between several adjacent tags due to the longer range of these protocols.

Chapter 5

Modular Linear Actuators and Magnetic Lead Screws

Every robotic or mechatronic system has *actuators* that move things relative to each other. Actuators consists of a primary power generating source, which is usually an electric motor, but can also be another source of stored energy (e.g., pressure reservoir, chemical reaction), and often also a *power transmission* element which is able to modulate between speed and force at a cost of a loss of energy to heat. This chapter introduces the MagnaCarta modular linear actuator system which is based on magnetic lead screws, and was previously published in [5], which forms the base of this chapter. These actuators were inspired by the industrial gantry machines like the CNC milling machine, waterjet and 3D printers used to built prototype parts in the CSAIL machine shop. The actuators presented in this section do not have the required stiffness to make practical CNC machines, but they can help to lay the groundwork for future CNC-grade modular linear actuators. Additionally this lack of stiffness allows for the compliance and the ability to sense forces that help simplify the task of assembly.

Most industrial linear motion systems use ball screws or belts as their power transmission elements. While these have many characteristics favorable for machines, they can not easily be turned into the *deeply* modular actuators necessary for scalable modular systems. This chapter discusses difficulties inherent in making linear actuators modular in Section 5.1, and provides a listing of linear transmission mechanisms and their suitability for creating modular systems. While there are some modular linear actuators for industrial applications, many of these are linear motors or rack and pinion drives, which present significant challenges for practical use in precision modular machines.

Magnetic Lead Screws (MLS) are like traditional mechanical screws, but instead of physical sliding or rolling contact contact they use magnetic fields that function as the threads. This results in extremely high efficiency as well as an inherent ability to gracefully handle impacts and engagements and disengagements of their threads, making them well-suited to modular systems. Magnetic lead screws are relatively new, and we are only aware of a handful of actual physical prototypes that have been constructed, and few uses in the robotics field. Section 5.2 gives an overview of this related work and further discusses the benefits and trade-offs of MLS.

The rest of the chapter discusses the design and characterization of a new modular Mag-

naCarta magnetic lead screw actuator. This system modifies the traditional MLS design in order to accommodate a modular form factor. Section 5.3 details the mechanical and electrical design of the MagnaCarta system. Section 5.5 provides characterization and analysis of several key aspects of the design of the MagnaCarta system, including the preload force and the track-to-track transition. Finally, Section 5.6 shares preliminary information regarding the prospect of combining multiple MagnaCarta actuators in series to increase the actuation force and stability.

5.1 Modular Linear Actuators Overview

It can be claimed that all power transmission mechanisms are series elastic actuators, just of (widely) varying stiffnesses [93]. A very stiff strain wave gear combined with a force/torque sensor is in some ways the same as a spring based series elastic actuator, as both measure forces by sensing the deflection of an elastic element. However, the spring in the force sensor based system is designed to be as stiff as possible, usually in order to maximize the position control loop bandwidth. The wide range of possible stiffnesses illustrate several of the trade-offs involved with designing force sensing actuator mechanisms, and explains some of the particular advantages of using magnetic springs as series elastic actuators.

Creating a modular linear actuator is more challenging than it might initially appear. Many of the most commonly used linear actuator mechanisms, (e.g., ball screws, lead screws, roller screws and belts) are fundamentally difficult if not impossible to truly make modular due to the interlocking structural loops inherent in their designs. While there are some "modularizable" linear actuator mechanisms, each of these have significant practical challenges, specifically: linear motors (low force/weight), rack and pinion system (requires lubrication and precision machined surfaces), and friction based drives (requires high normal forces).

Table 5.1 lists some of the common (and uncommon) linear actuator power transmissions, and comments on how modularizable they are. While there are many linear-to-rotational power conversion mechanisms, few of them are suited for creating deeply modular linear actuators. One of the most interesting potential solutions besides the MLS is a mechanism alternatively called the roller pinion drive or the roller gear mechanism [94]. This mechanism is similar to a rack and pinion, except it uses rolling pins and a cyclodial shaped rack. This mechanism claims to have zero backlash while also providing high stiffness, high efficiency, and high accuracy without the friction and need for oil that comes with standard involute-profile geared rack and pinions. While this transmission has not been used in many academic robotics projects, a company called Nexen [95] offers them as a product, although they are quite expensive. Roller gears might be a great candidate for future higher-stiffness modular linear actuators. However, one of the challenges is that their design necessitates a rather large diameter driving pinion wheel, which results in a low mechanical advantage ratio. While they can be combined with additional gearing to address this problem, this will increase the complexity, cost, and size for any roller-pinion based modular actuators.

Screws are arguably the most important category of actuators for machines and industrial motion. There are some interesting and exotic types of screws including the friction based drive screw, fluid screws, and roller screws that each have useful applications. However, these types of screws as well as the more well known ball and lead screws are difficult if

Table 5.1: Listing of rotary-to-linear motion mechanisms and discussion of their potential for creating deeply modular linear actuators. There are several broad classes of transmissions including screw-based, wheel based, and tension based. The most important practical characteristics machine designers consider when choosing between these include their stiffness, backlash, mechanical advantage ratio, form factor, and cost.

Type	**Name**	**Use**	**Mod Difficulty**	**Notes**
Screws	Lead Screws	common	difficult	
	Ball Screws	common	impossible	CNC machines
	Roller Screws	less common	impossible	ultra high force
	Fluid Screws	rare	impossible	mostly theoretical
	Magnetic Screws	rare	easy	no known commercial use
	Friction Screws	rare	possible	misc. machinery
Tensile	Belts	common	impossible	3D printers
	Chains	common	impossible	large industrial
	Cables	less common	impossible	robots and large systems
	Metal bands	less common	impossible	precision instruments
Wheel	Rack and pinion	common	moderate	diverse applications
	Friction drive	rare	moderate	i.e., wheels
	Roller Pinion	rare	moderate	large machines

not impossible to modularize. The fundamental requirement to create a deeply modular screw based actuator is to have the nut able to be separated from the screw without passing through either of the two bearings that support the rotating part of the screw. While there are some lead screws used in vices that have separable nuts, it is all but impossible for ball and roller screws. The sole exception to this is magnetic lead screws, which will be further discussed in the next section.

5.2 Magnetic Lead Screw Related Work Overview

While the feasibility of magnetic screws have been previously presented in prior work, very few actual functioning systems have been built outside of several benchtop prototypes from academic research laboratories. While the most commonly used magnetic gears are rotary-to-rotary and involve the use of iron pole segments which lead to eddy current losses [96], there are several types of iron-free magnetic gears which have mechanical efficiencies approaching 100%. These gearing mechanism include magnetic worm gears [97] presented in 1993 for rotary motion, and magnetic lead screws [98] designed for various linear applications including wave energy generation [99] and suspensions for cars [100]. While these technologies were presented years ago, we are not aware of any products based on these technologies. There are few systems shown in academic robotics literature, besides this interesting but low force application to modular modular robots presented in 2017 [14], and shown in Figure 2.1b. Two examples of MLS are shown in Figure 5.1, with the first taken from [99] and the second created as a prototype proof of concept for this project.

There has been extensive research related to various characteristics of magnetic lead

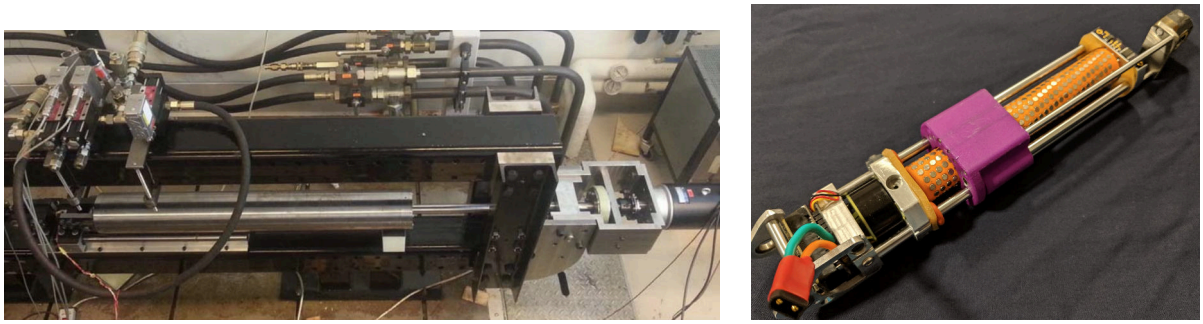

(a) (b)

Figure 5.1: Magnetic lead screws are fascinating high-efficiency power transmissions that are not yet in widespread use. This figure shows in (a) a benchtop prototypes from the wave energy generation project presented in 2013 [99]. This is a large expensive prototype that contains 8.5 kg of permanent magnets, and has a maximum force before the threads slip of 17 kN, resulting in a force to magnet mass (FTMM) ratio of 2. (b) Shows a prototype of low-cost magnetic lead screw actuators built to test the feasibility of creating the MagnaCarta system. This design contains 146 g of magnets and has a slip force of 220 N, and after accounting for length of the nut, it has a FTMM of 1.8. This number is only 10% lower despite using much simpler production methods, thereby validating the feasibility of the low-cost fabrication methods used to create the MagnaCarta system.

screws. The series elastic force sensing performance has been recently studied by Bu and Fujimoto in [101], who were able to demonstrate effective force sensing with a small benchtop prototype, as well as in 2014 in a patent by Rasmussen et al. [102]. Additionally, there have been many theoretical works related to MLS including evaluations of different possible magnet shapes [103], and various magnetic finite element analysis simulation works to help characterize relationships between variables including the lead, magnet dimensions, air gaps, efficiency and maximum axial force [104].

There are several practical challenges related to building magnetic lead screws. The first is that even small screws require hundreds if not thousands of individual magnets carefully placed into position. This task can be simplified by 3D printing, with Figure 5.1b providing an example, but until an industrial supply chain and bespoke tooling can be created it remains a time-consuming and frustrating task. A second challenge is the task of creating the linear bearing constraint. A MLS where the nut is perfectly centered on the screw needs no constraint forces, as Figure 5.10 illustrates. However, this is an unstable equilibrium, and in practice there can be significant radial forces that require stiff linear bearings to counteract. This is a different challenge than working with lead or ball screws, which function like bearings, and can sometimes lead to overconstrained when paired with additional linear bearings.

While most magnetic lead screws presented in related work are essentially the same form as a traditional lead screws with both threads replaced by permanent magnets, there are several works presented that have non-traditional configurations. One example of this a lead screw where the rotating part is ferro-magnetic instead of permanent-magnet based [105]. Another concept [106] shares some similarities with our design, but is designed for use in

transportation systems. This system also has a cut in the non-rotating component as in our system; however, this system does not include any modular segments. Additionally, this system does not appear to include any physically realized mechanism for constraining the screw and the nut.

Magnetic lead screw actuators have many characteristics that match those needed for human like robots that interact with their environments. We have presented a first prototype of such an actuator, and have demonstrated its use in several novel robotic systems. Our actuator is able to accurately measure forces, effortlessly handle impacts that would likely damage other actuators of similar size, and has high mechanical efficiency which is beneficial for battery powered untethered systems. These characteristics make MLS particularly suited for tasks involving assembly operations, such as when working with digital materials.

Magnetic lead screw actuators share basic characteristics with the other types of screw based actuators, including lead screws, ball screws, air screws and roller screws. The basic characteristic of any screw is the lead, which is defined as the amount of linear distance traveled per revolution of the screw. By using the equation 5.1 we can relate the torque of the motor to the force felt at the output of the screw. The important point here is that the screws have a high mechanical advantage as compared to other linear transmission mechanisms. It is difficult to make the pitch of MLS as fine as that of a ball screw, or especially a lead screw. The shortest pitch possible with a MLS is the width of two magnets plus any spacer material between them. Assuming the screw is constructed out of individual cubic or cylindrical magnets, as the desired pitch decreases the required magnet size also decreases which makes it more challenging to fabricate.

$$\text{force} = \frac{torque \cdot 2\pi}{\text{lead}} \times \text{efficiency} \tag{5.1}$$

5.3 Design of MagnaCarta Modular Linear Actuator

This section presents the design of the MagnaCarta system. This brushless-motor-powered modular actuator is the core enabling technology for self-assembling modular robotic gantries in the FrFlFuFa system. This actuator is intended to produce large forces, and to perform precise motions, while still having compliance in the direction of motion. To facilitate easy combination in series or parallel the actuator is robust enough to withstand slight misalignment, can be back-driven, and has high mechanical efficiency. The magnetic field acts as a spring which allows force sensing by treating it as a series elastic actuator. In this thesis we build upon previous research in the MLS field to develop a novel type of magnetic lead screw suited for modular robotic applications.

A typical MLS replaces the interlocking threads of a traditional lead screw's shaft and nut with permanent magnets, arranged in two helices of opposite polarity 5.2. We reimagine the magnetic lead screw as a modular robotic *cart* that slides along modular *track segments*, illustrated in 5.3. This can be seen as a modification of the typical MLS where the spinning part (shaft/cart) has been made shorter than the non-spinning part (nut/track), and the non-spinning part has been cut in half parallel to the axis of the screw. The resultant magnetic force also functions as a preload to bind the cart to the track. The only physical connection between the cart and the track is six small wheels, which are arranged in a

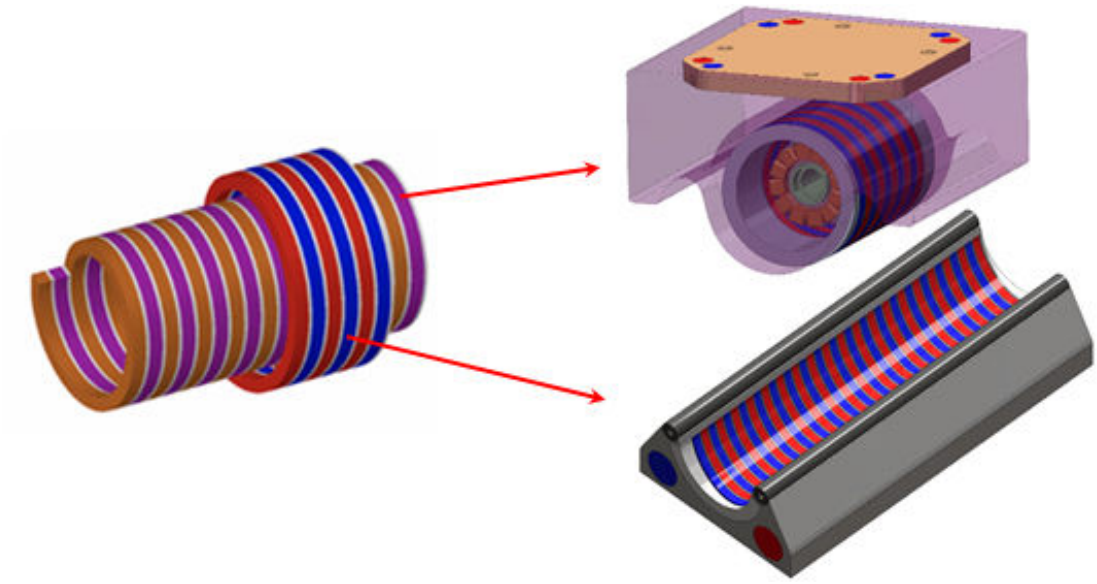

Figure 5.2: A typical MLS (left) consists of a shaft and nut each with two matching opposite polarity permanent magnet helices. We re-imagine the MLS as a modular cart and track (right). The motorized shaft forms the cart, while the nut has transformed into the track by being stretched and cut in half. This design change allows the sidestepping of the challenge to modularity presented by having the rotational bearings on the longer segment seen with a traditional screw form factor.

quasi-exact constraint arrangement, as seen by the *dark purple* cylinders in Figure 5.3. The rotating element of our design called the *spindle* is shown in the middle of the bottom part of Figure 5.3. The spindle integrates both the magnets for the brushless motor and the rotating part of the MLS. The pitch of the MagnaCarta MLS is 10 mm, therefore for every full rotation of the spindle the cart nominally moves 10 mm.

Because the entirety of the actuation forces (i.e., forces along the direction of movement) between the cart and track are transmitted through an air gap (in this system, nominally 1 mm, illustrated by the white space seen in Figure 5.3) by magnetic fields, connecting and disconnecting carts and tracks is easy. Combining carts either in series or in parallel is also feasible due to the high efficiency and tolerance to slight misalignment afforded by the magnetic field. If the stiffness or force of a single cart, as shown in Figure 5.9, is not sufficient, two or more carts can be connected together to make a stronger, stiffer, and more stable combined actuator. Additionally, carts are able to hyper-extend (i.e., travel beyond the travel length of a track) all the way to complete separation of the track and the cart, which can simplify reconfiguration algorithms.

5.3.1 Design of the Spindle and Motor

This section will discuss the core part of the MagnaCarta system, the rotating element referred to as the *spindle*, as well as its brushless motor. The spindle integrates both the magnetic circuit for the motor, and the magnetic lead screw transmission into a single roughly 400 gram component. The spindle is in the direct load path between the magnets on the

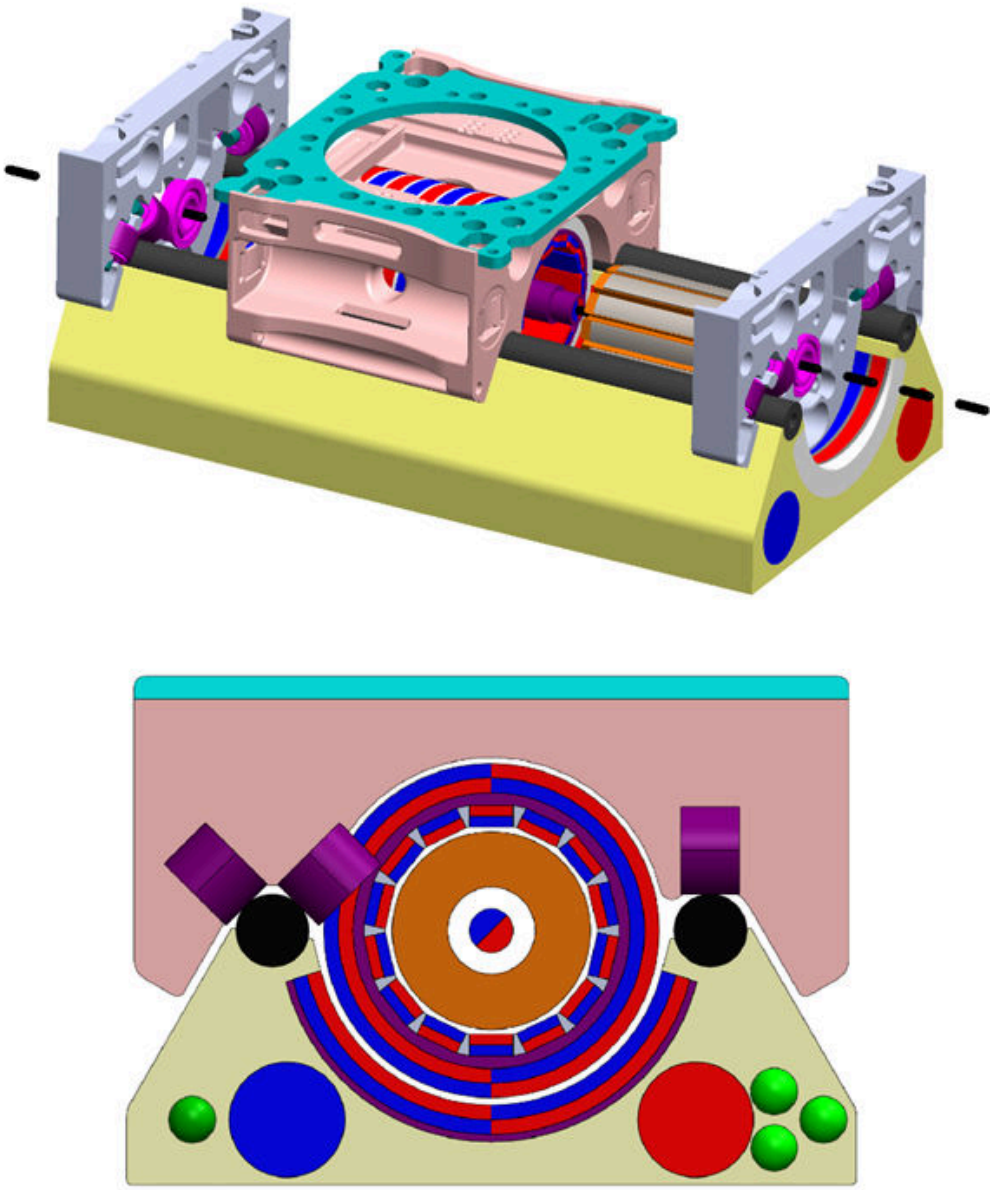

Figure 5.3: This figure illustrates the assembly of the cart module and track segment with an exploded-view (top) and a cross-sectional view (bottom). The core spinning element, the *spindle*, is shown in the center, which is supported by two ball bearings *pink* along the main axis of rotation *dotted line* which are pressed into two machined aluminum side plates *gray*. The two alternating helical magnet arrays *red and blue* on the exterior of the spindle interface with matching helices on the track in order to translate the rotation of the spindle into linear motion. A brushless motor (Turnigy Multistar 2834) with custom high torque-constant windings is the shown in *orange and gray* in the center. Six *purple* wheels provide a sliding constraint between the track and cart. The electronics (not shown) are mounted in a spacer *light red*, which holds the modular connector in, which is shown in *teal*.

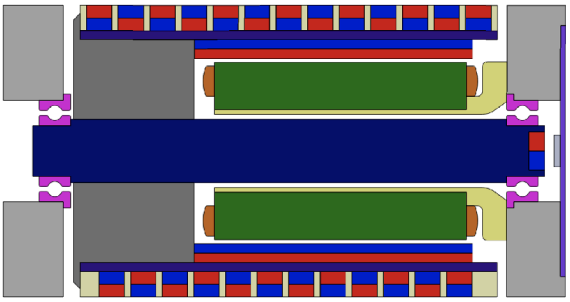

Figure 5.4: This cutaway cross-section of the MagnaCarta spindle illustrates the two magnetic circuits and the mechanical structure of this core component of the modular linear actuator. The 360 outermost 4 mm square *red and blue* N48 permanent magnets form the helical magnetic 'threads' for the magnetic lead screw system, and interact magnetically with matching helices in the tracks. Next is the *thin blue* pair of horizontal lines, which is a precision thin steel tube that provides structural strength to the right cantilevered portion of the magnetic helix, as well as work to align and complete the magnetic circuits for both sets of magnets. Next, also in *red and blue* are the motor rotor magnets, which are N42SH grade (high demagnetization temperature) neodymium magnets that work with the *green and orange* brushless motor rotor to spin the spindle. Finally in *dark blue* is the central precision shaft, which connected on either side to the *gray* aluminum structural side plates through two 8x16x5mm flanged four-point-contact ball bearings.

cart and the track, and thus it has to be able to withstand high forces. These forces might be even more significant when the cart and track are snapped together vertically after being separated.

The detailed design of the spindle can be seen in Figure 5.4. Inside the spindle and attached to the right aluminum structural side plate, is a modified hobby brushless motor (Turnigy Multistar 2834-800) which applies a torque to the rotor magnets on the inside of the spindle. This motor was designed for model aircraft, and had windings with very low torque constant. As can be seen in Figure 5.5 the motor had to be painstakingly rewound in order to increase the K_t enough to generate meaningful torques with the limited available current provided by the two onboard 18650 battery cells.

The core of the spindle is constructed from a precision configurable stepped shaft from Misumi which is 10 mm diameter in the center, and has two 8 mm stepped ends to transfer thrust loads to the two primary spindle bearings. Attached to the core shaft is a turned aluminum spacer which has been reamed and press-fit onto the core shaft. Moving radially outward, a 38 mm outer diameter, 1 mm thick configurable precision steel tube is pressed onto the spacer, which forms the back-iron for the spindle magnets as well as the magnets for the rotor of the motor. These three metal parts are then securely fixed into place with three dowel pins machined at 120 degree radially outward increments in order pin these components together and ensure that it can handle any impact forces encountered during use. The 360 4 mm cube magnets comprising the magnetic threads are pressed into a 3D-printed sleeve which slides over the steel spacer and which sets their position into the required helical shape. Finally, the magnets are set into place with a thin epoxy, and the

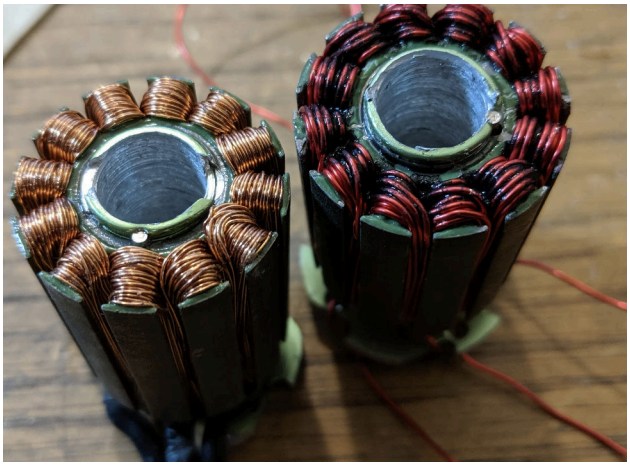

Figure 5.5: On the left this image shows the original as-purchased brushless motor rotor which has a low-torque-constant, low-resistance copper coil windings. On the right is the stator after being hand-rewound to increase its torque constant. A higher torque constant allows for reasonable battery powered operation with the low currents available to the brushless motor controller circuit board. Intuitively the thinner the wire, the higher the torque constant, but after some measurement it was discovered that the original windings have 6-8 fine wires that are all *in parallel* with each other. This likely allows for a better packing density, and potentially a higher surface area to volume ratio for cooling.

whole assembly is lightly sanded and cleaned to try to minimize any chance of protrusions catching on the tracks while it is rotating.

5.3.2 MagnaCarta Electronics System

The electronic system consists of a series of connected custom PCBa boards controlled by a Teensy 3.6 microprocessor. These boards integrate a custom brushless motor control system based on the A4915 mosfet driver, combined with an on-axis magnetic encoder (AK7452) to measure the absolute angle of the spindle. This custom BLDC driver shares a similar schematic as the driver described in Section 6.4, but in a different form factor.

Additionally a set of four three-axis hall effect sensors (ALS31313) are located on the two ends of the cart and are used to determine the cart's position relative to the track, and to detect when the cart extends past the edge of the track. They accomplish this task by measuring the presence of the magnetic field from the track, and with further calibration and software development could be used to estimate the absolute linear position of the cart relative to the track.

The control circuit board can alternatively draw roughy 8 V of voltage from two onboard 18650 battery cells, the *green* cylinder in Figure 5.6b, or up to 24 V through the modular interface connector embedded in the top of the module. The three carts that have been constructed each have different versions of the electronics, and some of the features that are intended to be included in the final version included a Decawave radio module, a small LCD screen, and the ability to share power through the connector.

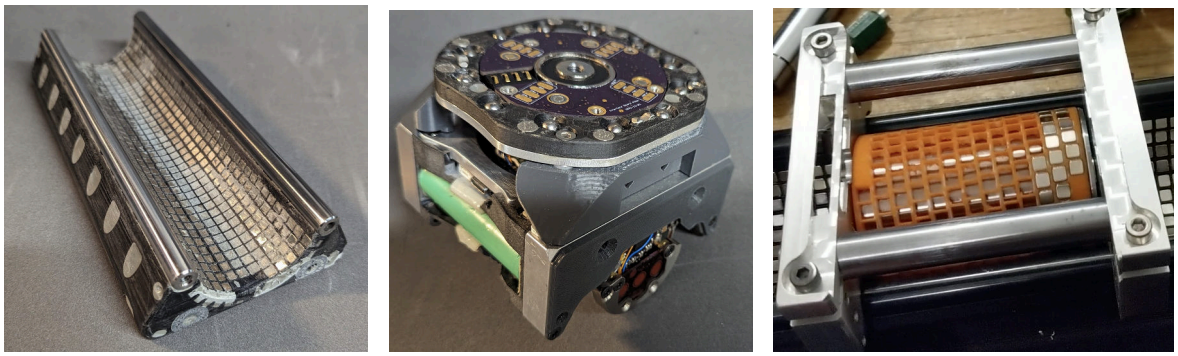

(a) (b) (c)

Figure 5.6: These three images show the final track (a) and cart (b-c) as fabricated. The manufacturing process for these prototypes was quite involved, as the 3D printed parts deformed slightly during assembly. In order to achieve the dimensional accuracy to successfully transition between tracks, the tracks had to be filled with machinable epoxy, and have various mechanical features including the rail positions carefully re-machined.

5.3.3 MagnaCarta Prototype Fabrication Details

Photos of the finalized tracks and carts can be seen in Figure 5.6. A total of three tracks and three carts have been fabricated, along with many spare parts. These prototypes were constructed out of CNC machined and turned metal in the CSAIL machine shop as well as several 3D printed components.

The tracks were built out of a single large 3D printed element which was produced on a HP multi-jet fusion 3D printer through an online fabrication service. This 3D printed part includes individual square holes for each of the roughly 520 4 mm cubic magnets, which were then secured by glue. Several challenges were encountered while assembling these parts, mostly due to deformation causes by the fitting of the magnets into the square holes. The deformation caused the two guide rail positions to move enough so that the cart rubbed against the track leading to increased friction. In order to fix this, the old track rail positions were filled in with machinable epoxy, and the tracks were precisely positioned in a CNC mill by their kinematic couplings and new guide rail positions were milled with a ball endmill.

The design for the cart centers on two half-inch thick 7075 machined aluminum side plates. These plates were carefully machined so that all of the critical relative dimensions between the bearings were machined in a single fixturing. These two plates are held together by two hollow 12 mm precision-ground metal tubes that form the primary structural support between the two plates, as shown in Figure 5.6c. This image shows the partially assembled spindle showcasing the 3D printed magnet spacer as well as the tops of the two aluminum side plates.

5.4 Characterization of the Linear Actuator

MLS are significantly less stiff than traditional power transmission mechanisms that involve physical contact. The linear position of the cart relative to the track can function as a

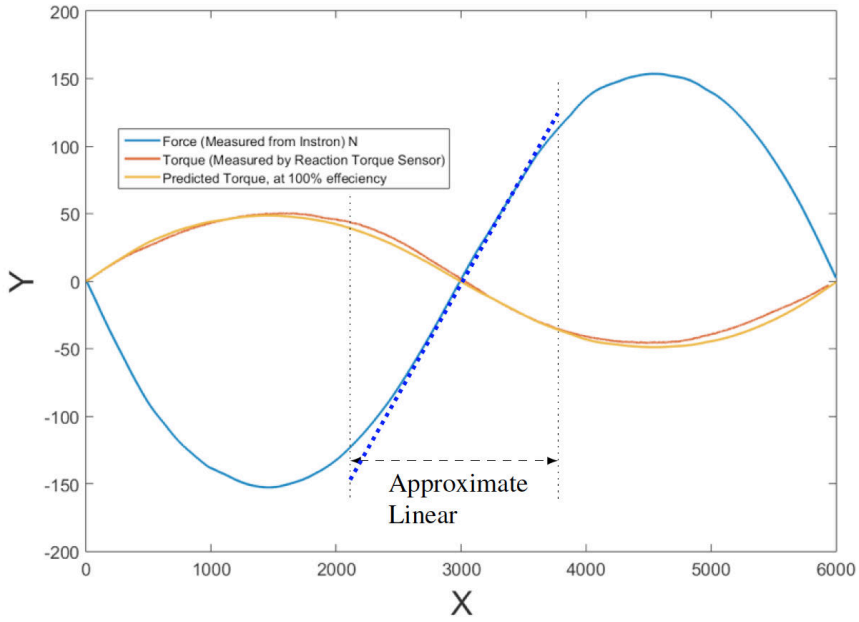

Figure 5.7: This graph shows the force and torque versus distance of a single 10 mm magnetic pole pair of a prototype magnetic lead screw (not the MagnaCarta). The numbers shown on the x-axis represent data sample numbers, and the entire width of the graph is 10 mm. As expected the force is sinusoidal with the force and torque measurements indicating a measured efficiency exceeding 99%.

spring with a stiffness that is determined by the combination of the stiffnesses of all of the magnet pairs. Since calculating these interactions using finite element simulation is challenging, we opted to measure the physical hardware experimentally, the results of which can be seen in Figure 5.9. This experiment involved fixing the rotation of the spindle, and then pushing down on the cart using an Instron machine and measuring the force versus distance relationship. This experiment shows a maximum force of 410 N and the characteristic sinusoidal force vs distance shape found in previous MLS literature, as well as from measurements of a previous prototypes which are shown in Figure 5.7. Because the preload binding the cart to the track decreases as the magnetic threads become offset by half a pole pair, the track and cart eventually disconnect.

In a series elastic actuator, there are two design elements which lead to conflicting requirements, the stiffness (k) and the travel range (l) of the elastic element. Making the elastic element very stiff has several advantages; the most important one is that the control bandwidth of a SEA increases [93]. This is relatively intuitive to understand: imagine the difference in trying to push a heavy mass attached to a very flimsy spring versus pushing the same block with a rigid rod. However, the downsides to stiff SEA are twofold. At higher stiffnesses, the deflection (x) of the element at moderate to low forces is very small and difficult to measure without exotic and often delicate sensors (e.g., strain gauges). Additionally, as the stiffness of an elastic element increases, the travel range (l) decreases, limiting a systems ability to successfully absorb impacts that are high speed or of high magnitude

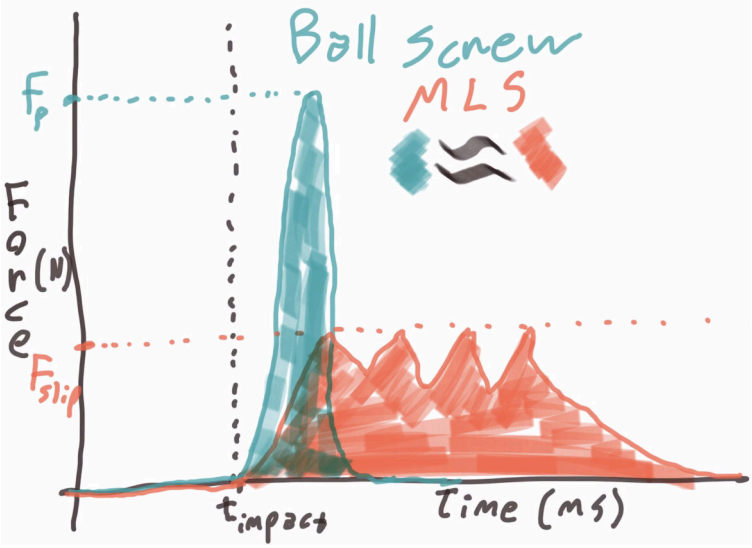

Figure 5.8: This figure shows a sketch of the force-versus-time graph for both a MLS actuator as well as a traditional ball screw actuator during a sharp impact. While the energy dissipated in the impact depends on the rotational inertia, the peak force for the MLS cannot at any time exceed the slip force. In contrast, for the ball screw actuator this force can be of arbitrary magnitude depending on the duration of the impact, thus leading to potential damage of the mechanical elements in the load path for the ball screw like the shaft-support ball bearings and the ball nut itself.

without either breaking the elastic element or colliding with the stops that limit the elastic element's range and transferring that impact to the rest of the actuator. This safe limiting of peak forces inherent in MLS is sketched in Figure 5.8 and is especially important in prototype systems where there are real possibilities of errant motor commands and unexpected collisions, as well as for assembly operations.

In contrast to the existing elastic elements which are used in traditional SEA, the magnetic elastic elements inherent in every magnetic gear form a sweat spot and solve several of the challenges inherent in traditional SEA spring designs. The key advantages include a relatively high stiffness, a predictable and easy to quantify stiffness curve, low-cost, and due to the built in overload clutch, an essentially infinite effective travel range. As can be seen in Figure 5.7, the force versus displacement curve for a magnetically geared actuator is almost a sine wave. This allows for reliable and scalable force sensing, as the region near zero is approximately linear, and the sensors can be simple and high bandwidth kinematic position sensors. This will help to provide a similar quality and bandwidth force and torque data as is achieved through expensive and sometimes fragile strain gauge based force-torque sensors. A final advantage of magnetic elastic elements is that in contrast to physical clutches the magnetic clutch immediately re-engages once the over-force condition is removed.

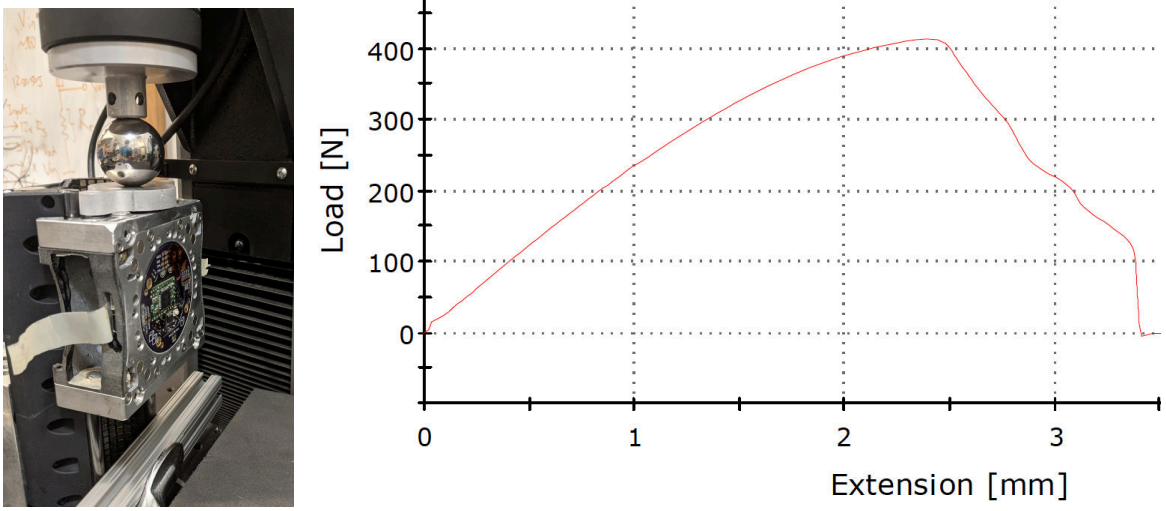

(a) (b)

Figure 5.9: This figure shows the force distance relationship for a single cart measured with a Instron machine (model 5944) that is pushed along a track with its spindle mechanically prevented from rotating. The maximum force before the cart separated from the track at roughly a quarter of the lead (2.5 mm) is 410 N (90 Lbs). As shown in other research, e.g., [107], the force/distance graph for a MLS is sinusoidal with a period of the lead. This can allow for simplified force sensing through series elasticity using a linear approximation in this case with a spring constant of about 230 N/mm.

5.5 MagnaCarta Magnetic Transmission Properties and Analysis

The MagnaCarta system was designed mostly through intuition and experience learned through building a sequence of different types of magnetic gears, including magnetic worm gears and traditional magnetic lead screws, in addition to a scale prototype cart-and-track system. Although the MagnaCarta generally functions well as a modular linear actuator, there are a few aspects of the system which can benefit from further analysis. Some basic characteristics for the magnet screw in this project compared with two other transmissions can be found in Table 5.2.

5.5.1 Analysis of Magnetic Preload Force

Previous work related to magnetic screws has suggested that the primary variables which set the maximum slip force (F_{slip}) can be estimated to a reasonable accuracy based on a heavily simplified model of magnetic attraction. The two most important variables are the (1) *area* of the air gap, and (2) the height or thickness of the air gap. As might be intuitive the F_{slip} is proportional to the area of the air gap (ignoring edge effects), but decreases non-linearly with an increasing air gap. However, attempting to make the air gap too small can cause the

Table 5.2: This table shows some of the basic parameters for the magnetic transmission element of the MagnaCarta system and compared with two other magnet lead screw transmissions. The force-to-magnet-mass (FTMM) radio is the ratio of the slip force to the total mass of the magnets in units of Newtons per gram. The FTMM value roughly represents how effectively the magnets are used in the transmission.

Design	Pitch	Stiffness	Magnets (g)	F Slip	FTMM
MLS [99]	20 mm	3416 N mm	8500 g	17000 N	2
(Figure 5.1b)	8 mm		118 g	220 N	1.8
MagnaCarta	10 mm	220 N mm	410 g	410 N	1

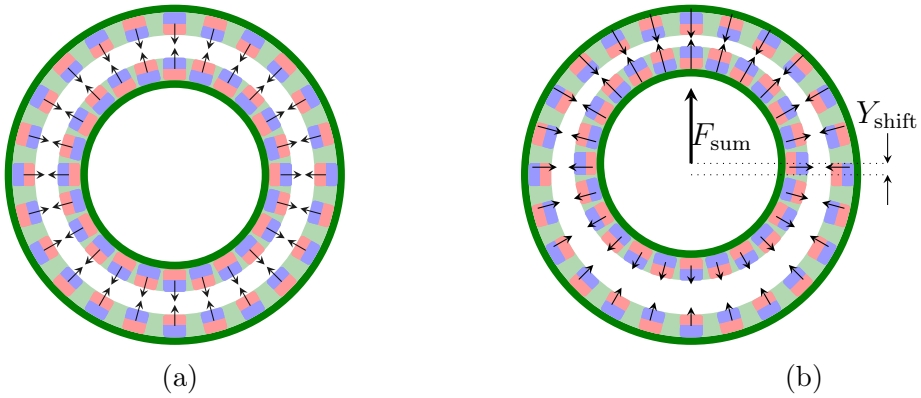

Figure 5.10: Magnetic ring cross-section image showing a representation of the sum of radial forces in a standard magnetic lead screw. (a) For a perfectly centered traditional magnetic screw, the resultant radial force F_{sum} is zero. However, this is a unstable equilibrium, because due to the nonlinear nature of magnetic forces, even a slight offset to any direction (e.g., Y_{shift}) will result in an unbalanced force. This makes the linear bearing constraint design of traditional magnetic lead screws an important design feature.

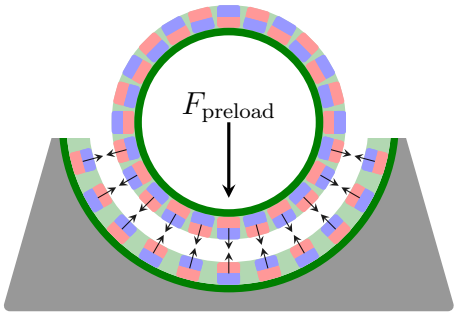

Figure 5.11: In the case of the MagnaCarta system, this sum of forces is what provides the preload force to attach the cart to the track. Due to symmetry all of these forces balance in the X direction, but sum to $F_{preload}$ in the negative Y direction. This force holds the cart down to the track, but also causes complications when the cart passes over the seam between two tracks if they are not securely attached.

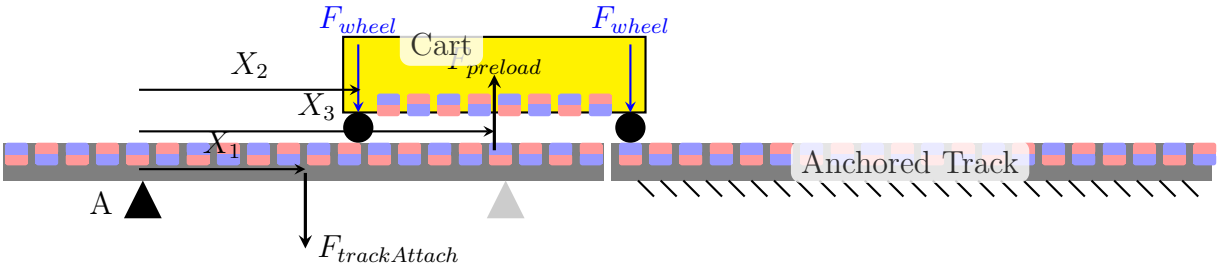

Figure 5.12: This diagram shows a simplified model of the cart and track system as it transitions over the seam between the two tracks. The goal of this model is to analytically predict the maximum force required to hold the track down, in order to have no dislocation happen.

spindle to touch the track either because of manufacturing tolerances or deflection caused by the magnetic preload. If the nut and the screw touch, high frictional torque, stiction and other adverse effects including vibration and the generation of magnetic dust can occur.

Due to the unbalanced nature of the magnet arrangement in this design shown in Figure 5.11 a large force binds the track to the cart. This force can be estimated through Equation 5.2 by taking only the Y component of each pair of magnets. Symmetry about the Y axis helps to reduce this to only five magnet pairs which can be roughly calculated to be about 60% of the sum of all of the pairs of magnets. This percentage could be reduced in future designs by omitting the magnets at the bottom and adding more on the sides where the Y forces cancel out. Further work would need to be performed to analytically relate this force to the slip force.

$$F_{\text{sum}} = 2\sum_{i=1}^{N/2} F_{\text{magnet,i}} \sin(\theta_i) \tag{5.2}$$

5.5.2 Track Seam Transition Problem and Model

The carts touch the track with wheels on either end of the spindle, and between these two wheels there is a slippery plastic part that is designed to contact only if one of the wheels is not fully touching, although this significantly increases the friction. We can develop a torque balance equation around the *black triangle* shown in the left of Figure 5.12 in order to determine what force is required to hold down the track in the worst case scenario (just before the right wheel transitions from the right track to the left track). Equation 5.3 shows this torque balance about one of the kinematic interface points on the bottom of the track. Taking several simplifying assumptions and assuming that F_{wheel} is equal to half of $F_{preload}$, the maximum force lifting up the track is almost half of the preload force, which is estimated to be about 160 N.

$$\sum \text{Torques}_{\text{about } A} = 0 = X_3 \cdot F_{\text{preload}} - X_2 \cdot \frac{F_{\text{preload}}}{2} - X_1 \cdot F_{\text{trackAttach}} \tag{5.3}$$

In practice this force is larger than the magnetic force due to the connectors on the

bottom of the track. Every time a cart moves over a seam between two tracks that aren't both bolted down, the cart slightly pulls one of the tracks vertically until the plastic part of the cart spacer touches the linear guide rail. While this doesn't stop the cart from being able to move between tracks this is an unanticipated problem that would require attention in future work.

5.6 Combining MagnaCarta Actuators in Parallel and Series

Designing a modular lattice based system poses a foundational challenge: a choice regarding the basic lattice cell size must be made at the outset. Altering this choice later is exceedingly difficult, as all of the connectors and robots and components are defined by this size. This makes the design of actuators for modular systems specifically challenging. Often the torque or force available from an actuator like an electric motor scales with its volume. If the motors are the same size as the unit lattice cell, this means full-cell sized actuators in a system with length L will have 8 times the power as those with half the cell height.

In order to have a single modular system be able to create resulting machines at differing size scales, some solution allowing for elegantly combining actuators together must be realized. Traditional power transmission elements prevalent in industry don't lend well to this task due to their non-backdrivable nature and fixed lengths. In contrast, the *MagnaCarta* actuators, characterized by their magnetic transmission and unique linear constraint mechanism, are backdrivable and exhibit predictable compliance. This makes them theoretically suitable for both serial and parallel combinations to augment the force, stiffness, and stability of larger systems.

A preliminary experiment combing three carts together has been performed as a proof of concept for this idea. An image showing this experiment can be found in Figure 5.13. In the experiment three carts are each bolted to the 1x3 structural block and are sent a coordinated signal to drive upwards. The combined actuator was able to lift a 30 pound weight, and was able to accomplish this task even when one of the carts was inactive, with the other two carts successfully back-driving the disabled cart.

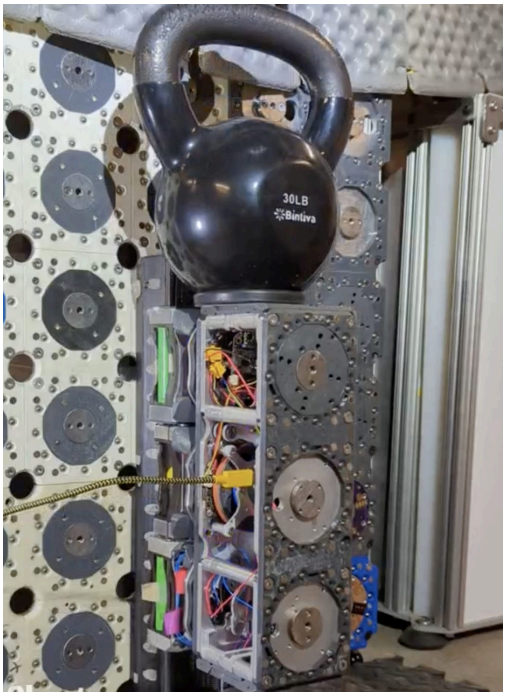

Figure 5.13: This figure shows a preliminary experiment which uses three separate MagnaCarta carts in series to lift a heavy weight against gravity. The three carts are attached to the 1x3 structural block and are able to lift a 30 pound weight 100 mm in about 2 seconds.

Chapter 6

Belty the Assembler: Embodying the Benefits of Proprioceptive Actuation

This chapter introduces the design of Belty, a compact assembler robot notable for its use of custom high-power proprioceptive quasi-direct-drive actuators. With these actuators, Belty can dynamically navigate on a cubic lattice structure and quickly manipulate and assemble modular components using its two modular connector-fitted feet.

The robotics community has recently been invigorated with the introduction of quasi-direct-drive proprioceptive actuators [108], as showcased by the highly dynamic mobile robots like the MIT Mini Cheetah [109], and compliant low cost robotic arms like Berkeley Blue arm [110]. These brushless motor-based actuators, unlike conventional, highly geared, servo-based designs, enable robots to operate faster, move with greater peak power, and handle environmental impacts with heightened sensitivity and grace.

Despite their undeniable advantages, this actuator revolution has yet to make its mark within the Modular Self Reconfiguring Robots (MSRR) domain or the field of robotically assembled structures. The majority of modular robotic systems still heavily rely on electric motors paired with highly-geared servo motors. Yet there are emerging exceptions such as the work by K Cheung et al. at NASA Ames [68], which is in part derived from the Bill-E robot and is focused on reconfigurable space structures.

This chapter presents a novel approach to assimilating brushless actuators into the compact bounding box imposed by lattice assembler robots. Capitalizing on these actuators, Belty can execute dynamic tasks that necessitate a video slow-down to view. This is in contrast to the (sometimes excruciatingly) slow nature of most of the MSRR related work systems. Moreover, Belty stands out for its agility and the pioneering ability to hop between lattice positions while carrying modules, a feature discussed in Section 7.3.2. This unique capacity to leverage its payload's momentum enables Belty to place blocks in positions that are difficult to reach through statically stable motions, and also allows it to operate in very tight spaces that larger assembly robots can't fit into.

After providing some context regarding proprioceptive actuators in Section 6.1, Belty's design goals are discussed in Section 6.2, its mechanical design in Section 6.3, and electrical system in Section 6.4. The chapter concludes up with a detailed experimental characterization of the capabilities of its actuators in Section 6.5.

6.1 Proprioceptive Actuators Overview

There is increasing interest in expanding robots from their traditional rigid position-controlled factory environment origins to be able to physically interact with the world in the same fluid and capable way as humans and animals. One of the grand challenges in robotics is to create actuators that are comparable to biological muscle, which is difficult simply because muscle is an incredible actuator. Biological muscle has a high power-to-weight ratio, is able to measure and precisely modulate forces, and is resilient to unexpected impacts. Traditional robotic actuators have mostly the opposite characteristics due to their complex inefficient gear trains. However, traditional robotic actuators do exceed the capabilities of muscle in at least two aspects: they have higher stiffness, and are better able to move to, and hold, precisely specified positions.

The series elastic actuator (SEA), presented by Pratt et al., in 1995 [93] is one path towards solving this grand actuator challenge of making robotic actuators that have properties similar to muscles. Series elastic actuators combine a relatively highly geared actuator (e.g., ball screw or strain wave gear) in series with a spring which introduces compliance and therefore a method of measuring output forces and absorbing limited impacts. Examples of modern robots using series elastic actuators include the Anymal [111] robot quadruped, as well as several commercial robots like Baxter from Rethink Robotics and various humanoids [112]. While SEA are effective at measuring forces, the transmissions often use significant gear reductions which brings downsides including reduced efficiency, higher reflected inertia, lower *power*-to-weight ratio (*not* torque-to-weight), and the inability to handle impacts that exceed the range of motion of the elastic element. Due to this added complexity, size, and fragility of many of the presented designs, SEA's have remained as a niche solution.

More recently proprioceptive actuators [108] have become increasingly popular as an alternative to SEA in mobile and human-safe robots. The core idea of proprioceptive actuators is to use electric motors which are optimized for *torque density* combined with minimal gearing. Because torque output for a motor is the tangential electromagnetic force times radial distance, electric motors with larger diameters and thin axial lengths, aka 'pancake motors' are the optimal shape for creating high-torque-density motors. This style of motor does have several drawbacks compared with traditional electrical motors. Specifically they require the complicated addition of electronic commutation as it is not practical to use brushes due to the large radius and the necessity of a large number of pole pairs. These motors have recently been popularized due to the remote control drone industry, as some of their characteristics including their low cost (no brushes), ease of cooling due to their exposed coils and large surface area to volume ratio and their high torque density (no gearing required) make them ideal for flying machines.

Despite the widespread adoption of pancake style motors in hobby flying machines, their use in robotics was not been practical until the wide availability of simple and inexpensive *on-axis* absolute magnetic encoders. These encoders, as shown in Figure 6.1, are the unsung heroes behind the proliferation of brushless DC motor based proprioceptive actuators. The motors in flying machines can get away with using a commutation scheme called back electromotive force (back-EMF), which uses software to determine where the rotor position is based on the voltage generated by the motion of the rotor itself, and generally do not

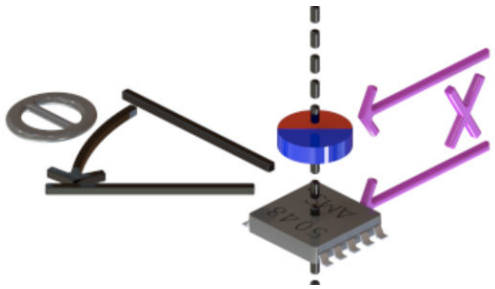

Figure 6.1: Diagram of an absolute on-axis magnetic encoder. These encoders are less costly, easier to use, and more robust than traditional optical encoders, and are more precise than the discrete hall sensor communication used to commutate certain brushless motors. They provide the absolute angle of a magnet that is attached to the motor rotor in the plane of the sensor (θ), as well as sometimes providing the vertical distance between the magnet and the sensor (x). In 2023 these sensors are commercially available from several different manufactures for prices around 10 dollars, and often have angular resolutions between 12 to 16 bits per revolution, and bandwidths often exceeding 10 kHz. Most of the recent quasi-direct-drive actuators now use some version of these sensors.

need the added electrical and software control complexity and rigid mechanical constrains required by encoders (as most on-axis encoders must be close to and exactly in-line with the rotating axis of the motor). The downside of the sensorless approach is that back-EMF driven commutation only works at medium-to-high speeds, which for flying machines is not a significant drawback, as the motor will never operate at any significant torque at low speeds, and the motors temporarily operate (poorly) as a stepper motor to get up to speed.

On-axis magnetic encoders are now widely available, and often even implement the commutation algorithm onboard which simplifies the engineering challenge of developing the electronics necessary to drive the commutation signals for brushless motors. Every motor driven axis in the FrFlFuFa project with the exception of the stepper motor in the force-distance measurement block uses a brushless DC motor paired with either the AKM AK7452, or Austrian Micro Systems AS5147 on-axis magnetic encoders. These encoders provide reasonably accurate, highly repeatable, high resolution (14 bits) of angular position data at high bandwidths up to 10 kHz, with more details presented in Section 6.4.

While proprioceptive actuators have many advantages as compared to traditional servos, they suffer from several significant disadvantages which require careful consideration to overcome, and they are not appropriate in all situations. The primary disadvantage of these actuators is that due to their high efficiency they require constant power in order to apply a constant torque (or force). Consider a proprioceptive actuator to a non-backdrivable actuator as analogous to holding a weight stationary at arms length (requires constant power) versus putting the weight on a shelf (requires no power), but the same physical *work* (zero) is being performed in both situations. While high gear reductions have many negative consequences, they do significantly increase the maximum torque or force of the actuator, which is sometimes the most important design requirement. Because little energy is lost in their power transmission, proprioceptive actuators in general can output higher average power than similarly sized servos. An additional disadvantage is that the large diameter of the

Table 6.1: Comparison of various robots based on actuator designs. The percentage motor mass metric attempts to estimate the total mass of the active part of the motor, i.e., only the magnets, the steel flux concentrators, and the copper coils themselves. All three of these components have similar densities, so in cases where it is difficult to measure these masses directly, an approximation based on volume and several reference motors is used for those indicated by the † symbol. Robots with a larger percentage of their mass comprising the actual power generating elements anecdotally have higher dynamic performance due to their higher baseline power capabilities.

Robot Name	Mass (kg)	Actuators	Motor Mass %	Notes
MIT Mini Cheetah [109]	9	12	32%	6:1 planetary gear
Belty	2.1	3	25%	5:1 belt drive
Bill-E [27]	0.6	5	5% †	100:1 geared servo†
Berkeley Blue Arm [110]	8.7	7	15% †	7:1 belt drive

motors limits the design freedom due to the sheer size and provides a certain inflexibility in terms of placing the motors in the constrained spaces necessitated in lattice based robots.

Beginning with the Tiger Motor U8-based actuator presented in the MIT Mini Cheetah in 2018 [113], similar copies and variants have spread rapidly, including several which are now commercially available, or are in mass produced products, including the Unitree Go1 quadruped, which has a MSRP around $4000 and includes twelve actuators. The most common methods of gear reduction include planetary gears or timing belts, and gear reductions under 10:1 are generally considered [110] to qualify as a quasi-direct-drive actuator.

However, due to the downsides of even limited gearing, removing them entirely and going 'direct-drive' is another common actuation scheme. Although direct-drive is conceptually older [114], it has also been increasing in prevalence, and for the same reasons as QDD and proprioceptive actuators. Several direct-drive legged robots have been built recently, including [115] in 2016, and commercial products like the Diablo robot from a company simply called Direct Drive. Applications for direct-drive actuators include those where high control bandwidth and mechanical robustness are the paramount goals, and include gimbals for cameras, high-speed low-force robotic arms, and increasingly mobile robots. Increasing the torque density and affordability of direct-drive actuators has been a focus of research and development, and due to their simplicity and robustness it is likely that direct-drive actuators will spread further. The first prototype of the assembler robot for this project used direct-drive (see Section 6.5), but was unable to generate enough torque without extensive engineering development, hence the addition of the belts. Although with more engineering effort direct-drive actuators will likely be the better choice long-term for lattice structure assembling robots.

6.2 Belty Design Goals and Principles

The design for Belty the assembler robot is inspired from the incredible capabilities that proprioceptive actuators have shown for legged robots. The key insight is that the task of assembly in a modular lattice is not all that different from the task of legged locomotion in

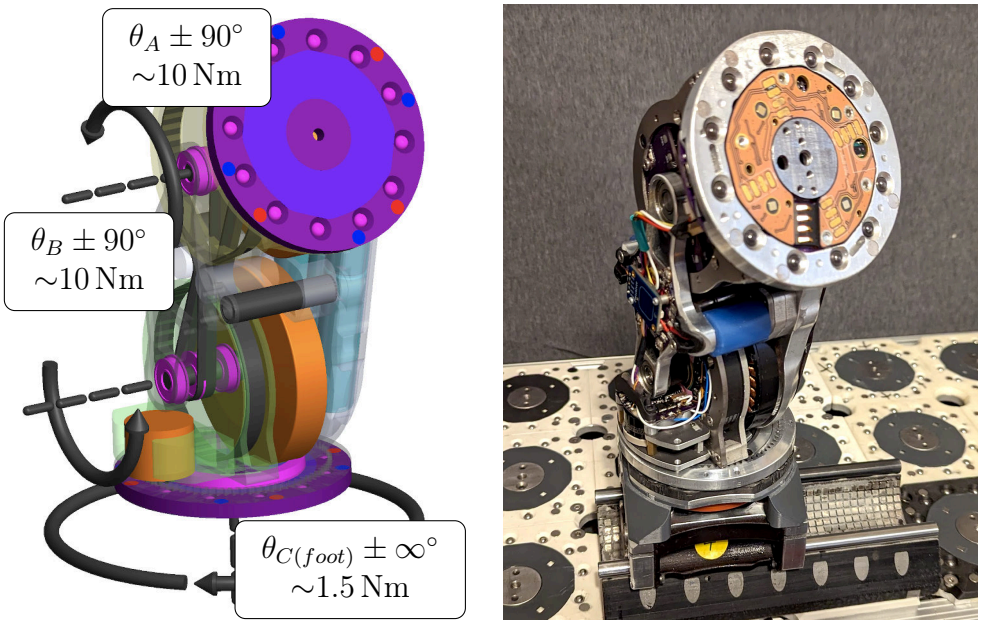

(a) Belty Design Schematic (b) Image of Belty

Figure 6.2: Image (b) and 3D sketch (a) of Belty the assembler robot, with *orange* representing the motors, *gray* showing belts and gears, *pink* showing bearings, and *purple* representing the modular connectors. Belty has three actuated degrees of freedom, and four independently moving assemblies.

unstructured environments. Both tasks require control of forces and handling of impacts, and assuming the use of alignment mechanisms in the modules, neither require all that precise position control. Due to the quick drop in strength over distance for permanent magnets, the maximum torques required for lattice assembling robots are of very short duration, which is well suited to QDD, and potentially direct-drive actuators. Think of the way that a toddler is able to assemble structures out of Duplos to quite high precision - in this case the actuators have extremely low position control precision and basically use low bandwidth force control to push components together. A toddler uses collisions and physical alignment features on the blocks to help guide assembly, in a similar way that an animal 'feels' the ground as it moves. Despite the limitations of the biological actuators that assemble them, structures built out of Duplos have high repeatability due to the digital nature of the building blocks, which embody the precision necessary to create accurate structures.

As long as the building blocks of the lattice system have connectors with a wide area of acceptance, and high repeatability as discussed in Chapter 4, low position loop stiffness is actually beneficial as once two connectors are brought close together their magnetic forces will backdrive the robot and 'snap' it into position. Assembler robots operating on a lattice with permanent magnetic connectors face two general categories of forces: high but short-duration forces involved with disconnecting from the lattice, and then the longer-duration but lower-magnitude forces required to lift and accelerate its mass and the mass of the payload.

The power and torque achievable from motors are fundamentally limited by thermal

effects, basically the limiting constraint comes down to the ability to dissipate waste heat from the coils in the motor. Therefore, low-gear-ratio high-torque-density motors are well suited for task this as long as their peak force never has to be sustained for long enough that the thermal limit is reached. Most of the similar lattice assembly robots use servo motors, which allow for high torque, and quick design cycles, but at a cost of dynamic capability and the possibility for further mechanism design optimization which can be achieved by integrating the actuators into the robot. It could be argued that Belty is over-optimized in this regards by trying to pack too much complexity into a small space, but so far the design has proven to be robust and capable, undergoing hundreds of moves and many jumps without any noticeable degradation or damage to its actuators or belt system.

The primary design goals for the development of Belty include:

- Use of backdrivable proprioceptive actuators for each axis in order to utilize the systems dynamics for motions like hopping and passing parts between different robots.
- Prioritize increasing the peak power-to-weight ratio for the primary actuators.
- Properly constrain each degree of freedom with appropriate strength preloaded bearings.
- Robust fully metal primary load path throughout the entire robot from foot to foot.
- Inclusion of protective rubber stops at the extreme extents of its motion as to be robust to impacts and forces experienced while being back-driven.
- Tight integration of electronics and mechanical structure in order to fit maximum capability in a small volume, and provide enough robustness for extensive testing.
- Integration of the power source on board unlike many robots in related work in order avoid the complications introduced by external wires while moving on the lattice.

6.3 Mechanical Design of Belty the Assembler

The design of Belty the lattice assembly robot can be seen in Figure 6.2. The robot shares a similar morphology with several traditional MSRR robots including the MTRAN [28] from 2002, but is kinematically simpler than other relative assembler robots like Bill-E or the robot in SMAC [52]. Belty has only three actuated degrees of freedom, occupies only two lattice cells in its most compact configuration, and does not have the long cantilevered arms seen in SMAC and Bill-E. The two primary axes (A and B) each consist of a single high torque density U8 BLDC motor paired with a 5:1 timing belt gear transmission that can rotate just over 90 degrees in either direction before hitting a rubber stop. Axis C, which is shown in Figure 6.3, uses a smaller BLDC motor with a 7:1 internal ring gear power transmission that can rotate continuously.

There are seven discrete assemblies in the design, including the motor rotors, all of which are constrained to rotate relative to each other with a total of thirteen bearings, with three of the connections deviating from the generally accepted practice of using two, and only

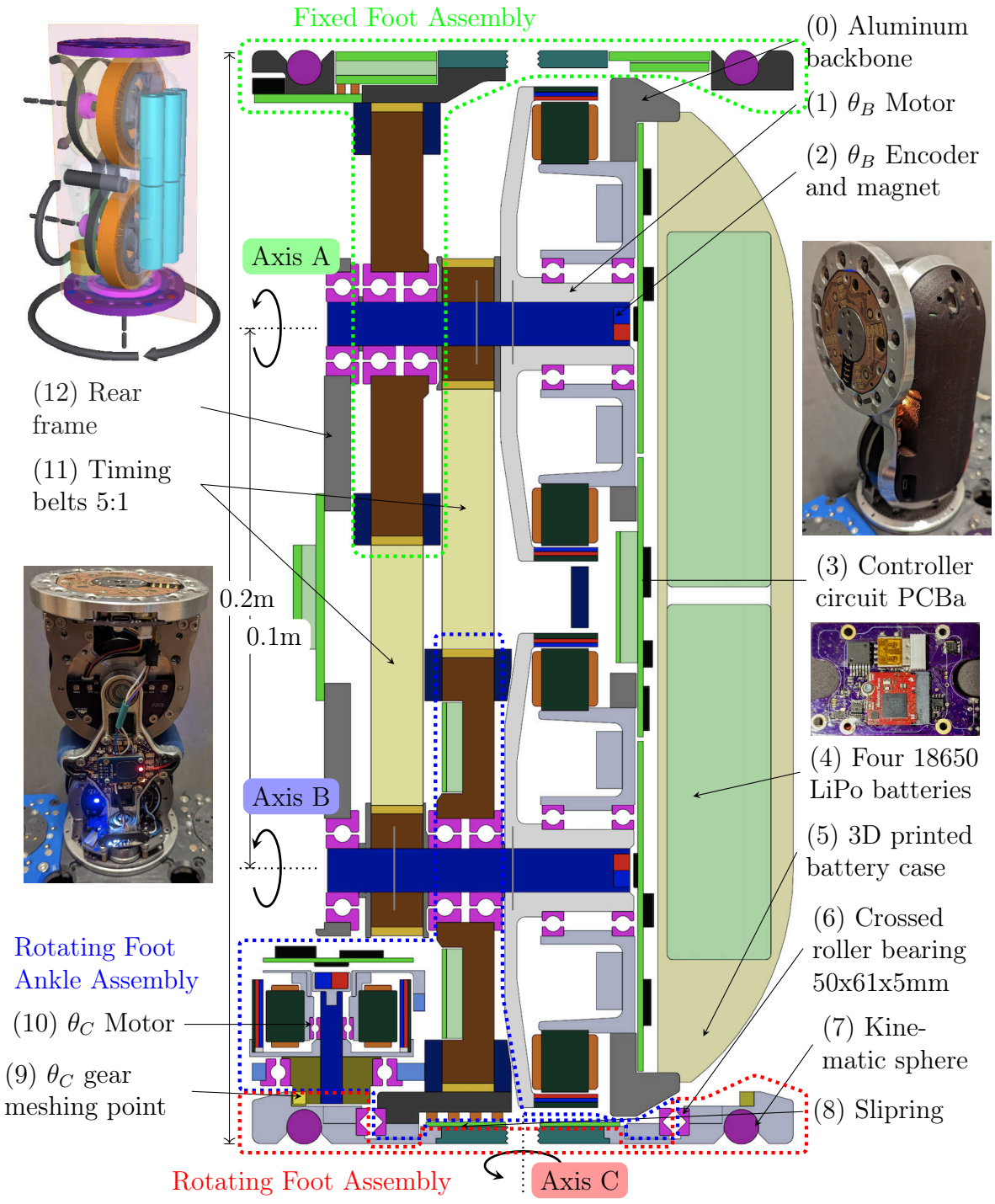

Figure 6.3: Cutaway diagram of Belty the assembler robot highlighting the four independent rotating parts (*red, blue and green* regions), and the uncolored core part. Belty's two primary axes, θ_A and θ_B, are each driven by a U8 brushless DC motor operated by a custom Teensy 3.2 based BLDC driver through a timing belt (*tan strips*) to its two feet with a gear reduction of 5:1. The third axis (θ_C) consists of the compactly repurposed parts of a smaller BLDC motor (MultiStar 2312-460) with a 7:1 module-one internal-gear reduction transmission.

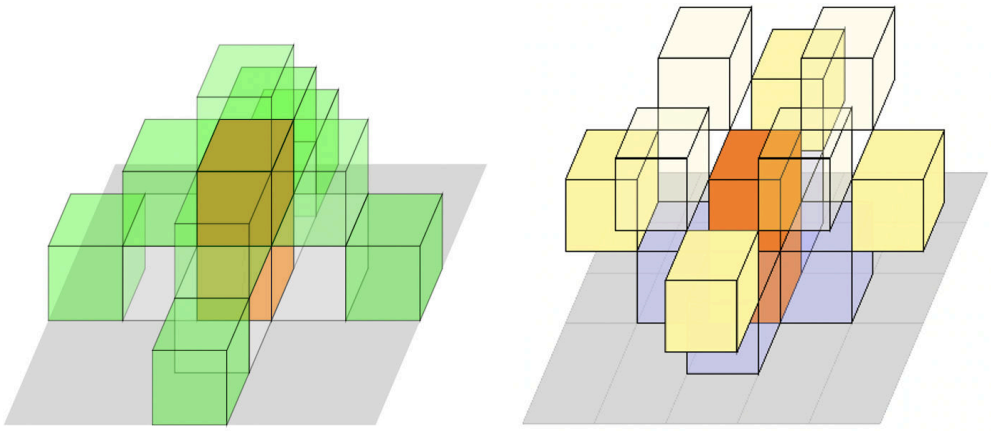

(a) (b)

Figure 6.4: This figure shows the workspace for Belty the assembler robot under two conditions. (a) Shows the workspace of statically reachable positions. (b) Shows the workspace that can be reached through dynamic motions, with blue representing possible blocks that can be picked up, and yellow representing drop-offs. However, these moves are not always as reliable as statically reachable moves.

two, bearings for each independently rotating element. Two of these exceptions are the two core shafts for axes A and B, which are supported by three bearings, since there are two bearings in each of the U8 Motors, and one in the outer frame. However, due to the precise manufacture of the U8 motor frame combined with a very slight clearance fit for the rotor shaft these two bearings effectively function as one, and these axes appear to function normally without any binding. Additionally axis C (described further in Section 6.5.2) uses a single crossed roller bearing to constrain the rotation of the foot.

Belty was intentionally designed with limited degrees of freedom in contrast to the more complicated, but more capable systems seen in related work. The intention of this choice was to determine if creating the simplest possible assembly robot, but giving it high performance actuators can lead to a more-effective and biologically-inspired way of assembling structures. By intentionally using the robot's own momentum, the momentum of its payloads, intentional (or unintentional) impacts with the lattice environment, and implementing under-actuated motion sequences (i.e., think using 'twists' to snap a block free), many more possibilities for lattice reconfiguration are opened up compared to traditional slower low-power assembly robots that do not attempt to embrace dynamics. An example of this expanded workspace through dynamics can be seen in Figure 6.4. While these moves provide interesting new possibilities, further algorithmic development is needed to improve their probability of success.

6.3.1 Frame Design Details

The core frame for Belty consists of two machined aluminum plates connected by 12 mm diameter configurable M8 hollow threaded steel standoffs from Misumi (part number: PSPJW12-48-M8-N8). The four bolts that clamp the two halves of the frame together have been hol-

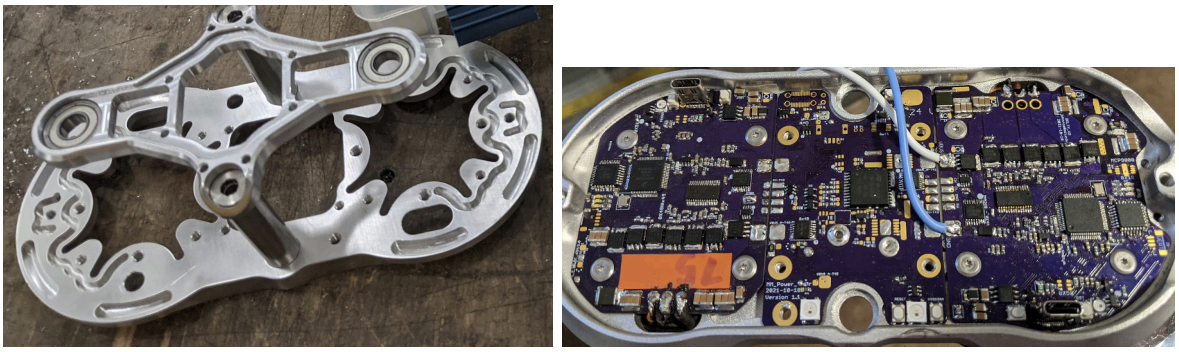

(a) (b)

Figure 6.5: Belty's backbone is machined out of a 12.7 mm thick 7075 aluminum plate in order to have high stiffness, and to help distribute the heat from the motors. The frame (a) consists of two machined aluminum plates held together with two 12 mm diameter steel standoffs. Additionally, the bathtub-shaped design (b) of the backbone allows the control circuitry to be protected from impacts.

lowed out in order to provide a protected tunnel to pass wires from the front to the back side of Belty. Two blue rubber tubes are placed over these standoffs (not shown in Figure 6.5, which act as end stops for the A and B axes and to attempt to mitigate damage from impacts or over-extension of these actuators. The two U8 motors are securely bolted into form-fitting machined cut-outs in the backbone in order to provide a rigid connection and to use the frame as a heat spreader to help dissipate waste heat from the motors. Bearings for the two intermediate shafts (*dark blue* in Figure 6.2) that hold the bearings for the two primary output axes are embedded in the cross-shaped outer rear frame component. This frame weighs a total of 250 grams, and while potentially over-designed has proven to be robust, even during several unfortunate incidents where Belty jumped off of a table onto the concrete ground.

6.4 Belty's Electronics System

The electrical system for Belty the assembler robot is built as a distributed network of six custom printed circuit boards which are connected to each other, and to any external modules through its connectors, with a normal two-wire CAN bus. The CAN bus protocol was designed for the automobile industry and was originally released in 1986. The CAN bus is primarily designed for robustness and reliability, featuring extensive electrical and software protections. This includes multiple layers of software error checking and electrical safeguards, such as the capacity to withstand shorts on either of the wires at voltages up to ±60 volts. These same features that make the CAN bus idea for cars, also are effective in robots. The large voltage protection range is especially important for modular robots which often have exposed electrical connectors, and where accidental shorts during movements are likely. In this version of Belty all of the boards and the connectors all share the same CAN bus, but in future versions it would be prudent to split this into several buses in order to increase the ability to recover from short-circuits.

Belty integrates a power source consisting of between four to six high discharge rate (30C) lithium polymers batteries which power all of the robots functions, including the ability to share power through the two connectors. The flow of electrical power through the system is shown schematically in Figure 6.6. After several instances involving the release of the 'magic smoke' contained within circuit elements, protecting the high current path from over-current and shorts has been a design priority. This has been accomplished through the use of the TPS26633 electronic fuse from Texas instruments. This device protects against many possible electrical faults, and will first hold a current limit, and then automatically shut down during adverse events.

The code is developed in the Arduino language using the many open source libraries for the Teensy microntroller system provided through the company PJRC. Libraries that are used extensively include the CAN library, the USBHost library, and the littleFS file system libraries. The electrical system architecture is inspired by the system presented by Ben Katz in his Thesis [113] and used by the Mini Cheetah [109]. Every custom circuit board contained in Belty is manufactured by OSHpark and then lovingly hand soldered in Medford, MA.

At the time development on Belty began, there were not many commercially available circuit boards for powering U8 style brushless motors. Recently there have been a proliferation of these boards, many of which have better features and specifications than those used here. However, the benefits of creating these boards include the immense lessons learned through their design process, as well the ability to tightly integrate them into the design. One of the challenges with creating modular lattice traversing robots in general is that the lattice grid cells force the designer to think *inside the box*. Small issues such as the location and orientation of USB connectors, the location of components on the circuit board and the thickness of the PCBa itself can make a substantial difference in the overall size and packaging of the robot. It is far easier to control all of these parameters when co-designing the frame and circuit board for a robot, although it takes more time and effort.

6.4.1 Core Processor

The core processor board can be seen in Figure 6.7 and is a custom carrier board for the 600MHz ARM Cortex-M7 Teensy micromod card-style module that serves as the primary processor and power management controller for the robot. This board manages the included four to six removable 18650 batteries and provides power distribution through several integrated power switches. Additionally it monitors the power consumed by the other boards through several Texas Instrument INA260 I2C current monitor chips. An emergency cut-off feature is created with a physical pull tab that drives the various power distribution chips through logic gates to cut power to the entire system in the event of an emergency. Communication with the outside world is handled through a combination of the CAN bus from one of the two connector circuit boards and either a wireless USB keyboard/mouse or a Decawave DWM1000 based mesh radio system.

6.4.2 Brushless Motor Drivers

Two variants of custom brushless motor driver boards based on the Teensy 3.2 chipset power the each of Belty's three axis of motion. Both of these boards use the A4915 power stage

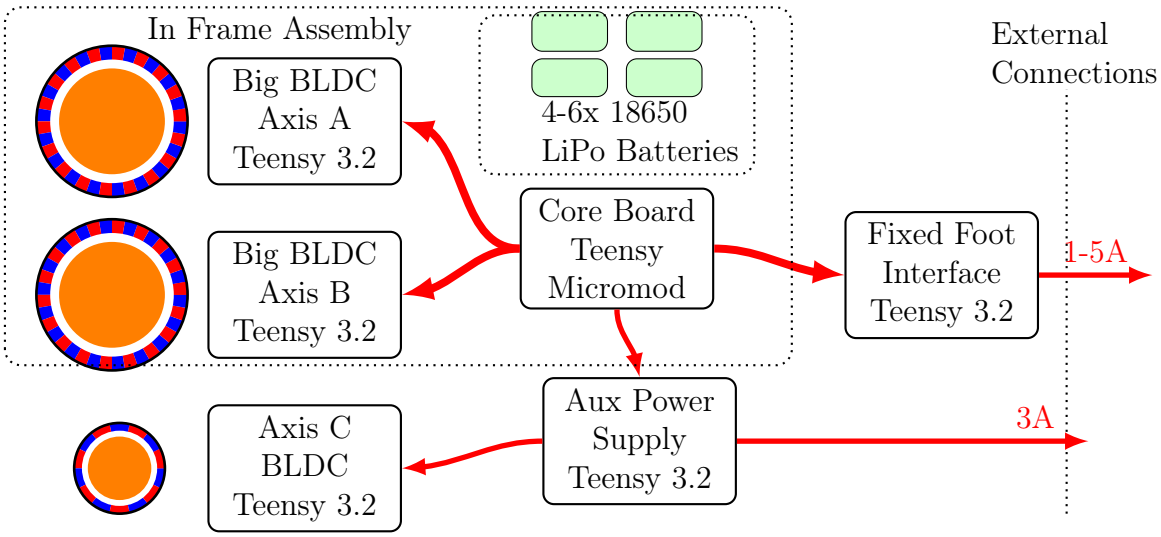

Figure 6.6: This diagram shows the six PCBa's that together form the electrical system for Belty the assembler robot. The core processor is custom carrier board for a Teensy micromod card that manages the battery, manages radio communications as well as distributes commands to the other five boards. There are three custom brushless motor driver boards based on the Teensy 3.2 chipset that each run one of the axes of motion on the robot. In addition there are two Teensy 3.2 based boards that manage the two connectors and have miscellaneous sensing and interface electronics.

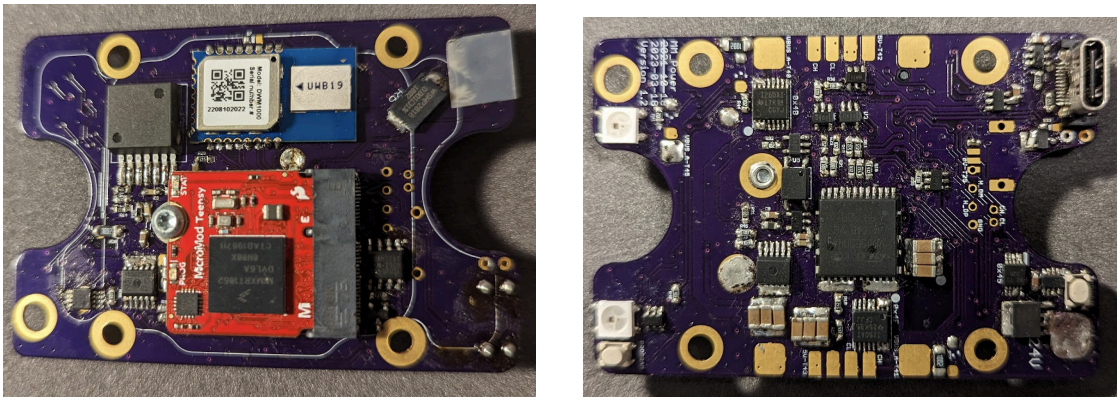

(a) (b)

Figure 6.7: Belty's primary custom controller circuit board with the front (a) and back (b) shown. This board uses the Teensy Micromod microcontroller, which with a 600 MHz ARM Cortex-M7, has more than enough computational power for the tasks required. Additionally this board manages four to six 18650 LiPo batteries and distributes power of up to 15 Amps to each of two adjacent primary U8 Motor controllers (axes A and B) PCBa and up to 5 A to other three circuit boards combined. Additional important features include USB host support, which allows for simple control of the robot through an off-the-shelf keyboard, multiple CAN controllers, and enough memory to store accumulated diagnostic data captured during movements.

predriver that runs the six SO-8 sized N-Channel power transistors that power the motors three phases. Each board also uses an on-axis magnetic encoder to generate the signals for commutation, with the larger board 6.8a using an AK7452 sensor which outputs the UVW phase commutation signals directly to the predriver, while the axis C board uses an AS5147 encoder with commutation handled by the main processor and a look up table. Neither of these boards currently implement field oriented control as used by many equivalent controllers due to a desire for simple software, but this feature could be added in the future.

These boards implement a simpler, although less accurate, method of current sensing than many comparable boards. Many similar boards use two high bandwidth current sensors to monitor the actual phase current of two of the three phases. This allow for high current control bandwidth, which is often in the range of 10 to 20 kHz. The boards used here use a single Texas Instruments INA260 current monitor to measure the low-side ground connection of the mosfets, which, while simpler, is lower bandwidth (max 1 kHz), and misses the effects of currents that recirculate in the coils [113]. In practice this approach is suitable for applications like Belty where the motors rarely move at high speeds and are mostly applying torques at near zero speed.

The two primary axes use the larger board shown in Figure 6.8a, which is tightly integrated with a U8 brushless motor. These two boards fit tightly with the core processor described in the previous section; this integration can be seen in Figure 6.5b. These boards also incorporate a significant amount of bulk ceramic capacitance and several varistors to help stabilize the power supply and suppress voltage spikes caused by inductive effects from the motors during sudden, sharp bursts of power. The physical layout of these boards were co-designed with the frame backbone and the battery case in order to minimize the thickness of this part of the robot, and to ensure that there was enough space to fit the belt transmission mechanism.

Axis C uses a much smaller variant of this similar design, shown in Figure 6.8b-c, which includes most of the same circuitry as the larger boards, just in a much smaller physical package. This board also has strict mechanical size constraints, and therefore has components on both the top and bottom in order to fit it in the constrained space next to the rotating foot.

6.5 Belty's Actuator Design and Characterization

The two primary axes (A and B) each comprise a single high-torque-density U8 BLDC motor paired with a 5:1 9 mm wide Powergrip GT timing belt gear transmission, as illustrated in Figure 6.9a. These axes are capable of delivering up to 10 Nm of torque while drawing 15 A for brief durations, and they can execute high-bandwidth sine wave motions at full power, achieving frequencies of up to 100 Hz. These two motors are embedded in a single large bathtub-shaped machined aluminum backbone component which helps distribute and dissipate heat and protects the custom electronics from impacts. The third axis, denoted as θ_C and depicted in Figure 6.3, employs a smaller BLDC motor with a 7:1 custom CNC-machined internal ring-gear power transmission. This axis is capable of generating approximately 1.5 Nm of torque.

The torque versus current performance at stall for Belty's actuators has been character-

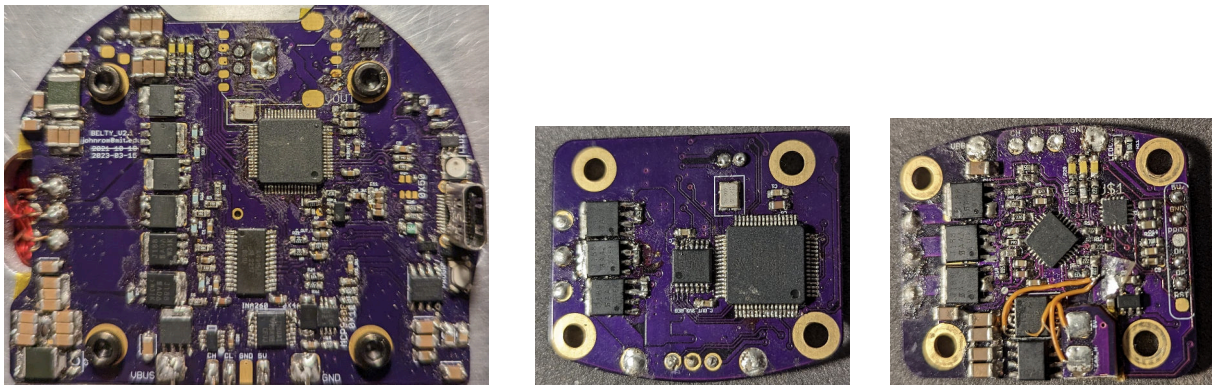

(a) (b) (c)

Figure 6.8: This figure shows the the two different brushless motor driver circuit boards that power Belty's three motors. These controllers use the A4915 predriver IC combined with an on-axis encoder to drive their respectively sized brushless motors. (a) Shows the board which powers the two primary axes, while (b) and (c) show the back and front respectively of the board which drives the gear-driven axis C. These boards are manufactured by OSHpark with a 2oz copper layer and 0.8 mm thickness PCB in order handle high currents while still being compact.

ized using two similar experimental setups built out of modular system elements as shown in Figure 6.9b-c. These experimental setups feature modules mounted on an electrically connected lattice substrate. Force measurements are captured by the load-cell equipped force-distance measurement block driven by a stepper motor, which is described in detail in Section 3.5.2. All measurements are transmitted and synchronized using the onboard CAN communication network with the data passing through modular connectors and stored in onboard memory as data files.

6.5.1 Primary Actuators Belt Drive Mechanism

The two primary degrees of freedom for Belty are implemented with 5:1 belt transmissions combined with U8 BLDC motors. Both pulleys started out as off-the-shelf components, but both required additional machining to make the design work. The 16-tooth pulley pinion was carefully machined on a lathe in order to shorten its length and increase the bore to fit around the 8mm central shaft, while still keeping the bore concentric with the teeth. The larger pulley was machined in order to securely hold the bearing as well as to attach to the two water-jet titanium plates that connect it to the feet. The choice to use belts as opposed to gears stemmed from the difficulty of working with custom high-strength gears, and the desire to keep as much space as possible in the radial direction available for the two feet. This requirement made it difficult to fit the off-the-shelf proprioceptive motors available at the time. However, for future designs it would likely be more practical to use off-the-shelf actuators or direct-drive actuators to simplify the design and make the robot more robust.

Belt transmissions have several downsides when compared with traditional gearing. These downsides include the need for a mechanism to apply constant tension to the belt, nonzero

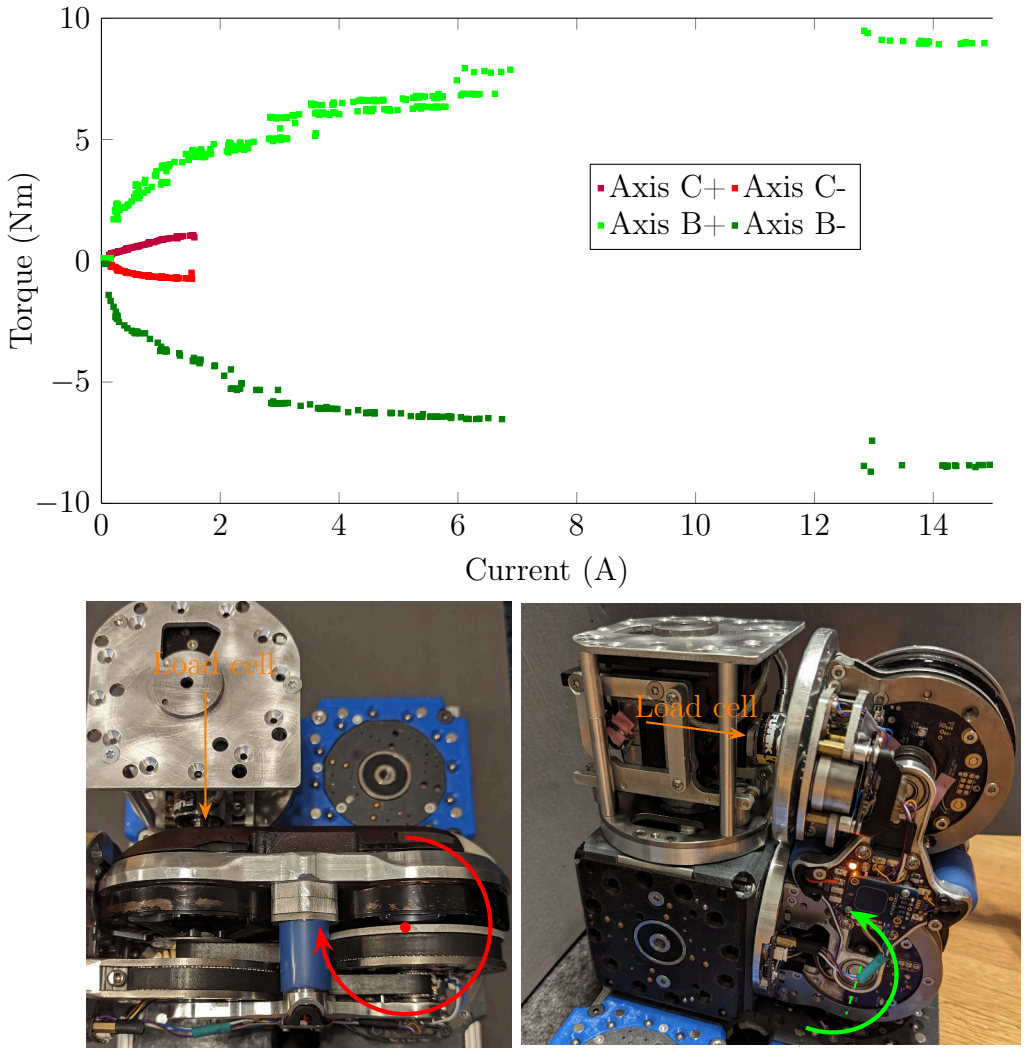

(b) Axis C setup (c) Axis B setup

Figure 6.9: Actuator stall torque vs. current for Belty's two actuator types, measured through an experimental setup created from compatible modular components. The primary actuators A and B max out at about 10 Nm of torque, but there appears to significantly diminishing returns for currents over about 5 A. The smaller Axis C 7:1 gear driven actuator uses a much smaller BLDC motor and is thermally limited to about 1.5 A which results in a peak torque of about 1.3 Nm. The gap in the data from 6 to 12 A is due to the motor temporarily shutting down after exceeding the software set thermal limit.

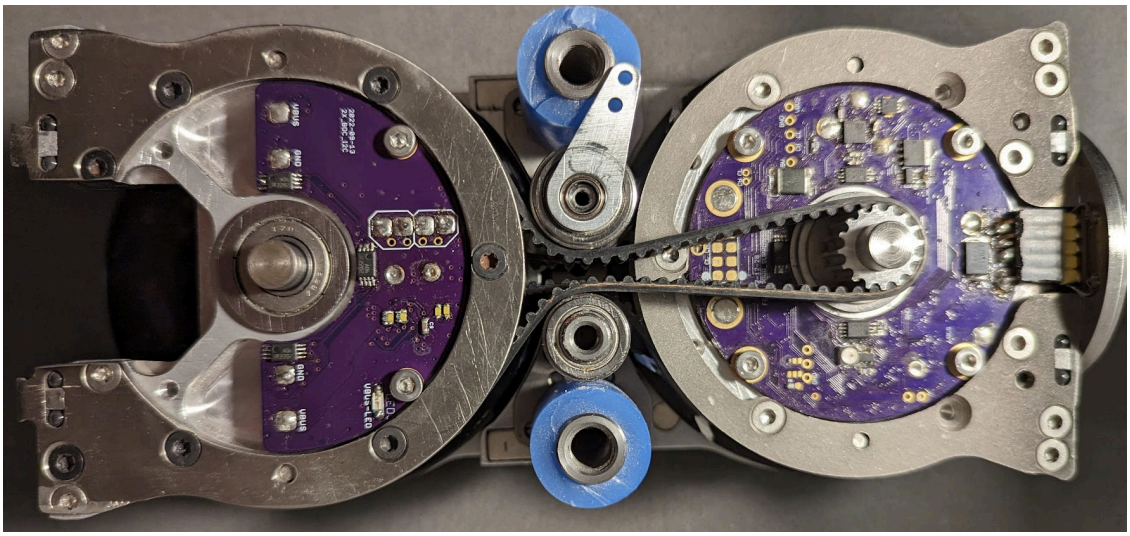

Figure 6.10: Top down view of the top layer of the belt drive power transmission in Belty. The cam that applies tension to the belt is visible in the top center of the image. While belts have many downsides, one advantage is that they provide design flexibility in circumstances where full output rotation is not required. In this example the cutout seen on the far left of the image is a result of cutting the belt and machining away the belt pulley in order to provide room for additional components.

backlash, and lower stiffness than many types of gears. The design of the tension mechanism especially is a difficult practical challenge in such a space-constrained design. The tensioners are implemented on each of the two belt layers independently with a small cam which pinches idler wheel against another fixed idler, as can be seen in Figure 6.10. In this design, the motor on the right drives the foot on the left, and vice versa. This two-layer configuration introduces non-symmetry into the design, causing torque to be transmitted around the bearings that support the 8 mm shaft of the rotating foot on the right side. While this design choice is effective, it has made assembly and maintenance challenging. Future designs should consider a simpler geared servo approach, such as the planetary gear-driven actuators utilized in recent proprioceptive quadrupeds' actuators.

6.5.2 Geared Rotating Foot Design and Slip-ring

In addition to the two primary belt-driven high-power actuators used for the two axes discussed in Section 6.5.1, one of Belty's feet has been fitted with a compact single stage 7:1 BLDC motor and spur gear reduction actuator, as shown in Figure 6.11, and in the lower right corner of Figure 6.3. The rotational constraint is provided by a 50x61x5mm crossed roller bearing, which allows for proper constraint in a small space without requiring the two matched bearings required elsewhere. Ideally both feet would be able to have rotating actuators, and this could be designed in future versions of Belty, but for the version presented here this was not pursued due to the lack of symmetry forced by the design of the belt mechanism for the primary actuators.

In order to compactly fit this axis in a constrained space the gear teeth for both gears

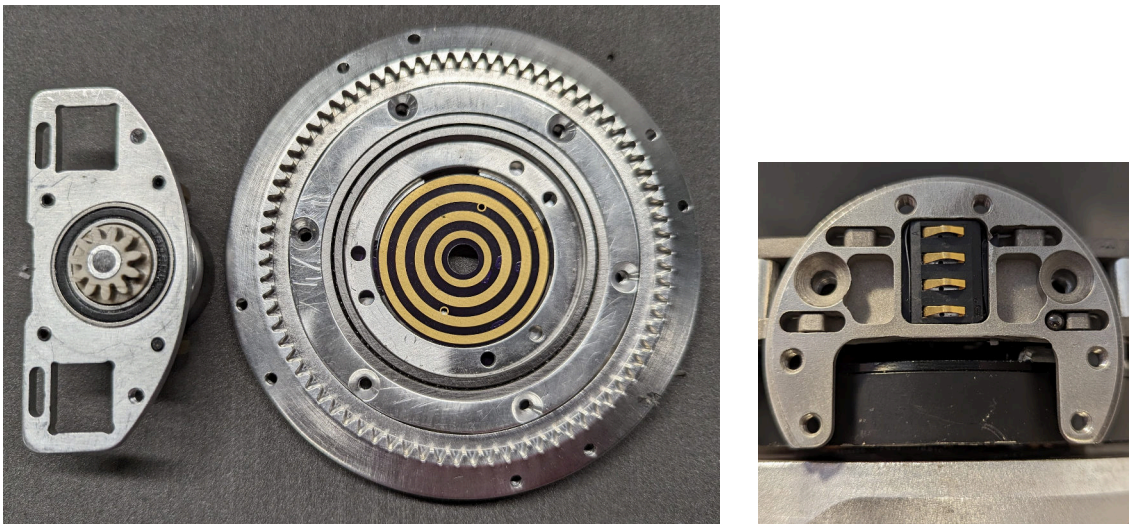

Figure 6.11: Image of the custom machined gearing and slip-ring system for the Belty's axis C rotating foot. This design uses the a 11-tooth spur gear machined out of PEEK to drive a 77-tooth internal gear which is directly machined into the output foot's frame. A custom four wire slip-ring is implemented using a PCB matched with an electrical spring contact in order to pass power and CAN bus signals through to the rotating foot connector.

were CNC machined using a small 1.1 mm end mill which traced out the gear profile from the top direction. This method of machining gears has the benefit that the teeth are supported on the bottom and are not cantilevered like traditional cut gears. The material for the larger 77-tooth internal gear is 7075 aluminum, which is a softer than the hardened steel used in many robot gears, but since the mating gear is machined out of high strength PEEK plastic, this has not proven to be an issue.

Axis C is able to rotate continuously, which makes connecting electrical signals to the foot require a slip-ring. No commercially available slip-rings were found which were able to fit in the constrained space which is forced by the presence of the large U8 motors, so a custom design was implemented. This slip-ring consists of the four concentric gold plated rings formed as the top face of a commercial PCB, and shown in the center of Figure 6.11a, which combine with four spring-loaded pads that can be seen in the adjacent figure. While this slip-ring works, it is not completely reliable, and this is also an area that could be improved in future work. However, the fact that it is able to successfully transmit CAN messages at 1MHz through it while actively rotating is a testament to the forgiving nature of the CAN protocol.

6.6 Direct-Drive Prototype: Flippy

For all of the reasons discussed earlier relating to the nature of the forces that assembler robots operating on a magnetic lattice encounter, direct-drive actuators are very enticing. Ultimately well-designed direct-drive actuators are likely to be the best long-term solution for lattice assembler robots, but it is important to consider the difficulties and challenges that

they present. This section will discuss the first prototype assembler robot, named Flippy, which is shown in Figure 6.12. This robot used two larger U10 brushless motors which drove the two primary axes (A and B) directly. The benefits of using direct-drive actuators are significant:

- No need for a power transmission reduces space requirements and design and assembly complexity.
- Stiffer structural loop from foot-to-foot due to fewer bearings, and less cantilevered design elements.
- Lack of any rotations exceeding 360 degrees removes the need to calibrate motor encoder.
- Faster control bandwidth.

However, the downsides that ultimately led to the redesign of the robot were related to more practical considerations. The first challenge is the requirement for high currents to achieve high torques in a battery-driven system. Despite the larger size and higher torque constant of the motor, the direct-drive motors necessitated significantly more current to attain similar torques compared to those provided by the U8 belt-drive actuators. Designing the power path to handle the currents required for simultaneously driving the two large BLDC motors at peak torque is a non-trivial task.

The second problem related to the lack of damping torque from the motor in brake mode. If the regular controller became disrupted for whatever reason (power failure, faulty control input, over-temperature, etc...) and the motor controllers shut down, the significant momentum stored by the robots payload basically went into free-fall. While nothing became damaged due to this, the level of software and controller maturity in the system at the time made this a real possibility. In a more professionally designed system with more reliable software and electronics, this will be less of a problem. However the dangers involved with the possible failure of a direct-drive system are worth careful consideration.

Figure 6.12: Before designing Belty a similar robot with direct-drive actuators was built and tested, named Flippy. There are many favorable characteristics of direct-drive actuators for assembly robot tasks including mechanical simplicity and high bandwidth control. However, the lower maximum torque and the lack of inherent damping made this prototype too difficult to safely operate given the maturity of the electrical system on the robot.

Chapter 7

Algorithms and Control

This chapter will discuss both control algorithms for specific moves in addition to more general control strategies, developing some analytical and theoretical tools for systems that are similar to FrFlFuFa as well as system level characterization and bench-marking of the existing hardware. The hardware described in previous chapters has many arbitrary elements that arose from the vagaries of the development process, and many sub-optimal implementations of elements like the motor drivers which could be improved with further engineering efforts. While this thesis does not focus on large scale algorithms or simulations, many large scale simulations of robotically assembled lattice structures for systems like the Bill-E system [35] can be found in related work.

Section 7.2 will introduce an abstraction of the magnetic cubic lattice and a new metric called the *Lattice Assembly Efficiency Factor* (LAEF) regarding the energy required to reconfigure elements of the system. This metric is in a way a discretized version of the cost of transport metric which is commonly used to evaluate energy use for vehicles and animals. Following this, Section 7.3 will introduce the experimental results and analysis for several basic motions, describe their definitions, and characterize them in terms of reliability, speed, and the newly defined LAEF metric. Finally Section 7.4 will discuss some of the challenges and opportunities in developing mid-level hardware specific controllers for reconfigurable systems like the FrFlFuFa system.

The following definitions are provided here to help define several classes of movements presented in this chapter; protected lattice moves, regular lattice moves and extra-lattice motions.

- *Regular lattice*: These are lattice motions that always involve at least one connected lattice connection, and could be stopped at any point during motion, and run in reverse. These motions include picking and placing blocks, traversing on the lattice, etc.

- *Extra-lattice motions*: Motions where the assembly robots disconnect from the lattice temporarily during the motion. Examples of this include hopping, or tossing and shoving a module into place.

- *Protected lattice*: These are motions during which at every point the motion robot is connected to the lattice by at least a single active structural interface connector, e.g., the AutoBolt (Section 4.8.1). This type of movement would be appropriate for

situations when robots could present a fall hazard. These moves are conservative in the sense that they have the lowest risk of accidental disconnection of the robot, but also require the most additional hardware and time to perform.

7.1 The Magnetic Lattice

As robots move around a lattice they form and break connections at every step. The FrFlFuFa system, like many others, uses eight permanent magnets which help to provide temporary forces in order to align and hold elements together. This section uses the term *magnetic lattice*, to mean a 3D cubic lattice where each connector stores energy in magnetic connections. Each of these connections stores energy as part of the magnetic bond, and energy must be input into the system in order to break these connections.

The set of eight lattice attachment magnets each has a diameter of 6.35 mm and is positioned with a slight 0.25 mm inward offset from the connection plane. However, the magnetic bond strength is highly sensitive to variations in this offset distance, as indicated by the steep slope at the beginning of the force-versus-distance graph in Figure 7.1. Based on data for these magnets, we estimate the maximum connection force to be approximately 90 ± 20 N and the bond energy to be on the order of 1.5 ± 0.5 J.

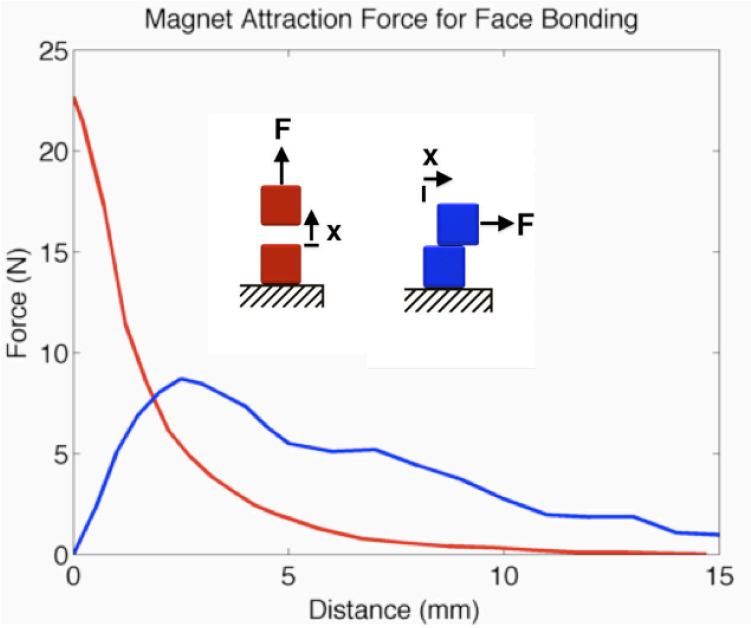

Figure 7.1: This graph provides the correct shape of the force versus distance characteristic for the forces encountered with the magnetic lattice. This figure is from the M-Blocks project [1], but the magnetic configuration is similar and the magnitude of forces is about four times higher, with a peak linear force in the range of 90 N. By integrating the area under this curve the bond energy can be calculated, which for the full FrFlFuFa connectors results in about 1.5 J.

7.2 LAEF Metric: Lattice Cost of Transport Efficiency Benchmark and Analysis

With the goal to evaluate systems based on relative comparison metrics regarding energy consumption, this section introduces a new metric termed the *Lattice Assembly Efficiency Factor* (LAEF). The LAEF is designed to compare structure-assembling systems based on the efficiency of their respective motions while moving a payload to new positions on a modular lattice. This metric reflects the amount of energy expended per unit of lattice movement, adjusted by a normalization factor that takes into account the lattice size and payload mass.

In order to present this metric in a more intuitive manner, we introduce the concept of *Payload Reference Energy* (P_{re}), which is defined as:

$$P_{re} = M_{module} \cdot g \cdot H \tag{7.1}$$

Here, P_{RE} represents the energy equivalent of raising the payload modular element by one lattice cell height against gravity. With this new constant, we can now express the LAEF as:

$$LAEF = \frac{E}{P_{RE}} \tag{7.2}$$

Where:

- E is the total energy consumed per lattice move including energy need to form and break connections.
- H is the lattice cell height.
- M_{module} is the mass of the modular payload element being reconfigured.

Equation 7.2 provides a standardized method to evaluate the energy efficiency performance of modular robotically assembled structures. It allows a comparative view of the actual energy required by the robot to move across a grid cell relative to a baseline energy, namely the gravitational potential energy needed to lift the payload module by one grid cell height. Belty has been experimentally determined to have a LAEF between 4 and 20, depending on the type of movement, with full results shown in Table 7.1. We estimate that existing modular assembly robots would have LAEF values on the order of 30 to 100 to move a single module due to their less efficient actuators.

7.3 Algorithms for Reconfiguration Motion Primitives

While an exhaustive dynamic simulation and extended characterization of possible motions will be valuable future work, this thesis highlights preliminary data from several specific moves. These motions consist of motion scripts performed by Belty under onboard battery power. These motions are shown in Figures 7.2-7.3.

In this system each of Belty's actuators includes an on-axis magnetic encoder (AK7452 or AS5147) to provide high bandwidth actuator position information, and a Texas Instruments

INA1260 power, current and voltage sensing chip to report the power consumption down to 10 mW resolution. These two measurements are both sampled at 200 Hz and are collected and time synchronized by the Teensy Micromod-based core controller circuit board. Additionally, for the moves carrying the block an extra 3 W is consumed by the block's electromagnet to securely attach it during the motion, which has been added to the data.

This section lists and compares the motion primitives for the system, which can be thought of as the lowest level algorithmic building blocks that can be composed in order to accomplish larger system goals.

Table 7.1: Summary of lattice movement experimental results in terms of energy consumption, speed, the LAEF metric, and trials attempted. For some of the movements energy consumption data was not measured. The number of moves attempted as well as the success ratio are estimated from videos taken during development and should be considered as a rough estimate.

Motion Name	Time (s)	Cells	Energy (J)	LAEF	Attempts	Success %
Simple traverse	1.8	1	17.9	-	85	95%
Hopping	1.7	1	18.7	20.7	115	75%
Overhead carry	2.1	4	20.1	5.6	8	100%
Cart traverse carry	1	1	-	-	47	100%
Extra-lattice drop-off	2	3	-	-	2	50%

7.3.1 Lattice Traversing

Traversing, or moving around, a lattice structure is perhaps the most basic movement that any modular robot system can perform. Belty is able to quickly traverse on a straight line, and can perform concave motions. However, due to its limited degrees of freedom, it is not able to perform convex traverses, which many other assembly robots, like those from the Bill-E or SMAC systems can perform. However, with help from additional helper modules, or by collaborating with another Belty robot, these moves become possible. The control algorithm for this move is demonstrated by the power data shown in Figure 7.2 and it consists of first detaching from the lattice using an aggressive shaking motion, then followed by rotating both actuators through almost their entire 180 degree range of motion, before placing the motors into brake mode right before contact and letting the magnetic lattice pull the second foot into place. These final steps helps to minimize the impact forces caused by the inertia of the robot by dissipating the energy through the BLDC motors.

7.3.2 Hopping to Assemble

Belty the assembler robot is the first modular robot able to move around a lattice through hopping. An overview of this motion can be seen in Figure 7.3.2. While hopping may not be appropriate in every situation, dynamic techniques can open up new ground for assembly robots. Each jump consumes 18.7 J of energy to carry a 900 g payload resulting in a LAEF of about 21. Jumping as a means of locomotion has several benefits including the possibility

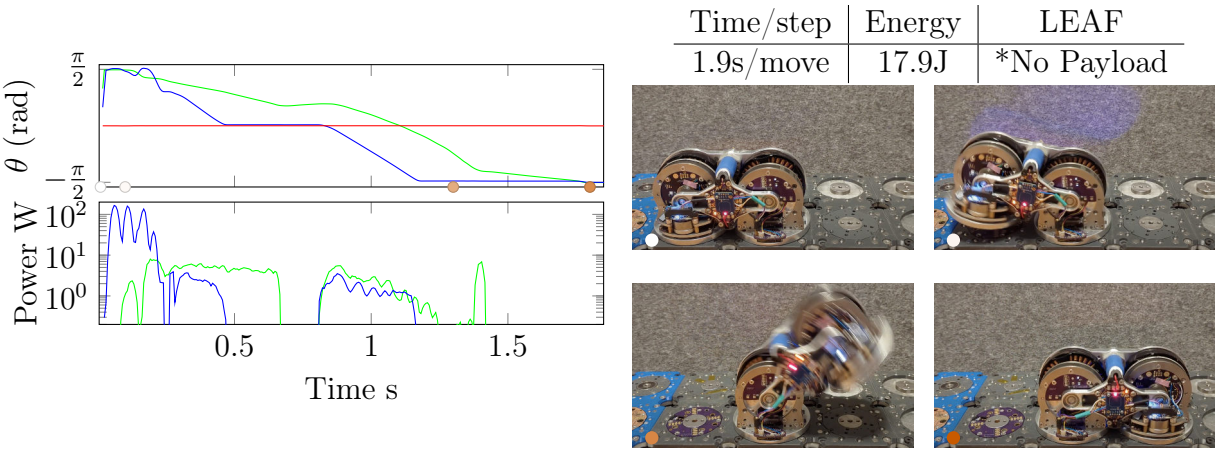

Figure 7.2: Single walking step. This move involves Belty taking a single step by rotating the two primary actuators π radians relative to each other. In the first 0.2 seconds the motor controlling the moving foot (axis B) shakes to free itself without disconnecting the alternate foot, which consumes about 10 J of energy before the foot breaks free. The entire motion is completed in about 1.9 seconds, and this could be further improved with a more optimized motion profile.

to continue indefinitely assuming proper lattice alignment at each step, as well as requiring a small collision-free motion bounding-box. This can allow reconfiguration in compact or obstructed environments where larger assembly robots like Bill-E would not be able to fit.

The initial control algorithm to perform the hopping action was determined through trial and error, and could likely be further optimized for both energy consumption and speed through machine learning techniques. The full sequence of actuator positions and actuator power usage can be seen in the graph of Figure 7.3.2. The move, shown in Figure 7.3, begins with Belty holding the payload vertically, before leaning about 30 degrees in the direction opposite of the intended motion. Once a preset angle is reached, Axis B slowly ramps up the torque so as to not accidentally disconnect the bottom foot from the lattice. Once the block is back to the starting position, but now with a substantial velocity in the direction of intended movement, axis A initiates two short 50 ms pulses at maximum power to first push off from the ground, and then to straighten out the foot in order to land with it parallel to the ground. Belty is airborne for about 100 ms, and it lands with the actuators in brake mode in order to aid in dissipating and absorbing the impact forces.

The primary failure mode for this movement is that Belty gets close to, but is not fully connected to the next connector position, while still being upright. Initial experiments prove that there are several strategies that can help to ensure alignment after the move, with the first one tested being a twisting wiggle motion from the axis C actuator which often causes it to shimmy into position. This motion can be seen on the power section of the Figure 7.3 graph as the red wiggles from 0.8 to 1.6 seconds.

While more quantitative experimentation would be the first future work step in improving the reliability of this motion, in informal testing it works about 75% of the time. One factor that highlights the prototype nature of this system is that Belty's rotating foot doesn't have the tag reader electronics necessary to detect if the landing position is actually a valid

connector. Since the other foot needs to use its tag reader to determine if they payload is properly connected, all of jumps were attempted from the rotating foot. In future versions of Belty-like robots, knowing this information would be vital for improving the accuracy of movements like jumping as corrective motions could be applied until the robot detects the connector snapping into place.

7.3.3 Overhead Module Carry

Belty is able to lift modules off from the ground by using the module's electromagnetic gripper to grip onto the module, and sliding it towards itself, as shown in the first 0.4 s in Figure 7.4. The A and B axis actuators are not able to directly lift the module, as doing so with the axis closer to the payload disconnects the other foot from the lattice, and doing so with the foot anchored to the ground would require roughly 20 Nm of torque which is the magnetic force of the magnetic bond times the moment arm consisting of two lattice cells. The trick to disconnect the payload through dragging is one of the simplifying assembly strategies that are possible due to the actuators and the robustness of the connectors to sliding motions. After breaking the module free, Belty lifts the block until it is aligned vertically. At this point, which is at about t = 1 s in Figure 7.4, a slight nudge is given by the anchored foot, t = 1.1 s in order to start the module pivoting in the direction of motion, at which point the actuators are placed into brake mode. While the move could be faster if this torque is increased, letting gravity and the magnetic lattice forces move the block into its final position helps to maximize the efficiency of the movement. This ability to use potential energy from the payload is an example of the efficiency benefits of using backdrivable actuators for lattice assembly tasks. Additional improvements in efficiency should be possible if the electronic system were able to use the motors to generate electricity on the way down and send it back to the batteries, but this feature was not implemented in this version of Belty.

Carrying the payload module by lifting and placing it on a grid is quite efficient with a LAEF per lattice cell movement of the payload of around 5.7, as compared to around 20 for the hopping movement. However, moving the payload module beyond four cells would either require either passing the module to another Belty robot, or extensive maneuvering on the lattice to be in a position to continue carrying the module.

7.4 Energy Driven High Level Controllers

Once the suitable hardware exists in sufficient quantities, algorithms and reconfiguration planners will need to be developed which are able to efficiently marshal this hardware to accomplish tasks. Some of this planning is generalizable and there has been much related work developing control strategies which attempt to be hardware agnostic, including [18]. However, actual systems will have many specific properties and unique features and quirks, which will likely require what is effectively a middle layer of control algorithms between the general high-level control commands (e.g., create this global shape) and the low-level control (specific motor commands and lattice moves) for each robot. This middle layer will need to prioritize and consider aspects such as number and type of modules required, energy

Time/step	Energy	LEAF
1.7s/move	18.71J	20.7

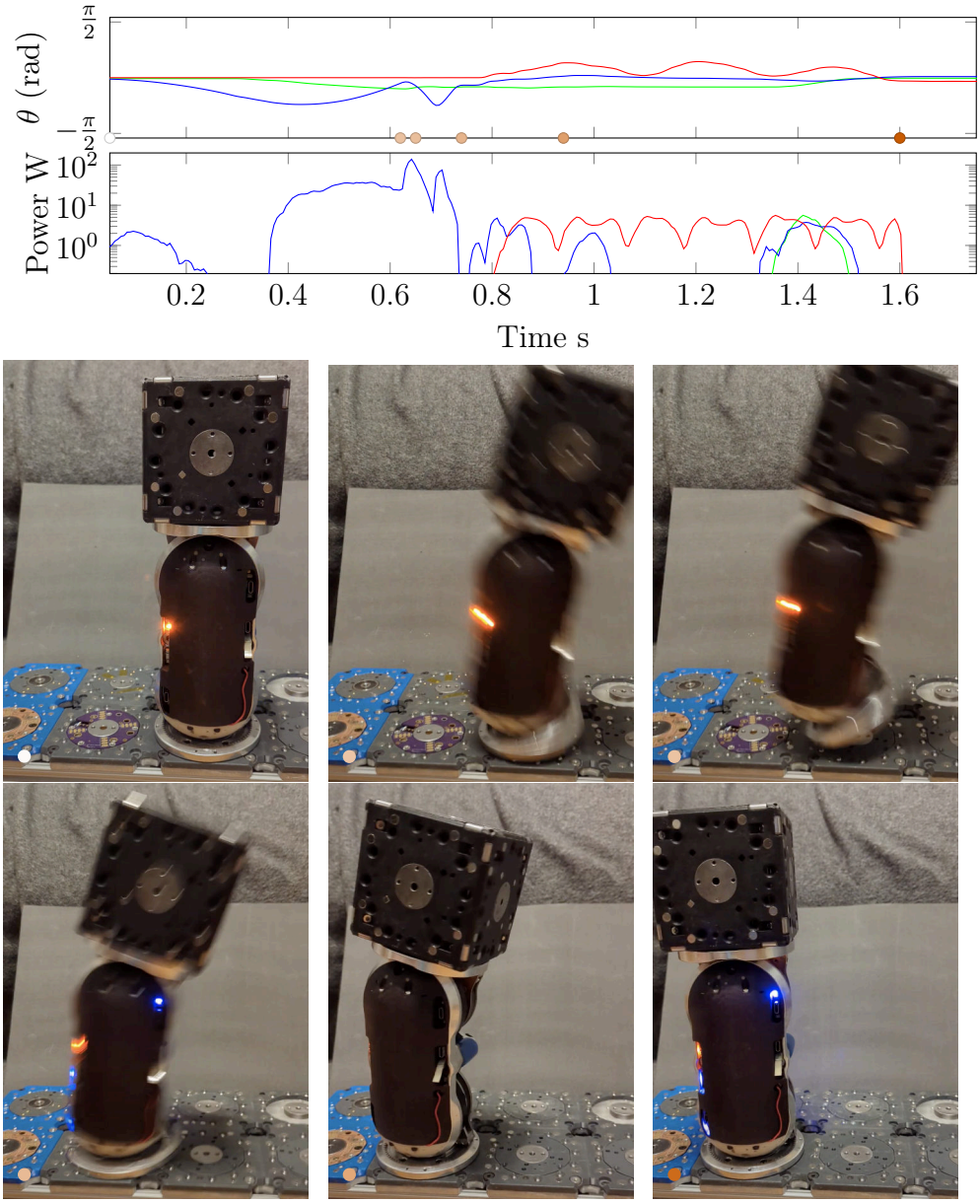

Figure 7.3: Belty moving a payload through hopping. By utilizing the momentum of its body and payload and a 50 ms pulse of 200 watts of power from the axis B actuator at t = 0.6 s, Belty hops to the next lattice position. While this method of locomotion would not be appropriate where the risk of falls is high, dynamic motions in general may increase the range of useful capabilities for simple assembler robots like Belty. Hopping has a success rate of roughly 75% and the wiggles from the axis C actuator (*red line*) help to align the connector in the case of slight misalignment. Additional model or machine learning driven optimizations and misalignment detection strategies are likely to increase the reliability, as when it does fail it usually remains upright.

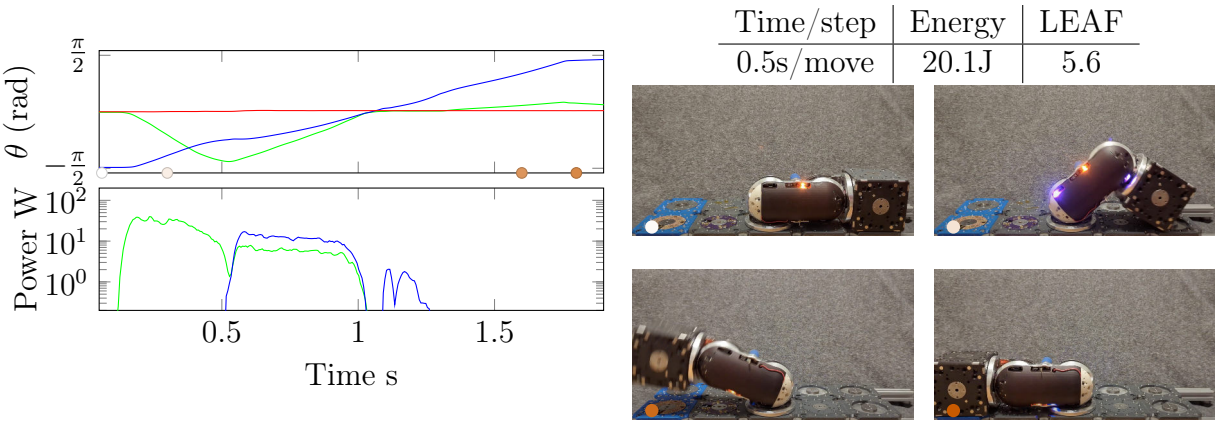

Figure 7.4: This figure shows Belty moving a payload cube by lifting it above itself and placing it four grid cells from its starting point in a straight line. It is important to note that moving the block further than this would require Belty to drop the cube and move around on the lattice to a new position, raising the LAEF for moves longer than four grid steps. In order to calculate the LAEF for this movement the average energy consumed per move is divide by the reference energy of $P_{RE} = 0.9$J.

consumption, reconfiguration speed, reliability of movements and management of conflicts and collaborations between modules. Because there are so many easily quantifiable factors, this area has broad potential for clever optimization algorithms to produce significantly improved results. Potentially because there have not been many actual large scale systems, this topic has been underdeveloped in the literature, and maybe rightly so. Why develop specific algorithms for a system that doesn't exist, when if it ever does exist, the details will inevitably be different. The rest of this section will discuss several potential concepts that can help guide this future development for FrFlFuFa like systems.

Thinking of the assembly process through the lens of energy and power consumption is a useful approach to begin to create meaningful progress towards efficient large scale practical systems. While there are some challenges associated with measuring these quantities, there are available high resolutions current and power monitoring chips that make the task of measuring power consumption relatively straightforward. In the development of large scale systems, it is likely that energy use will be one of the primary factors considered. Entire trajectories and movement sequences can be planned taking into account the energy use, the time, and the probability of success. For reconfigurable space structures energy consumption will likely be the dominating factor, because even if some magical endless source of energy is developed, waste heat production will also scale with the sum of energy consumed, and this can be a challenge for space systems to regulate.

Besides the energy and time required by the actual physical movements of reconfiguration itself, the costs associated with forming and breaking connections will likely be a significant consideration in any future controllers. Some of the systems from related work require that every movement involve an active connection or disconnection to that specific lattice square. For larger robots like Bill-E [27] it is likely not practical to rely solely on the magnetic alignment lattice to hold the robot during moves due to the significant torques introduced through the long moment arms caused by the robots long reach. While Belty can perform

many moves with solely the magnetic forces from the base magnetic lattice, it has a bad habit of disconnecting and falling off the lattice during particularly aggressive movements. Additionally, even just disconnecting from the lattice itself requires significantly more energy than is stored in the magnetic bonds themselves, with data from the traverse movement in Subsection 7.3.1 indicating the consumption of roughly 6 times the energy to disconnect (10 J) than is stored in the magnetic bond (1.5 J). While this can be further optimized, these initial experiments suggest that the energy to disconnect is at least on the same order of magnitude as that to move the modules, so strategies that are able to minimize connections in general, and energy consuming ones in specific will be necessary.

Many specific reconfiguration actions will be able to be accomplished through different methods by the use of metamodules. Reconfigurable machines can build temporary machines and structures that can help locally simplify assembly tasks. For example in this system, it is significantly more efficient and more reliable to move payloads on carts than it is for the assembler robots to try to carry them. If many modules had to be moved to the same location, it might make sense for a team of TrackBot metamodules to move in, create temporary tracks in that area, and then later tear them up to move them someplace else. There are many exciting possibilities to consider how best to create controllers which factor in all of these parameters in order to create new structures. Hopefully once sufficient hardware exists these algorithms can be a fruitful area of future work.

Chapter 8

System Experiments and Applications

While reconfigurable systems have been proposed for many potential use cases, including space structures and re-toolable factories, there are still many missing steps in order to be able to make any meaningful attempt at these goals. Many smaller and more easily digestible applications need to have solutions developed for them that can act as building blocks towards the more complex systems applications. This section presents several independent system experiments that utilize the hardware and demonstrate some of its unique capabilities. Most of these experiments combine several active modules into what is termed a *metamodule* which is a combination of one or more individual elements functioning as a single robot.

The first system experiment showcases precision alignment capability of the modular connectors combined with collaboration between individual robots in order to accomplish a task, and is shown in Section 8.1. The combination of Belty the assembler robot with one of the modular linear carts, which creates a metamodule named the RoombaCat is used to drive along an extensible one-dimensional linear track while picking up a module, and relocating it to a different lattice position. The repeatability of the connection is measured using a dial indicator.

The second system experiment showcases in Section 8.2 the ability to create and extend modular linear tracks using a metamodule called a TrackBot, which is able acquire tracks either by picking them up, or by having them handed off from another robot. This experiment demonstrates several aspects about the linear actuator module including the ability for it to gracefully engage and disengage from tracks, the ability to to work in series with multiple linear modules, and the ability of the semi-permanent connector system to securely attach the TrackBot together.

The third experiment in Section 8.3 demonstrates a simple 1.5 axis gantry machine, which consists of two carts, a 1x3 structural block and the force sensor block (Section 3.5.2) which has a simple magnetic gripper attached to the end of the load cell that is able to reach down, pick up blocks, and then slide them a new position along the primary linear axis. Future work could include more capable gantry machines, but not enough modules have been constructed to make them at the time of this writing.

Trials conducted	average Time (s)	Lattice Cells Moved	Repeatability Average
5	13	4	21 um

Table 8.1: Preliminary experimental results for precise pick-and-place system experiment repeatability analysis.

8.1 Linear System Pick and Place Experiment

While Belty the Assembler is able to traverse around a single level of a lattice structure independently, with the exception of hopping while carrying a payload, it is not able to carry a module while moving long distances. This is due to lack of a third gripping connector which several of the other lattice assembling robots have that allows them to traverse and carry modules at the same time. Belty is able to pick up and move modules with one foot planted on the ground, but with a limited work envelope (see Figure 6.4). This experiment is designed to demonstrate how metamodules, in this case specifically the RoombaCat module (named after the fun internet videos of cats riding ontop of roombas and reaching out and smacking things) dramatically increases the assembly work envelope as compared to a single Belty.

The experimental setup consists of one RoombaCat module on a two piece linear track, as shown in Section 3.3, moving a payload that consists of a metal sphere on a plate with embedded kinematic teeth, and is shown in Figure 8.1. After picking up the module with its included electromagnetic attach point from an independently moving cart, Belty drives along the track until it detects the end of the track. Next a pre-programmed motion algorithm then uses an impedance controller to avoid damaging the dial indicator by initially placing the module adjacent to the intended lattice position. After contact with the structural module has been detected, the robot maintains a slight downward force, and then rotates the C axis in order to slide the payload into position without hitting the dial indicator. After the payload snaps into position, the electromagnet is turned off, and Belty quickly twists the A axis to disconnect from the payload and lets it settle into the position with its kinematic connector. This experiment demonstrates several of the advantages of using proprioceptive actuators for lattice assembly operations, including the current sensing ability to detect the initial collision with the structural cube, and the back-driving of the C axis actuator when the payload snaps into place.

8.2 TrackBots and 1D Track Reconfiguration

While the mechanism of reconfiguration of this design differs from the previous work with the M-Blocks robots, some of the same elements are present. While the M-Block algorithms are based on the Pivoting Cube Model of reconfiguration, this system mainly uses linear motion. Potential future algorithmic research for FrFlFuFa -like systems should leverage the existing reassembly algorithms developed for the Sliding Cube Model (SCM) [18]. While this system does not follow the SCM model exactly at the module level, it might be possible to abstract parts of the system to facilitate similar reconfiguration capabilities. Additionally, these algorithms can contribute to more complicated construction of structures like bridges

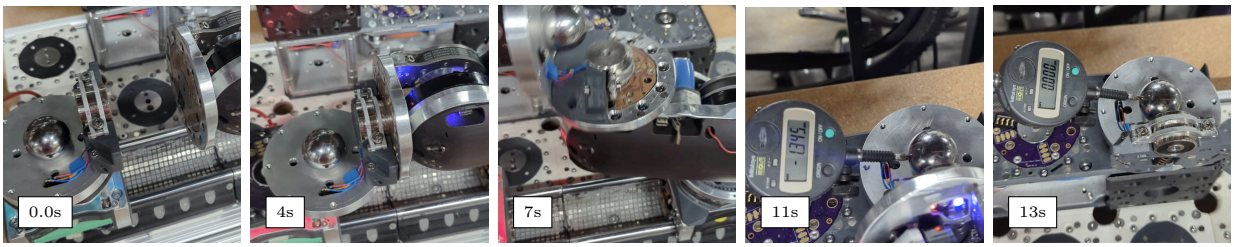

Figure 8.1: Frames from an experiment where Belty moves a payload to a cell and measures the offset with a dial indicator. Five experiments were performed with a resulting standard deviation of 21 um, which is poor for an industrial kinematic coupling, but is likely far more accurate than comparable MSRR connectors. In more than one of the experiments the offset reading of the dial indicator was exactly zero, and it is possible that for some of the experiments the impacts and motion of the robot slightly misaligned the dial indicator, therefore contributing to the observed errors.

or gantries.

We assume some means of delivering new track segments to the gantry, which in the future could be achieved using carts. The algorithm is reminiscent of algorithms developed for the Sliding Cube Model (SCM) [18]. While the individual modules proposed in this paper do not follow the SCM exactly, it would be interesting to try to find ways to apply the SCM to groups of modules, as we work to develop more general algorithms for reconfiguration.

Given robot modules capable of performing various reconfiguration primitives–like connecting and disconnecting tracks, and translating and rotating tracks–we can employ *reconfiguration algorithms* to reconfigure larger groups of modules and do useful work. These algorithms comprise building blocks of future work on general reconfiguration and self-assembly, and showcase that (1) reconfiguration primitives can be achieved by coordinated actuation of cart modules' brushless motors, (2) reliable localization on a track segment can be achieved by querying carts' Hall effect sensors, and (3) system-scale reconfiguration is possible via intuitive planning on the level of modular actuation and sensing.

The goal of 1D track reconfiguration is to move a series of connected tracks, e.g. from left to right. Algorithm 1 accomplishes this using a multi-module robot that we call a *TrackBot*, shown in Table 3.2, which repeatedly disconnects the leftmost track segment from the others, moves it to the right, and connects it back to the line.

A TrackBot has two carts connected by a single Belty module. Belty acts as two servos connected by a rigid bar, forming a kinematic chain of three segments. Each TrackBot therefore has five brushless motors (one in each cart, and three in Belty). Recall that each cart has Hall effect sensors on its left and right sides. These sensors enable the cart to detect when it passes over the end of a track segment, because we intentionally omit a small number of magnets from the ends of each cart. For planning, we assume the sensors raise flags as follows:

- A *track-track-connection flag* is raised when the sensor passes over the connection between two tracks.
- An *end-of-track flag* is raised when the sensor reaches the unconnected end of a track.

Algorithm 1 uses these flags to know when a step of reconfiguration has been completed.

Algorithm 1: Reconfiguration with a single TrackBot.

```
// (13): Get into position to disconnect the leftmost track segment
   from the line (right cart's left side flush with the leftmost
   track-track connection).
```
while *no flag raised by the right cart's left sensors* **do**
    drive both carts to the right
```
// (13): Disconnect track segment from line.
```
while *no flag raised by the left cart's right sensors* **do**
    drive left cart to the right while holding right cart's position
```
// (13): Pick up track segment (and left cart).
```
rotate both servos 90 degrees clockwise
```
// (13): Translate lifted track segment.
```
while *no flag raised by high (originally left) cart's left sensors* **do**
    drive high cart to the right; hold low cart's position
```
// (13): Carry track segment to right.
```
while *no end-of-track flag raised by the low cart's right sensors* **do**
    drive low cart to the right
```
// (13): Put track segment down.
```
rotate both servos 90 degrees clockwise
```
// (13): Connect track back to line.
```
while *no track-track-connection flag raised by the left (originally right) cart's right sensors* **do**
    drive right cart to the right while holding left cart's position
```
// (13): Return to starting configuration.
```
while *no end-of-track flag raised by left cart's left sensors* **do**
    drive both carts to the left

We can extend Algorithm 1 to handle multiple TrackBots working together to perform reconfiguration more quickly. The summary of this algorithm is as follows. The leftmost TrackBot begins as before, and all other TrackBot's wait with one of their carts up. The leftmost TrackBot performs steps (0–3) of Algorithm 1, then carries the track to the next TrackBot, which has one cart up with its motor deactivated, ready to receive the track. The leftmost TrackBot translates the raised track over, deactivates its motor, and returns to the left. After receiving a track segment, a middle TrackBot powers its motor, carries the track segment to the next TrackBot, and gives it away in the same way. After receiving a track segment and powering its motor, the rightmost TrackBot performs steps (4–6) from 1, before raising itself back up and returning to the left.

The single-robot version of this algorithm was implemented on the actual hardware, which is shown in Figure 8.2. This experiment made a few modifications from Algorithm 1 due to challenges related to the control software. The entire experiment took about a minute, but the times when it was actually moving was closer to 10 s, with many pauses built into the script to allow for debugging and human intervention in case things were not working

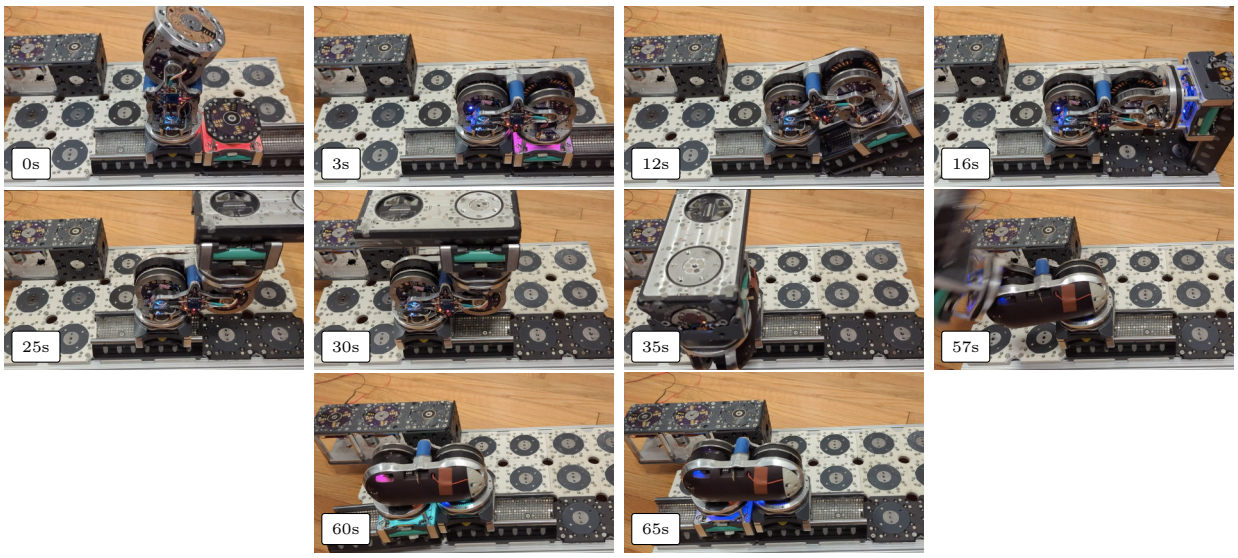

Figure 8.2: Select video frames from a track relocation experiment with a RoombaCat meta module. Belty starts by dropping down and forming an electromagnetic connection to the cart on the right. After forming this connection, the robot has turned into a TrackBot metamodule. The TrackBot then holds the right cart fixed, and uses the full strength of right cart's linear actuator to push to disconnect the mobile track from the lattice, which requires more force than Belty is able to generate. After disconnecting the track, Belty lifts the track up, and then commands the second, and then drives both tracks to the other end of their range of motion. Next Belty rotates 180 degrees, and drops the track back down to the lattice. In order to guarantee that the track successfully snaps into alignment it is necessary to wiggle the two linear actuators back and forth to allow the kinematic coupling connector to snap into place. The whole operation took about a minute, but most of this time was delays for debugging purposes, and total moving time was just around 10 seconds.

properly.

8.3 Modular Gantry Machines

By combining tracks, carts and structural blocks together, multi-axis gantry machines can be created, which share the same basic motion as many existing machines like 3D printers, or Milling machines. Due to cost and time considerations this project does not have enough blocks to make a full 3-axis gantry machine. Further design optimizations and control software will need to be developed before attempting to build such a machine. However, a rendering of an potential future 3D gantry system build out of FrFlFuFa modules is shown in Figure 8.4. If the machine has a source for additional parts, it is able to extend itself along one axis indefinitely, building both the structure and the linear rails as it moves along. This machine is mostly built out standard system modules, but it also is shown with a few non-standard-lattice thin structural plates which form the bottom of the Y axis. The need for parts like these non-standard plates is illustrates the challenge involved with adhering strictly to a cubic lattice, which is discussed in Chapter 9.

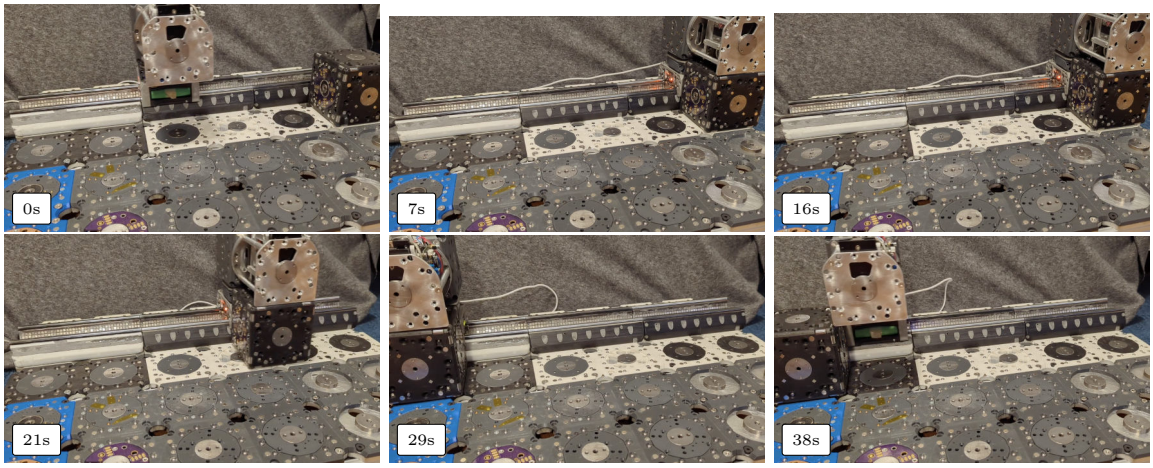

Figure 8.3: This figure shows a sequence of frames from a video where the XZ Gantry metamodule moves a single block along a six-cell long 1D path created by three MagnaCarta track segments. The robot used a magnetic gripper to grip and slightly lift up the blocks.

It is difficult to create multi-axis machines with the small number of MagnaCarta and structural modules that have been produced to date. This module has has been enhanced with a magnetic gripper at the end of the force sensor. This device is able to reach down by driving the linear stepper motor, and then using the stepper driven stage to pull the block away from its connection on the base plate. After lifting up the block, a mechanical stop is built into the module to prevent the block from extending more than about 3 mm from the connection plane. If the stepper motor drives further it will pull the block up against this stop and and drop it 3 mm to the base lattice below. The kinematic coupling is able to then self-align it accurately into the desired lattice cell. This is a preliminary method of picking and placing modules using a modification of the previous linear testing block without requiring an additional actuator to grip and release the block. Future versions of this should separate the linear motion from the gripping in order to more cleanly manipulate modules.

An example system is presented here that implements the XZ Gantry metamodule, as described in Section 3.3, which includes a cart, a structural cube, and the linear sensing block to create a 1.5 axis modular linear gantry machine. The half-of-an-axis description for the XZ Gantry metamodule in Table 3.2 is meant to signify that the Z axis is created out of the force distance sensing block which is not able to move more than about a third of a cell length. This machine is able to pick up modules which have an upward facing connector and move them along the track in either direction and then place them onto the grid, demonstrating a proof of concept modular robotic gantry system. The system was able to successfully move a payload module 6 lattice cells as shown in the video frames in Figure 8.3. The entire experiment took about 38 seconds, and was remote controlled through wireless keyboard commands to the cart module. A significant portion of that time involved struggling with the controlls, and with further software development the entire motion should take under 10 seconds.

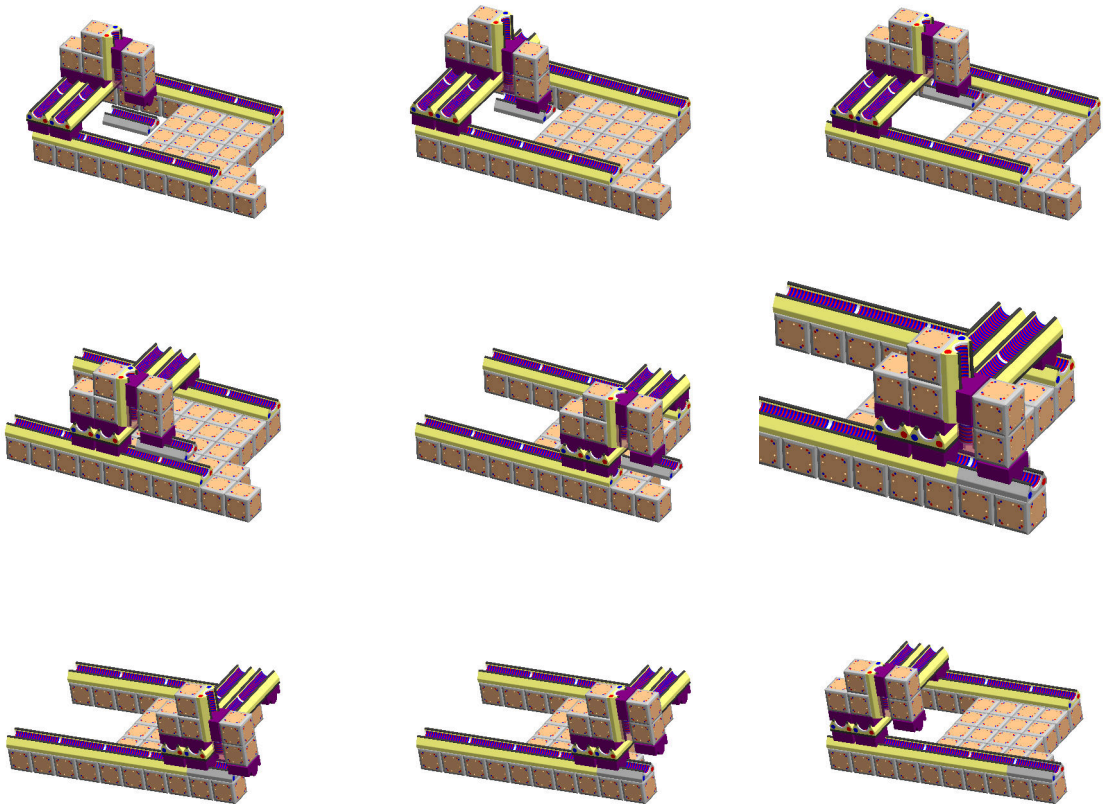

Figure 8.4: This figure shows an imagining of a three-axis gantry machine that is able to extend itself fully along one axis solely by using structural cubes, structural plates, and MagnaCarta actuator segments. This machine assumes that each of the structural blocks is able properly bind themselves together, and that the parallel axes are able to coordinate their motion adequately. During the sequence of moves the machine picks up the a track shown in *grey* using a cart as a gripper. It then moves this to the correct XYZ position and deposits the track.

8.4 Extendable Cantilevered Bridge Assembly Demonstration

The final experiment in this section consists of a preliminary example of the FrFlFuFa constructing a cantilevered bridge, in Figure 8.5. This experiment was a combination of short motion scripts and human in the loop remote control, and used almost all of the modules that were fabricated. This experiment demonstrates many of the important characteristics of the system including the following:

- Robots handing off modules to each other which is facilitated by the backdrivability of the actuators as well as the tag identification system and alignment capabilities of the connectors.
- Belty's ability to hop is necessary in order to traverse the structure while carrying the structural cube module.
- The autoBolt connector attachment sequence worked while being powered and directed through the modular connector from Belty.

The structural cube module is quite heavy, and the combined forces experienced by Belty's bottom connector approached the strength capability of the passive magnetic attachment system. Since only a single AutoBolt enabled structural cube was manufactured it has not yet been possible to determine how far of a bridge can be produced using this system.

The jumping step specifically here seems to be a limiting factor. The large forces experienced by the structure when the hop lands were almost enough to disconnect the whole 1x3 block from its connectors. Future algorithms using multiple Belty robots, or extending the tracks along the bridge to allow carts to carry the subsequent blocks would likely be more reliable.

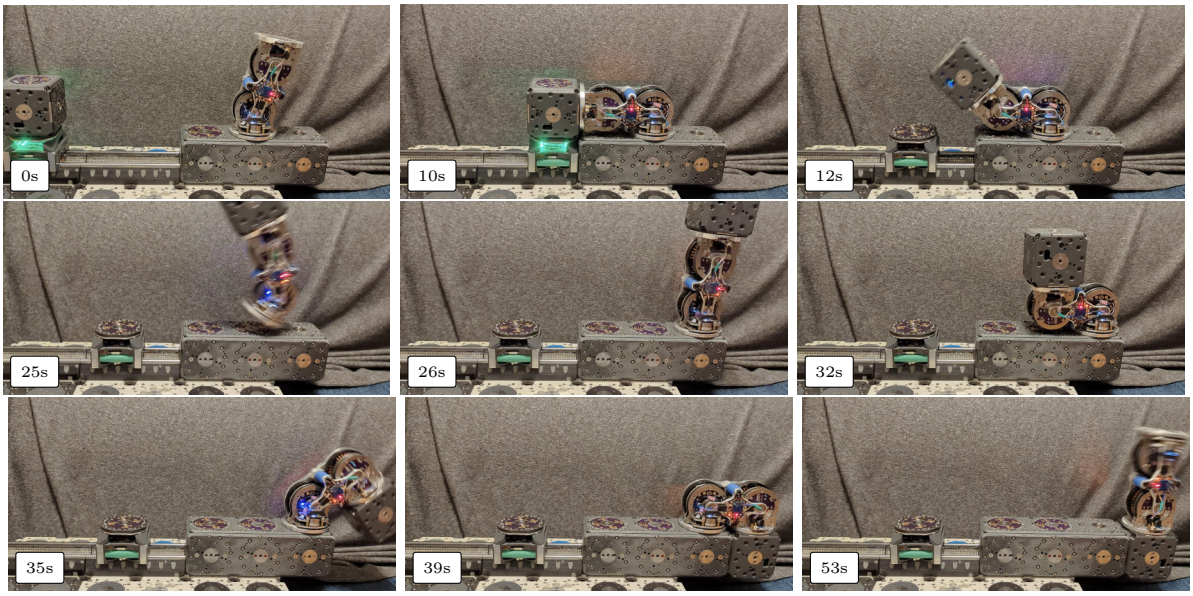

Figure 8.5: This figure shows video frames from a preliminary experiment that combines almost all of the elements of the system to build a single-module cantilevered bridge. In the first frame CartyB (the name of the second cart) brings the structural cube and hands it off to Belty. Belty then verifies that the ID number on the cube is the expected module. Next, Belty lifts the cube, and hops one square to the right. Next Belty carefully lowers the structural cube into positon, and then sends a command for the module to bolt itself to its neighbor.

Chapter 9

Conclusion and Future Work

9.1 FrFlFuFa System Summary

After discussing the ideas and motivation behind this work in Chapter 1, the state of the art in academic literature is reviewed in Chapter 2, with a focus on the modular connector and digital material assembly systems. Chapter 3 introduces the concept of the FrFlFuFa system and introduces the categories of modules and important concepts. Basic parameters regarding the function and design of the simple elements and several miscellaneous special function blocks are collected.

Chapter 4, discusses the challenge of creating a modular connector and shares insights and benchmarks in regard to topics like connector strength, accuracy and repeatability, and general design principles. A kinematic coupling enabled connector is introduced which has both high repeatability as well as a large capture area, or *area of acceptance*. Additionally, the design of the AutoBolt non-gendered bolting mechanism is presented and discussed which is able to securely bolt connectors together.

Chapter 5 introduces a novel modular linear actuator system based on magnetic lead screws that are modified from their traditional form to create modular gantry machines. The design of these actuators are described and an analytical model to help understand the preload force is presented. Additionally, various experiments involved in characterizing aspects such as the stiffness and force of these actuators are discussed.

Chapter 6 begins by discussing the concept of proprioceptive, or quasi-direct-drive actuation. A lattice assembler robot named Belty is then described which is able to perform dynamic motions including the ability to use momentum to jump while carrying lattice blocks. Belty is a self-contained roughly 2 kg robot with three degrees of freedom that can also provide power and communication to other modular elements through the connectors on its two feet.

Chapter 7 and Chapter 8, introduce initial physical reconfiguration algorithms developed to reconfigure systems elements. These motions are evaluated based on the basis of energy expenditure using a new metric, coined the LAEF for lattice assembly efficiency factor. The LAEF is intended to provide a simple single number representing the energy efficiency of moving modules on a 3D lattice to enable comparison in this regard to related work. This metric can perhaps help focus the reconfigurable robotics community more towards valuing

and measuring energy efficiency in assembly operations.

9.2 Lessons Learned

While many of the lessons that I learned throughout developing this work are difficult to transfer through text alone, there are a few general lessons that I will try to distill into this section. Many of these lessons have been only learned through repeated exposure to consequences caused from poor design choices that I made. Perhaps the 'deepness' that these lessons have been learned is proportional to the pain experienced while learning them. While some of these will undoubtedly need to be re-learned through personal experience of the reader, the following bullet points encapsulate some of these lessons:

- Make batteries and other consumable or commonly replaced parts of the design easy to access and replace. It is no fun to have to completely disassemble and desolder parts of a robot every time the battery needs to be swapped or checked out.

- Think deeply about the assembly process at the beginning of the design process. For many of the prototypes I have built, I ended up taking them apart and reassembling them *dozens* of times. Every time there was a needlessly difficult or delicate assembly step was an opportunity for things to go wrong and break or go missing. Often for prototypes it might make sense to use easily reversible connectors like bolts instead of more permanent methods like glue given the possibility of the need for multiple assembly cycles.

- Challenges involving electrical wires have probably given me more grief than any other single practical topic. Wires that don't have carefully considered stress-relief and mag-safe like ability to disconnect *will* eventually fail, and usually at the connection point where they attach, and usally at the worst possible time. If wires ever bend with short radii, they will fail at the solder joint, often times ripping up the copper on the PCBa in the process. If they dangle down from the side, they will catch on things and rip themselves apart. Loose wires are difficult to debug and can mercilessly short out even complicated lovingly hand-crafted circuit boards, and release their 'magic smoke'.

- Take advantage of the amazing resource that is the printed circuit board manufacturing industry. Learn how to make and use simple printed circuit boards as wire replacements, or even use them as primarily mechanical parts. PCBa manufactures embed lots of sophisticated manufacturing steps into an easy to use and order and surprisingly inexpensive process. Where else can you order a 10x quantity of precisely milled composite-material with hundreds of precisely drilled copper-plated holes for only a few dollars, that *also* happens to include as many embedded copper wires as you want?

- No matter how important you think designing for robustness and implementing sound design principles is, it is likely more so. I have seen many people in graduate school who tried to choose a quick hack to solve an important problem almost go mad facing the consequences of that choice. From my experience, in general putting the effort to

do things the *right* way from the beginning will ultimately end up saving more time overall. If a problem keeps coming up in your work, for example difficulties involved with pressing bearings into parts, don't just push harder or hit it with a hammer (solutions I have at times seen my colleagues attempt), instead learn about reamers and press-fit tolerances and do it right!

- Many of the interesting solutions to problems in the robotics world seem to come from applying principles learned elsewhere. There is certainly value in learning about a broad range of other topics, even if initially they don't seem relevant to your research. If an area is exciting or interesting, read about it, and think of how it might be applied to your specific problems.

One important topic I have struggled with is how deeply to go down the rabbit hole of building or rebuilding things from the ground up. On one hand, rebuilding basic parts, for example making a new brushless motor controller, machining custom gears or developing a new software operating system can be seen as wasteful reinventing of the wheel. However, in many cases, especially the densely-packed designs common in modular robots, there are significant efficiencies to be had from designing custom parts. Also, sometimes by redesigning something from the ground up you will deeply learn the principles involved in the operation of the system. This knowledge is useful even if the device that you designed does not end up being used; it helps you to understand and meaningfully compare and contrast existing off-the-shelf solutions.

My takeaway lesson here is to rebuild things from the ground up when the potential knowledge might be important to your overall goals. However, periodically reevaluate along the process to see if this condition still applies. There were certainly a few situations where I stubbornly made my life more challenging than necessary by continuing to develop my own solution while a better off-the-shelf solution was available. Once the problem is understood, and knowledge about what is available and has been done before is obtained, consider the value of giving up - view the sunk costs as simply well-earned knowledge. However, there are also times when persevering beyond what felt reasonable has ultimately led to useful innovations and simplifications.

9.3 Future Work

While developing a modular robotic system is potentially an open ended project, obtaining a degree is not (or at least shouldn't be!) While many of the initial goals of this project were met, there are many interesting directions for future research, both immediate and practical and theoretical aspects of the work that feel unfinished. However, the hope is that these contributions will be incorporated in some capacity into a future set of standards for modular machines. This section will discuss a few of the more straightforward future work goals to fix some of the most obvious problems identified throughout this work.

In regards to the high level mechanical design, further simplification and optimization should be possible to create even more efficient and faster versions of each of the physical robots presented in the previous chapters. Specifically the assembler robots should probably be able to be implemented as purely direct-drive systems, omitting the name-sake belt

transmission inside Belty the assembler robot. While this was briefly experimented with while testing prototypes for the current system, it was deemed to be too dangerous due to higher electrical currents and lack of damping to create with the knowledge and engineering resources available at the time. However, implementing direct-drive should simplify the design as well as also allow more room in the center of each of the assembler robot's feet for payloads such as stronger motors and/or active connectors such as the electromagnetic gripper (Section 4.9) or screw connectors (Section 4.8) presented in Chapter 4. At the same time, removing this transmission eliminates four bearings that are in the primary load path, making the robot both stiffer and simpler to model and control. Additionally, making the primary actuators direct-drive would eliminate the need for sensor calibration after every power cycle that is currently needed.

In regards to the connector, there are a few straightforward changes that should be undertaken. One challenge is that since the CAN network is shared through the whole connected structure, if a single short occurs anywhere along this, the network will temporarily go down. It is prudent to break up the CAN network into several electrically isolated networks that can be patched together by special CAN bridging nodes, which would pass messages from one network to the other. While this will slow down the message passing from nodes that are far from each other, it is a practical necessity. Occasionally during testing, one of the exposed connectors would short out on the metal central portion of a connector which would stop all messages from getting through, requiring intervention from a human in order to keep moving.

The AutoBolt mechanism needs mechanical refinement, especially in regards to the control electronics and the driving motor as well as the mechanism's form factor. It is likely possible to make a design that functions in a similar manner that takes up significantly less space. Improving the functionality and space efficiency of the AutoBolt connector, and being able to embed it in more modules, would go a long way towards making the FrFlFuFa more useful. The motor that drives the AutoBolt should have additional torque in order to more firmly bond the modules together. An additional source of friction between the flanged nut and the plate it sits in should also be added. This friction is necessary to stop the occasional issue where the flanged nut spins in place instead of extending the screw, which currently depends on the friction between the screw and the threads being less than between the flanged nut and the outer plate.

There are several aspects of the existing MagnaCarta actuators that should be fixed in future versions. The first is that a solution needs to be found for the track seam traversal problem which is discussed in Section 5.5.2. One solution could be to increase the magnetic attraction between the tracks and the structure that they are attached to. An additional solution could also involve some form of spring-loaded alignment pins that work to prevent the relative vertical motion of one track relative to the other. Additional challenges include the need to integrate power sharing and active connector control into the cart's circuit boards. The location of the height of the center-line of the spindle rotating axis should likely move upwards in order to be in the center of the lattice cell. This would allow for active connectors to be embedded in each track, as well as allowing for special functions like turn-tables or track-switching schemes to be placed below special track segments.

One of the takeaways from the experimental measurements regarding the repeatability and accuracy of the connectors done in Section 4.4 is that the repeatability is currently

much better than the accuracy of the fabrication. This result is not too surprising given the sometimes sub-optimal manufacturing methods used to fabricate this system. The development of precision fixtures and molds combined with more accurate manufacturing methods like potting (encasing precisely located components in epoxy) and injection molding would greatly increase the dimensional accuracy of the components.

9.4 Discussion

While this project has lead to several interesting designs, a few flashy videos and significant personal learning, it has arguably not *yet* achieved one of the key initial goals: to create actually *useful* systems. I believe that the potential benefits that true modular architectures will eventually bring to the design and operation of machines of all types is truly vast. I also believe that this is the type of grand challenge that society in its current form does not appear to be able to suitably prioritize given the scale of the potential benefits such a solution might bring.

What will it take to finally move towards a useful real-world system? Together with the extensive collection of related research, hopefully this work can help to guide this process. Whether these systems are ultimately built for quickly scaling adaptable disease testing for the next pandemic, or for creating large-scale space telescopes assembled in orbit, they will face many of the same challenges discussed in this work. How can the rate and energy efficiency of the assembly process best be maximized? How accurate is the final structure given the known parameters of the constituent modular pieces? And finally, how can we bring the hardware and system operation costs (i.e., robustness and reliability) to a point where these systems make financial sense? Answering these questions will likely involve the creation of a new iteration of open source specifications that will allow multiple researchers to work together,and collectively move (hop?) towards this goal.

The next steps towards this goal beyond the obvious engineering work and standardization to further refine and implement a more finalized version of this system with more modules is unclear. More importantly it is worth reflecting on what choices were made in this system, and whether they were the right ones, and what other fundamental choices might better support useful systems. These include choices such as actuator type, lattice size, whether the connectors are gendered or not, and the lattice specifications. The following paragraphs will include a few thoughts on these questions, but hopefully this thesis can inspire more discussion and debate about other parameters as well.

While the lack of proper linear bearings and the compliance of the magnetic screw transmissions make this system a poor choice for traditional CNC machines like mills or lathes, one could imagine an adaptation of this system that fixes these shortcomings. The core idea of a 3D lattice grid that connects machine elements to each other through repeatable kinematic couplings and which can dynamically detect its own configuration is certainly a worthy future direction of research. Future factories might have distant descendants of this work implemented as larger and stiffer industrial Lego-like blocks. These systems could allow the manipulation of the parts being fabricated as well as rearranging the CNC machine elements. For example, several simple two or three-axis machines could be temporarily combined to form a large 6-axis machine center depending on demand. While the favorable

economics of hyper-optimized conventional mass production are difficult to overcome, the benefits afforded by modularity including the ability to quickly scale good designs and adapt to sudden changes might begin to change the economic calculus for modular machine tools.

While the magnetic screw-based cart system is interesting and has been fun to build, future modular linear actuators should likely be based on either rack and pinion-like systems for cost-conscious applications, or direct-drive linear motors for those systems which require high speed motion. Linear motor driven systems are beginning to become more common including several that are commercially available as a 1-DOF bases to extend the range of industrial robot arms. The mechanical advantage given by the magnetic screw is significant, especially in battery powered systems that have a limits to their power generation and thermal constraints. However, switching to a linear motor dramatically simplifies the design of the linear modules, while also significantly increasing assembly speed at a moderate disadvantage in force/weight and absolute force capability. Interestingly enough, the existing tracks are theoretically already able to be used as the platen for a modular linear motor assuming the 10 mm pole pair pitch and the slight angle of the adjacent magnetic strips are able to be overcome. Dual-use systems that have modules either using the high mechanical advantage slow motion from a magnetic screw, or the high-speed low-force capability of a linear motor are possible.

The lattice cell size of 100 mm for this system was chosen mostly because it is a nice round number (in base 10 at least), as well as because it is the size for the cubesat standard for satellites [116]. Given the larger size of many of the elements commonly seen in real-world industrial systems, like stepper motors and linear rail bearings, perhaps increasing the size of the lattice cells is a promising direction to go. There might be several different size-classes of systems, similar to the different connector sizes between Duplos and Legos. However, making too many different specializations begins to erode the benefits achieved from modularity. Perhaps dedicated size systems can be developed for different application domains, like modular space systems, versus factory automation versus precision measurement applications. Which designs and challenges remain the same over different size scales, and which are dependent of the scale?

Additionally, the choice to have each connector be non-gendered is a *very* restricting requirement. This choice was made partially because it seemed like a fun challenge to try to solve, and also because the existing related work literature involved with modular self-reconfigrable robots tries to implement such connectors in order to simplify reconfiguration algorithms. Perhaps future systems should compromise on the requirement to have non-gendered connectors. Are the simpler designs allowed by adopting a gendered connector approach worth the extra complications involved with control algorithms? My answer to this question given everything that I have learned working on this project is a solid *probably*. While the extreme flexibility given to systems which have non-gendered connectors is enticing, many real-world manufacturing systems involve quite simple and repetitive tasks, and thus would probably not lose too much from the move to gendered connections.

There will always be a conflict inherent in trying to force disparate parts into a standardized box. There are definitely places in this work where it feels like too much functionality and space efficiency are compromised by adhering to a strict lattice cell. Perhaps a better approach is to generally *try* to keep to a cubic lattice, but allow for many non-standardized components to integrate seamlessly into the system. Intelligently utilizing elements like the

linear MagnaCarta actuators allows for positioning of modules at arbitrary positions along multiple axes, which makes this task seem feasible. Fully thinking through how this can allow for modules of non-standardize systems is a worthwhile task. While the last few years have involved thinking very much *inside* the box, maybe the old saying has it right, it *is* worthwhile to try to think outside the box.

References

[1] J. Romanishin, "M-blocks: Three dimensional modular self-reconfigurable robots," M.S. thesis, Massachusetts Institute of Technology, 2018.

[2] T. Li, J. Hou, J. Yan, R. Liu, H. Yang, and Z. Sun, "Chiplet heterogeneous integration technology—status and challenges," *Electronics*, vol. 9, no. 4, p. 670, 2020.

[3] L. Fridman. "Neil gershenfeld: Self-replicating robots and the future of fabrication." Lex Fridman Podcast no. 380. (2023), [Online]. Available: https://www.youtube.com/watch?v=YDjOS0VHEr4&t=1668s.

[4] I.-W. Park, D. Catanoso, O. Formoso, C. Gregg, M. Ochalek, T. Olatunde, F. Sebastianelli, P. Spino, E. Taylor, G. Trinh, *et al.*, "Soll-e: A module transport and placement robot for autonomous assembly of discrete lattice structures," in *2023 IEEE/RSJ International Conference on Intelligent Robots and Systems (IROS)*, IEEE, 2023, pp. 10 736–10 741.

[5] J. Romanishin, J. M. Bern, and D. Rus, "Self-reconfiguring robotic gantries powered by modular magnetic lead screws," in *2022 International Conference on Robotics and Automation (ICRA)*, IEEE, 2022, pp. 4225–4231.

[6] T. G. Howsman, D. O'Neil, and M. A. Craft, "A stigmergic cooperative multi-robot control architecture," in *Ninth International Conference on the Simulation and Synthesis of Living Systems (ALIFE9)*, 2004.

[7] S. Bonardi, M. Vespignani, R. Moeckel, and A. J. Ijspeert, "Collaborative manipulation and transport of passive pieces using the self-reconfigurable modular robots roombots," in *Intelligent Robots and Systems (IROS), 2013 IEEE/RSJ International Conference on*, Ieee, 2013, pp. 2406–2412.

[8] S. Hauser, M. Mutlu, P.-A. Léziart, H. Khodr, A. Bernardino, and A. J. Ijspeert, "Roombots extended: Challenges in the next generation of self-reconfigurable modular robots and their application in adaptive and assistive furniture," *Robotics and Autonomous Systems*, vol. 127, p. 103 467, 2020.

[9] M. Yim, W. Shen, B. Salemi, D. Rus, M. Moll, H. Lipson, E. Klavins, and G. S. Chirikjian, "Modular self-reconfigurable robot systems: Challenges and opportunities for the future," *Robotics and Automation Magazine*, vol. 14, no. 1, pp. 43–52, 2007.

[10] S. Chennareddy, A. Agrawal, and A. Karuppiah, "Modular Self-Reconfigurable Robotic Systems: A Survey on Hardware Architectures," *Journal of Robotics*, vol. 2017, 2017.

[11] G. Liang, D. Wu, Y. Tu, and T. L. Lam, "Decoding modular reconfigurable robots: A survey on mechanisms and design," *arXiv preprint arXiv:2310.09743*, 2023.

[12] T. Abukhalil, M. Patil, and T. Sobh, "Survey on Decentralized Modular Swarm Robots and Control Interfaces," *International Journal of Engineering (IJE)*, vol. 7, no. 2, p. 44, 2013.

[13] M. Koseki, K. Minami, and N. Inou, "Cellular robots forming a mechanical structure (evaluation of structural formation and hardware design of "chobie ii")," in *Distributed Autonomous Robotic Systems*, Jun. 2004, pp. 131–140.

[14] Y. Suzuki, Y. Tsutsui, M. Yaegashi, and S. Kobayashi, "Modular robot using helical magnet for bonding and transformation," in *Robotics and Automation (ICRA), 2017 IEEE International Conference on*, IEEE, 2017, pp. 2131–2137.

[15] B. K. An, "Em-cube: Cube-shaped, self-reconfigurable robots sliding on structure surfaces," in *IEEE International Conference on Robotics and Automation (ICRA)*, Pasadena, USA, May 2008, pp. 3149–3155.

[16] B. Piranda, G. J. Laurent, J. Bourgeois, C. Clévy, S. Möbes, and N. Le Fort-Piat, "A new concept of planar self-reconfigurable modular robot for conveying microparts," *Mechatronics*, vol. 23, no. 7, pp. 906–915, 2013.

[17] C. Jones and M. J. Matarić, "From Local to Global Behavior in Intelligent Self-Assembly," in *IEEE International Conference on Robotics and Automation (ICRA)*, Taipei, Taiwan, 2003, pp. 721–726.

[18] Z. Butler, K. Kotay, D. Rus, and K. Tomita, "Generic decentralized control for a class of self-reconfigurable robots," in *Proceedings 2002 IEEE International Conference on Robotics and Automation (Cat. No. 02CH37292)*, IEEE, vol. 1, 2002, pp. 809–816.

[19] K. Stoy and R. Nagpal, "Self-reconfiguration Using Directed Growth," in *In Proc. 7th Int. Symp. on Distributed Autonomous Robotic Systems*, Citeseer, 2004.

[20] Y. Zhu, D. Bie, S. Iqbal, X. Wang, Y. Gao, and J. Zhao, "A Simplified Approach to Realize Cellular Automata for Ubot Modular Self-Reconfigurable Robots," *Journal of Intelligent & Robotic Systems*, vol. 79, no. 1, pp. 37–54, 2015.

[21] D. J. Christensen, U. P. Schultz, and K. Stoy, "A Distributed and Morphology-independent Strategy for Adaptive Locomotion in Self-reconfigurable Modular Robots," *Robotics and Autonomous Systems*, vol. 61, no. 9, pp. 1021–1035, 2013.

[22] P. Levi, E. Meister, and F. Schlachter, "Reconfigurable Swarm Robots Produce Self-assembling and Self-repairing Organisms," *Robotics and Autonomous Systems*, vol. 62, pp. 1371–1376, 2014.

[23] M. Yim, B. Shirmohammadi, J. Sastra, M. Park, M. Dugan, and C. Taylor, "Towards Robotic Self-reassembly After Explosion," in *Intelligent Robots and Systems*, San Diego, USA, 2007, pp. 2767–2772.

[24] J. Neubert and H. Lipson, "Soldercubes: a Self-soldering Self-reconfiguring Modular Robot System," *Autonomous Robots*, vol. 40, no. 1, pp. 139–158, Jan. 2016, ISSN: 1573-7527. DOI: 10.1007/s10514-015-9441-4. [Online]. Available: https://doi.org/10.1007/s10514-015-9441-4.

[25] J. White, M. A. Post, and A. Tyrrell, "A novel connection mechanism for dynamically reconfigurable modular robots," in *International Conference on Informatics in Control, Automation and Robotics (ICINCO) 2022: proceedings*, IEEE, 2022.

[26] J. Neubert, A. Rost, and H. Lipson, "Self-soldering connectors for modular robots," *Transaction of Robotics*, vol. PP, no. 99, pp. 1–14, 2014.

[27] B. Jenett and K. Cheung, "Bill-e: Robotic platform for locomotion and manipulation of lightweight space structures," in *25th AIAA/AHS Adaptive Structures Conference*, 2017, p. 1876.

[28] S. Murata, E. Yoshida, A. Kamimura, H. Kurokawa, K. Tomita, and S. Kokaji, "M-tran: Self-reconfigurable modular robotic system," *IEEE/ASME transactions on mechatronics*, vol. 7, no. 4, pp. 431–441, 2002.

[29] K. Kotay, D. Rus, M. Vona, and C. McGray, "The self-reconfiguring robotic molecule," in *Proceedings. 1998 IEEE International Conference on Robotics and Automation (Cat. No. 98CH36146)*, IEEE, vol. 1, 1998, pp. 424–431.

[30] M. Nisser, L. Cheng, Y. Makaram, R. Suzuki, and S. Mueller, "Electrovoxel: Electromagnetically actuated pivoting for scalable modular self-reconfigurable robots," in *2022 International Conference on Robotics and Automation (ICRA)*, IEEE, 2022, pp. 4254–4260.

[31] A. D. Marchese, H. Asada, and D. Rus, "Controlling the locomotion of a separated inner robot from an outer robot using electropermanent magnets," in *2012 IEEE International Conference on Robotics and Automation*, IEEE, 2012, pp. 3763–3770.

[32] K. W. Gilpin, "Shape formation by self-disassembly in programmable matter systems," Ph.D. dissertation, MIT, 2012.

[33] K. Gilpin, A. Knaian, and D. Rus, "Robot Pebbles: One Centimeter Robotic Modules for Programmable Matter through Self-Disassembly," in *International Conference on Robotics and Automation*, Anchorage, AK, May 2010, pp. 2485–2492.

[34] T. Tosun, J. Davey, C. Liu, and M. Yim, "Design and Characterization of the EP-Face," in *IEEE Intl. Conf. on Robotics and Automation (ICRA)*, 2016.

[35] M. M. Smith, "Recursive robotic assemblers," Ph.D. dissertation, Massachusetts Institute of Technology, 2023.

[36] C. Chen, T. Collins, and W. Shen, "A Near-optimal Dynamic Power Sharing Scheme for Self-reconfigurable Modular Robots," in *2016 IEEE International Conference on Robotics and Automation (ICRA)*, May 2016, pp. 5183–5188. DOI: 10.1109/ICRA.2016.7487724.

[37] M. Park, S. Chitta, A. Teichman, and M. Yim, "Automatic Configuration Recognition Methods in Modular Robots," *The International Journal of Robotics Research*, vol. 27, no. 3-4, pp. 403–421, 2008.

[38] S. Funiak, P. Pillai, M. P. Ashley-Rollman, J. D. Campbell, and S. C. Goldstein, "Distributed Localization of Modular Robot Ensembles," *IJRR*, vol. 28, no. 8, pp. 946–961, 2009.

[39] J. W. Romanishin, J. Mamish, and D. Rus, "Decentralized control for 3d m-blocks for path following, line formation, and light gradient aggregation," in *2019 IEEE/RSJ International Conference on Intelligent Robots and Systems (IROS)*, IEEE, 2019, pp. 4862–4868.

[40] J. Werfel and R. Nagpal, "Extended Stigmergy in Collective Construction," *IEEE Intelligent Systems*, vol. 21, no. 2, pp. 20–28, Mar. 2006, ISSN: 1541-1672. DOI: 10.1109/MIS.2006.25.

[41] Y. Zhu, D. Bie, S. Iqbal, X. Wang, Y. Gao, and J. Zhao, "A simplified approach to realize cellular automata for ubot modular self-reconfigurable robots," *Journal of Intelligent & Robotic Systems*, pp. 1–18, 2014.

[42] K. Lin, J. Rojas, and Y. Guan, "A Vision-based Scheme for Kinematic Model Construction of Reconfigurable Modular Robots," in *Intelligent Robots and Systems (IROS), 2017 IEEE/RSJ International Conference on*, IEEE, 2017, pp. 2751–2757.

[43] B. T. Kirby, B. Aksak, J. D. Campbell, J. F. Hoburg, T. C. Mowry, P. Pillai, and S. C. Goldstein, "A Modular Robotic System Using Magnetic Force Effectors," in *Intelligent Robots and Systems*, 2007, pp. 2787–2793.

[44] J. Liedke, R. Matthias, L. Winkler, and H. Wörn, "The Collective Self-Reconfigurable Modular Organism (CoSMO)," in *Advanced Intelligent Mechatronics (AIM), 2013 IEEE/ASME International Conference on*, IEEE, 2013, pp. 1–6.

[45] H. Kurokawa, K. Tomita, A. Kamimura, S. Kokaji, T. Hasuo, and S. Murata, "Distributed Self-Reconfiguration of M-TRAN III Modular Robotic Systems," *International Journal of Robotics Research*, vol. 27, no. 3-4, pp. 373–386, Apr. 2008.

[46] J. Werfel, Y. Bar-Yam, D. Rus, and R. Nagpal, "Distributed Construction by Mobile Robots with Enhanced Building Blocks," in *Robotics and Automation, 2006. ICRA 2006. Proceedings 2006 IEEE International Conference on*, IEEE, 2006, pp. 2787–2794.

[47] J. Wang and E. Olson, "AprilTag 2: Efficient and Robust Fiducial Detection," in *Proceedings of the IEEE/RSJ International Conference on Intelligent Robots and Systems (IROS)*, Oct. 2016.

[48] Y. Tu and T. L. Lam, "Configuration identification for a freeform modular self-reconfigurable robot-freesn," *IEEE Transactions on Robotics*, 2023.

[49] A. Slocum, "Kinematic couplings: A review of design principles and applications," *International journal of machine tools and manufacture*, vol. 50, no. 4, pp. 310–327, 2010.

[50] M. E. Karagozler, J. D. Campbell, G. K. Fedder, S. C. Goldstein, M. P. Weller, and B. W. Yoon, "Electrostatic latching for inter-module adhesion, power transfer, and communication in modular robots," in *Intelligent Robots and Systems, 2007. IROS 2007. IEEE/RSJ International Conference on*, IEEE, 2007, pp. 2779–2786.

[51] P. White, V. Zykov, J. Bongard, and H. Lipson, "Three Dimensional Stochastic Reconfiguration of Modular Robots," in *RSS*, Cambridge, USA, Jun. 2005, pp. 161–168.

[52] C. Wagner, N. Dhanaraj, T. Rizzo, J. Contreras, H. Liang, G. Lewin, and C. Pinciroli, "Smac: Symbiotic multi-agent construction," *IEEE Robotics and Automation Letters*, vol. 6, no. 2, pp. 3200–3207, 2021.

[53] M. S. Moses, H. Ma, K. C. Wolfe, and G. S. Chirikjian, "An architecture for universal construction via modular robotic components," *Robotics and Autonomous Systems*, vol. 62, no. 7, pp. 945–965, 2014.

[54] S. Hossain, C. A. Nelson, and P. Dasgupta, "Rogensid: A rotary plate genderless single-sided docking mechanism for modular self-reconfigurable robots," in *International Design Engineering Technical Conferences and Computers and Information in Engineering Conference*, American Society of Mechanical Engineers, vol. 55942, 2013, V06BT07A011.

[55] J. Mrázek and J. Barnat, "Roficom–first open-hardware connector for metamorphic robots," in *2019 IEEE/RSJ International Conference on Intelligent Robots and Systems (IROS)*, IEEE, 2019, pp. 2720–2725.

[56] J. Neubert, A. Rost, and H. Lipson, "Self-soldering connectors for modular robots," *IEEE Transactions on Robotics*, vol. 30, no. 6, pp. 1344–1357, 2014.

[57] P. Swissler and M. Rubenstein, "Fireantv3: A modular self-reconfigurable robot towards free-form self-assembly using attach-anywhere continuous docks," *IEEE Robotics and Automation Letters*, 2023.

[58] P. Swissler and M. Rubenstein, "Fireant3d: A 3d self-climbing robot towards non-latticed robotic self-assembly," in *2020 IEEE/RSJ International Conference on Intelligent Robots and Systems (IROS)*, IEEE, 2020, pp. 3340–3347.

[59] D. J. Christensen and K. Stoy, "Selecting a meta-module to shape-change the atron self-reconfigurable robot," in *International Conference on Robotics and Automation*, Orlando, USA, May 2006, pp. 2532–2538.

[60] A. Sproewitz, A. Billard, P. Dillenbourg, and A. J. Ijspeert, "Roombots-mechanical design of self-reconfiguring modular robots for adaptive furniture," in *Robotics and Automation, 2009. ICRA'09. IEEE International Conference on*, IEEE, 2009, pp. 4259–4264.

[61] R. MacCurdy, A. McNicoll, and H. Lipson, "Bitblox: Printable digital materials for electromechanical machines," *The International Journal of Robotics Research*, vol. 33, no. 10, pp. 1342–1360, 2014.

[62] B. Jenett, A. Abdel-Rahman, K. Cheung, and N. Gershenfeld, "Material–robot system for assembly of discrete cellular structures," *IEEE Robotics and Automation Letters*, vol. 4, no. 4, pp. 4019–4026, 2019.

[63] Y. Terada and S. Murata, "Modular stucture assembly using blackboard path planning systems," in *International Symposium on Automation and Robotics in Construction*, 2006, pp. 852–857.

[64] M. E. Carney, "Discrete cellular lattice assembly," Ph.D. dissertation, Massachusetts Institute of Technology, 2015.

[65] K. H. Petersen, N. Napp, R. Stuart-Smith, D. Rus, and M. Kovac, "A review of collective robotic construction," *Science Robotics*, vol. 4, no. 28, eaau8479, 2019.

[66] S. El-Sayegh, L. Romdhane, and S. Manjikian, "A critical review of 3d printing in construction: Benefits, challenges, and risks," *Archives of Civil and Mechanical Engineering*, vol. 20, pp. 1–25, 2020.

[67] Y. Terada and S. Murata, "Automatic assembly system for a large-scale modular structure-hardware design of module and assembler robot," in *2004 IEEE/RSJ International Conference on Intelligent Robots and Systems (IROS)(IEEE Cat. No. 04CH37566)*, IEEE, vol. 3, 2004, pp. 2349–2355.

[68] O. Formoso, G. Trinh, D. Catanoso, I.-W. Park, C. Gregg, and K. Cheung, "Mmic-i: A robotic platform for assembly integration and internal locomotion through mechanical meta-material structures," in *2023 IEEE International Conference on Robotics and Automation (ICRA)*, IEEE, 2023, pp. 7303–7309.

[69] Q. Lindsey, D. Mellinger, and V. Kumar, "Construction of cubic structures with quadrotor teams," *Proc. Robotics: Science & Systems VII*, 2011.

[70] M. Allwright, N. Bhalla, H. El-faham, A. Antoun, C. Pinciroli, and M. Dorigo, "Srocs: Leveraging stigmergy on a multi-robot construction platform for unknown environments," in *Swarm Intelligence: 9th International Conference, ANTS 2014, Brussels, Belgium, September 10-12, 2014. Proceedings 9*, Springer, 2014, pp. 158–169.

[71] K. H. Petersen, R. Nagpal, and J. K. Werfel, "Termes: An autonomous robotic system for three-dimensional collective construction," *Robotics: science and systems VII*, 2011.

[72] E. Niehs, A. Schmidt, C. Scheffer, D. E. Biediger, M. Yannuzzi, B. Jenett, A. Abdel-Rahman, K. C. Cheung, A. T. Becker, and S. P. Fekete, "Recognition and reconfiguration of lattice-based cellular structures by simple robots," in *2020 IEEE International Conference on Robotics and Automation (ICRA)*, IEEE, 2020, pp. 8252–8259.

[73] D. Gyimothy and A. Toth, "Experimental evaluation of a novel automatic service robot tool changer," in *2011 IEEE/ASME International Conference on Advanced Intelligent Mechatronics (AIM)*, IEEE, 2011, pp. 1046–1051.

[74] J. P. Wulfsberg, S. Grimske, N. Kong, B. Röhlig, J. Storjohann, and J. Müller, "A function integrated and intelligent mechanical interface for small modular machine tools," *Precision Engineering*, vol. 38, no. 1, pp. 109–115, 2014.

[75] A. J. Hart, "Design and analysis of kinematic couplings for modular machine and instrumentation structures," *SM Thesis, Massachusetts Institute of Technology*, 2001.

[76] P. J. Willoughby, A. J. Hart, and A. H. Slocum, "Experimental determination of kinematic coupling repeatability in industrial and laboratory conditions," *Journal of manufacturing systems*, vol. 24, no. 2, pp. 108–121, 2005.

[77] K. C. Galloway, R. Jois, and M. Yim, "Factory floor: A robotically reconfigurable construction platform," in *2010 IEEE International Conference on Robotics and Automation*, IEEE, 2010, pp. 2467–2472.

[78] N. Peek, "Making machines that make: Object-oriented hardware meets object-oriented software," Ph.D. dissertation, Massachusetts Institute of Technology, 2016.

[79] N. Peek, J. Coleman, I. Moyer, and N. Gershenfeld, "Cardboard machine kit: Modules for the rapid prototyping of rapid prototyping machines," in *Proceedings of the 2017 CHI Conference on Human Factors in Computing Systems*, ACM, 2017, pp. 3657–3668.

[80] J. W. Romanishin, K. Gilpin, and D. Rus, "M-blocks: Momentum-driven, magnetic modular robots," in *Intelligent Robots and Systems (IROS), 2013 IEEE/RSJ International Conference on*, IEEE, 2013, pp. 4288–4295.

[81] J. W. Romanishin, K. Gilpin, S. Claici, and D. Rus, "3d m-blocks: Self-reconfiguring robots capable of locomotion via pivoting in three dimensions," in *Robotics and Automation (ICRA), 2015 IEEE International Conference on*, IEEE, 2015, pp. 1925–1932.

[82] S. Claici, "Aggregation for Modular Robots in the Pivoting Cube Model," M.S. thesis, Massachusetts Institute of Technology, 2016.

[83] C. Sung, J. Bern, J. Romanishin, and D. Rus, "Reconfiguration Planning for Pivoting Cube Modular Robots," in *Robotics and Automation (ICRA), 2015 IEEE International Conference on*, IEEE, 2015, pp. 1933–1940.

[84] S. Claici, J. Romanishin, J. I. Lipton, S. Bonardi, K. W. Gilpin, and D. Rus, "Distributed Aggregation for Modular Robots in the Pivoting Cube Model," in *Robotics and Automation (ICRA), 2017 IEEE International Conference on*, IEEE, 2017, pp. 1489–1496.

[85] M. Rubenstein, C. Ahler, and R. Nagpal, "Kilobot: A Low Cost Scalable Robot System for Collective Behaviors," in *International Conference on Robotics and Automation*, Minneapolis, USA, May 2012, In Press.

[86] C. Liu, Q. Lin, H. Kim, and M. Yim, "Smores-ep, a modular robot with parallel self-assembly," *Autonomous Robots*, vol. 47, no. 2, pp. 211–228, 2023.

[87] N. Eckenstein and M. Yim, "Modular robot connector area of acceptance from configuration space obstacles," in *2017 IEEE/RSJ International Conference on Intelligent Robots and Systems (IROS)*, IEEE, 2017, pp. 3550–3555.

[88] A. H. Slocum, *Precision machine design*. Society of Manufacturing Engineers, 1992.

[89] USB Implementers Forum, Inc., *Usb type-c specification*, USB Implementers Forum, Inc. 20XX. [Online]. Available: https://www.usb.org/documents?search=type-c.

[90] A. J. Hart, A. Slocum, and P. Willoughby, "Kinematic coupling interchangeability," *Precision Engineering*, vol. 28, no. 1, pp. 1–15, 2004, ISSN: 0141-6359. DOI: https://doi.org/10.1016/S0141-6359(03)00071-0. [Online]. Available: https://www.sciencedirect.com/science/article/pii/S0141635903000710.

[91] M. L. Culpepper, "Design of quasi-kinematic couplings," *Precision Engineering*, vol. 28, no. 3, pp. 338–357, 2004.

[92] PJRC. "Teensy 3.2." (2023), [Online]. Available: https://www.pjrc.com/teensy/teensy31.html.

[93] G. A. Pratt and M. M. Williamson, "Series elastic actuators," in *Intelligent Robots and Systems 95.'Human Robot Interaction and Cooperative Robots', Proceedings. 1995 IEEE/RSJ International Conference on*, IEEE, vol. 1, 1995, pp. 399–406.

[94] C.-H. Kim, H.-C. Nam, and S.-M. Kwon, "Linear drive systems using roller gear mechanism," *Journal of the Korean Society of Manufacturing Technology Engineers*, vol. 21, no. 5, pp. 702–707, 2012.

[95] Nexen Group. "Nexen group - rotary motion control: Roller pinion gears." (Accessed: 2024-01-11), [Online]. Available: https://www.nexengroup.com/rotary-motion-control/roller-pinion-gears.

[96] K. Atallah and D. Howe, "A novel high-performance magnetic gear," *IEEE Transactions on magnetics*, vol. 37, no. 4, pp. 2844–2846, 2001.

[97] S. Kikuchi and K. Tsurumoto, "Design and characteristics of a new magnetic worm gear using permanent magnet," *IEEE Transactions on magnetics*, vol. 29, no. 6, pp. 2923–2925, 1993.

[98] T. Shinshi, J. Hashimoto, B. Chen, K. Sato, and A. Shimokohbe, "A new magnetic lead screw and its basic characteristics," *Transactions of the Japan society of mechanical engineers. C*, vol. 64, no. 618, pp. 310–317, 1998.

[99] R. K. Holm, N. I. Berg, M. Walkusch, P. O. Rasmussen, and R. H. Hansen, "Design of a magnetic lead screw for wave energy conversion," *IEEE Transactions on Industry Applications*, vol. 49, no. 6, pp. 2699–2708, 2013.

[100] N. I. Berg, R. K. Holm, and P. O. Rasmussen, "Design and test of a novel magnetic lead screw for active suspension system in a vehicle," in *2014 International Conference on Electrical Machines (ICEM)*, IEEE, 2014, pp. 470–477.

[101] L. Bu and Y. Fujimoto, "Novel force estimation method for magnetic lead screw-based rotlin actuator," *IEEE Transactions on Industry Applications*, vol. 58, no. 6, pp. 7297–7307, 2022.

[102] K. Trangbaek, V. Suplin, R. K. Holm, N. I. Berg, and P. O. Rasmussen, "Method and apparatus for measurement and control of linear actuator," US9628001B2, Nov. 2015.

[103] K. Lu, Y. Xia, W. Wu, and L. Zhang, "New helical-shape magnetic pole design for magnetic lead screw enabling structure simplification," *IEEE Transactions on Magnetics*, vol. 51, no. 11, pp. 1–4, 2015.

[104] J. Wang, K. Atallah, and W. Wang, "Analysis of a magnetic screw for high force density linear electromagnetic actuators," *IEEE Transactions on Magnetics*, vol. 47, no. 10, pp. 4477–4480, 2011.

[105] N. Ils, A. B. Christiansen, R. K. Holm, P. O. Rasmussen, *et al.*, "Design and test of a reluctance based magnetic lead screw pto system for a wave energy converter," in *2017 IEEE International Electric Machines and Drives Conference (IEMDC)*, IEEE, 2017, pp. 1–8.

[106] Z. Ling, W. Zhao, P. O. Rasmussen, and K. Lu, "Design and development of a magnetic lead screw propulsion device for general transport system," *IET Electric Power Applications*, vol. 14, no. 3, pp. 492–499, 2020.

[107] S. Christensen and S. E. Mark, "Analysis and control of a magnetic lead screw for servo application," 2014.

[108] P. M. Wensing, A. Wang, S. Seok, D. Otten, J. Lang, and S. Kim, "Proprioceptive actuator design in the mit cheetah: Impact mitigation and high-bandwidth physical interaction for dynamic legged robots," *Ieee transactions on robotics*, vol. 33, no. 3, pp. 509–522, 2017.

[109] B. Katz, J. Di Carlo, and S. Kim, "Mini cheetah: A platform for pushing the limits of dynamic quadruped control," in *2019 international conference on robotics and automation (ICRA)*, IEEE, 2019, pp. 6295–6301.

[110] D. V. Gealy, S. McKinley, B. Yi, P. Wu, P. R. Downey, G. Balke, A. Zhao, M. Guo, R. Thomasson, A. Sinclair, *et al.*, "Quasi-direct drive for low-cost compliant robotic manipulation," in *2019 International Conference on Robotics and Automation (ICRA)*, IEEE, 2019, pp. 437–443.

[111] M. Hutter, C. Gehring, D. Jud, A. Lauber, C. D. Bellicoso, V. Tsounis, J. Hwangbo, K. Bodie, P. Fankhauser, M. Bloesch, *et al.*, "Anymal-a highly mobile and dynamic quadrupedal robot," in *2016 IEEE/RSJ international conference on intelligent robots and systems (IROS)*, IEEE, 2016, pp. 38–44.

[112] F. Negrello, M. Garabini, M. G. Catalano, J. Malzahn, D. G. Caldwell, A. Bicchi, and N. G. Tsagarakis, "A modular compliant actuator for emerging high performance and fall-resilient humanoids," in *2015 IEEE-RAS 15th International Conference on Humanoid Robots (Humanoids)*, IEEE, 2015, pp. 414–420.

[113] B. G. Katz, "A low cost modular actuator for dynamic robots," Ph.D. dissertation, Massachusetts Institute of Technology, 2018.

[114] H. Asada and T. Kanade, "Design of direct-drive mechanical arms," 1983.

[115] G. Kenneally, A. De, and D. E. Koditschek, "Design principles for a family of direct-drive legged robots," *IEEE Robotics and Automation Letters*, vol. 1, no. 2, pp. 900–907, 2016.

[116] H. Heidt, J. Puig-Suari, A. Moore, S. Nakasuka, and R. Twiggs, "Cubesat: A new generation of picosatellite for education and industry low-cost space experimentation," 2000.